Journal of the OPTICAL SOCIETY *of* AMERICA

VOLUME 26
No. 4

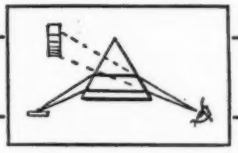

APRIL
1936

Wave-Length Identification Lists for the Extreme Ultraviolet . . . . . J. C. BOYCE AND H. A. ROBINSON 133

Behavior of the 4930A Absorption Band of Uranine Solutions Under High Pressure . . . . . WILLIAM JAMES LYONS 144

Spectrometer for Studies at High Pressures . . . . . W. JAMES LYONS AND FRANKLIN E. POINDEXTER 146

Infrared Absorption Spectra of Mixtures of Alcohol and Water . . . . . DUDLEY WILLIAMS, R. D. WEATHERFORD AND E. K. PLYLER 149

On the Figuring and Correcting of Mirrors by Controlled Deposition of Aluminum . . . . . JOHN STRONG AND E. GAVIOLA 153

On the Quantitative Use of the Foucault Knife-Edge Test . . E. GAVIOLA 163

Objective Measurements of Graininess of Photographic Materials . . . . . A. VAN KREVELD 170

On the Characteristic Function of Hamilton, the Eiconal of Bruns, and Their Use in Optics . . . . . M. HERZBERGER 177

Applied Electron Optics . . . . V. K. ZWORYKIN AND G. A. MORTON 181

Gloss Investigations Using Reflected Images of a Target Pattern . . . . . RICHARD S. HUNTER 190

Erratum: Theory of Microscope Vision . . . . . M. HERZBERGER 196

Published monthly
at Prince and Lemon Sts., Lancaster, Pa.
by the
AMERICAN INSTITUTE OF PHYSICS
Incorporated
175 Fifth Avenue, New York, N. Y.
FOR AND UNDER THE EDITORIAL SUPERVISION OF
THE OPTICAL SOCIETY OF AMERICA

THE OPTICAL SOCIETY OF AMERICA

OFFICERS OF THE SOCIETY

A. C. HARDY, *President*
Massachusetts Institute of Technology
Cambridge, Massachusetts

R. C. GIBBS, *Vice President*
Department of Physics
Cornell University
Ithaca, New York

L. B. TUCKERMAN, *Secretary*
Bureau of Standards
Washington, D. C.

HENRY F. KURTZ, *Treasurer*
Bausch & Lomb Optical Company
Rochester, New York

The Board of Directors consists of the above officers; the Editor of the Journal; the Past President; and five elected members:

W. B. RAYTON, *Past President*
Bausch & Lomb Optical Company
Rochester, New York

F. K. RICHTMYER, *Editor*
Cornell University
Ithaca, New York

Elected Members

ARTHUR H. COMPTON
Ryerson Physical Laboratory
University of Chicago
Chicago, Illinois

K. S. GIBSON
Bureau of Standards
Washington, D. C.

G. R. HARRISON
Department of Physics
Massachusetts Institute of Technology
Cambridge, Massachusetts

HERBERT E. IVES
463 West Street
New York, New York

CARL W. KEUFFEL
Keuffel & Esser Company
Hoboken, New Jersey

THE OPTICAL SOCIETY OF AMERICA was organized in 1916 *"to increase and diffuse the knowledge of optics in all its branches, pure and applied, to promote the mutual interests of investigators of optical problems, of designers, manufacturers and users of optical instruments and apparatus of all kinds and to encourage cooperation among them."* It aims to serve the interests of all who are engaged in any branch of optics from fundamental research to the manufacture of optical goods.

MEMBERSHIP

Regular Members: "Any person who has contributed materially to the advancement of optics is eligible for regular membership."

Associate Members: "Any person who is interested in optics is eligible for associate membership."

Corporate Members: "Any corporation desirous of encouraging the work of the Society is eligible for corporation membership."

The Society cordially invites to membership all who are interested in any branch of optics, either in research, in instruction, in optical or illuminating engineering, in the manufacture and distribution of optical goods of all kinds or in physiological and medical optics.

ANNUAL DUES

Regular members, $7.50; Associate members, $5.00; Corporate members, $50.00. These dues include subscription to the Society's official journal, the *Journal of the Optical Society of America.*

MEETINGS

The Society holds two meetings per year: An annual meeting in the autumn and a midwinter meeting jointly with the American Physical Society.

For further information concerning the Optical Society of America address the Secretary, Dr. L. B. Tuckerman, Bureau of Standards, Washington, D. C.

ROCHESTER, NEW YORK SECTION OF THE OPTICAL SOCIETY OF AMERICA

C. C. NITCHIE, *President*
H. E. SEEMANN, *Secretary*

L. A. DUBRIDGE, *Vice President*
H. G. KINGSLAKE, *Treasurer*

Councilors: E. C. FRITTS, R. KINGSLAKE, H. F. KURTZ, T. R. WILKINS, C. J. STAUD (*ex-officio*)

Journal of the
OPTICAL SOCIETY
of AMERICA

VOLUME 26 APRIL, 1936 NUMBER 4

Wave-Length Identification Lists for the Extreme Ultraviolet*

J. C. BOYCE AND H. A. ROBINSON,† *George Eastman Research Laboratory of Physics, Massachusetts Institute of Technology*

(Received February 3, 1936)

Wave-length lists are presented to facilitate identification of lines in the extreme ultraviolet. These lists are based on published results from this and other laboratories and on some unpublished results from this laboratory. One table contains lines likely to be present in gas discharges, another gives the lines arising from the more common constituents of glass, and a third lists the principal line or group of lines of each of the first five spectra of a number of elements, where such line or group of lines is to be found in the extreme ultraviolet. While every effort has been made to select lines on a self-consistent scale of wave-lengths, it is emphasized that these lines should not be used indiscriminately as standards of wave-length.

BECAUSE of the use of vacuum spectrographs, often without any window between the source of light and the interior of the instrument, spectra in the extreme ultraviolet are frequently contaminated by lines due to impurities. The data by which such lines could be identified are scattered through the literature. Some years ago one of the present writers collaborated in the compilation of a list of the extreme ultraviolet lines from gas discharges.[1] The mimeographed edition in which that list was published has now become out of date and a revision seemed in order.

Table I contains the lines of hydrogen, of neutral and ionized helium, and of the several stages of ionization, up to the fifth spectrum when known, of carbon, nitrogen, oxygen, neon, argon, and mercury. These elements were chosen to include those apt to be present by design in most gas discharges as well as those usually encountered as impurities in the various types of light sources used with vacuum spectrographs. In cases of high excitation in discharge tubes made of glass the lines due to boron, sodium and silicon are frequently observed. Table II lists lines up to and including the fifth spectrum of each of these elements.

Doubtful cases of identification may often be tested by the presence or absence of the line or group of lines usually strongest in that stage of ionization of the atom. Where such principal lines lie in the extreme ultraviolet, Table III collects them for the elements included in Tables I and II and also for aluminum, krypton and xenon.

It should be strongly emphasized that lines in the present list should not be used inadvisedly as standards of wave-length, since it groups together the results from a number of laboratories which may not be on a consistent wave-length scale. Where two or more investigators have published

* A limited number of reprints of this article are available for distribution and may be obtained by sending 35 cents in United States postage stamps to the Secretary, Department of Physics, Massachusetts Institute of Technology.

† Irving Langmuir Fellow of the American Scandinavian Foundation, at present at the Physics Institute of the University, Uppsala, Sweden.

[1] J. M. MacInnes and J. C. Boyce, *Extreme Ultraviolet Lines from Gas Discharges* (Princeton, 1930).

BOSTON UNIV...
COLLEGE OF LIBERAL ARTS
LIBRARY

TABLE I. *Extreme ultraviolet lines from gas discharges.*

SPECTRUM	λ	INT.	REFERENCE
Hg II	1995.576	4	G8
C I	1993.65	2	L10
N II	1991.64	–	U6
C II	1988.05	1	L11
Hg II	1987.978	6	G8
Hg II	1981.45	2	M2
C III ?	1979.79	3	L11
C III	1979.35	4	L11
Hg II	1979.00	4	G8
Hg II	1977.94		M2
Hg II	1973.889	8	G8
A III	1973.780	4	T4
A II	1973.48	1	T4
O II	1964.25	0	L6 – C13
O II	1963.84	2	L6 – C13
A III	1962.74	2	T4
O II	1962.24	3	C13
A II	1961.356	2	T4
O II	1960.34	1	C13
Hg II	1958.52	1	G7
A III	1957.83	1	T4
O II	1957.42	0	C13
Hg II	1957.386	1	G8
N III	1953.80	3	L12
N III	1953.66	3	L12
N III	1952.20	1	L12
N III	1951.43	2	L12
N III	1949.81	4	L12
N III	1949.22	6	L12
Hg II	1948.66	2	G8
Hg II	1947.65	2	G7
N III	1946.99	5	L12
Hg II	1942.32	50	G7
A II	1941.062	2	T4
Ne II	1938.82	5+	T1
C III	1931.027	4	C12.5
C I	1930.900	5	T2
Ne II	1930.02	7 –	T1
Ne	1928.83	1	R1
Hg II	1927.64	1	G7
N III	1923.86	2	L12
C III	1923.40	2	U5
C III	1923.22	2+	U5
N III	1923.11	2	L12
C III	1923.01	3	U5
N III	1921.49	4	L12
N III	1920.86	8	L12
N III	1919.99	2	L12
N III	1919.71	2	L12
A III	1919.515	4	T4
N III	1919.44	1	L12
N III	1919.06	0	L12
N III	1918.69	0	L12
A III	1918.667	4	T4
A III	1918.06	1	T4
O III	1916.48	2	L8
Ne II	1916.09	8	T2
A III	1915.564	7	T4
A III	1914.653	3	T4
A III	1914.398	9	T4
A II	1909.58	1	T4
N III	1909.12	1	L12
N III	1908.27	7	L12
Ne II	1907.49	5	T2
N III	1907.44	4	L12
O III	1907.06	1	L8
N III	1907.05	1	L12
N III	1906.38	1	L12
Hg II	1904.755	4	G8
O III	1902.89	1	L8
Hg II	1900.194	2	G8
C III	1894.49	0	U6
Ne	1889.77	1	R1
Ne	1888.15	1	R1
N II	1887.434	4	G12
N III	1885.25	10	L12
Ne	1883.82	1	R1
Ne	1880.21	3	R1
N II	1878.60	2	L7
Hg II	1875.541	3	G7
Hg II	1870.783	0.5	G8
Hg II	1869.242	10	G7
N II	1869.13	1	L7
N II	1868.21	0	L7
Hg II	1868.027	0.5	G8
N II	1864.4	C	L7
N II	1862.57	2	L7
N II	1859.6	C	L7
N II	1859.22	5	L7
N II	1858.47	2	L7
N II	1857.83	3	L7
Ne	1854.11	1	R1
Hg II	1853.329	2	G8
Ne	1853.22	1	R1
N II	1850.0	1	U6
Hg I	1849.68	20R	L17
N III	1845.80	4	L12
N III	1845.64	5	L12
A ?	1843.19	2	G19
N III	1841.68	1	L12
Hg II	1840.592	0.5	G7
N III	1839.59	2	L12
A ?	1839.43	3	G19
N I	1836.739	2	G12
A ?	1836.42	5	G19
N II	1836.36	1	L7
N III	1835.587	6	G12
N II	1831.78	0	L7
N II	1830.71	00	L7
Hg II	1820.727	5	G8
Hg II	1808.289	6	G8
N III	1805.5	7	L12
N III	1804.3	6	L12
Hg II	1803.945	0.5	G8
Hg II	1800.837	0.5	G7
Hg II	1798.736	0.5	G7
Hg II	1796.20	10	G8
Hg II	1793.962	5	G7
Hg II	1792.46	3	G8
Hg II	1783.79	1	G8
Hg II	1780.00	0	M2
C III	1779.12	0	U5
Hg I	1775.20	2n	L17
N II	1766.08	1	L7
N II	1765.216	1	G12
N II	1763.820	2b	G12
C II	1760.818	4	T2
Hg II	1760.445	2u	G7
C II	1760.412	3	T2
Hg II	1756.07	3	G8
C I	1751.9	8	G13
N III	1751.75	10	L12
N III	1751.24	6	L12
N III	1747.86	9	L12
N I	1745.246	2	T2
N II	1743.22	2	L7
N I	1742.734	3	T2
N II	1740.315	0	C12.5
Hg III	1740.24	6	M1
Hg III	1738.49	10	M1
Ne	1732.69	3	R1
Hg II	1731.889	10	G7
N III	1730.04	8	L12
Hg II	1727.17	2	G8
C II	1722.21	0	U5
C II	1721.66	2	U5
C II	1720.99	1	U5
C II	1720.44	0	U5
N IV	1718.52	10	U6
Hg II	1707.13	4	G8
Hg II	1705.518	7	G7
Hg II	1702.58	1	G8
N III	1699.95	4	L12
N III	1699.32	5	L12
N III	1699.00	2	L12
N III	1698.16	2	L12
N III	1697.19	0	L12
N III	1696.54	3	L12
Hg II	1695.18	2	G8
N III	1694.79	0	L12
Hg II	1692.63	3	G8
Ne II	1688.38	4	T1
Ne II	1681.70	3	T1
Hg III	1677.91	10	M1
Hg II	1675.898	8	G8
N II	1675.83	5	L7
A III	1675.637	4	T4
A III	1675.484	7	T4
A III	1673.425	7	T4
A III	1673.241	3	T4
A III	1673.14	1	T4
Hg II	1672.617	10	G8
Hg III	1671.07	7	M1
Hg II	1669.87	1	G8
A III	1669.671	7	T4
A III	1669.304	5	T4
A III	1669.10	1	T4
Hg III	1662.74	6	M1
Hg III	1661.18	0	M1
C I	1658.126	3	T2
C I	1657.916	3	T2
C I	1657.380	2	T2
C I	1657.005	6	T2
C I	1656.280	4	T2
Hg II	1654.78	6	M2
Hg II	1653.69	1	G8
Hg III	1652.48	3	M1
Hg II	1649.959	30	G7
Hg III	1647.49	10	M1
C III	1645.06	1	U5
Hg II	1644.526	1	G7
He II	1640.409	C	G11
Hg II	1635.88	0.5	G8
N II	1629.86	0	L7
N II	1629.02	1	L7
Hg II	1628.247	1	G7
N II	1627.42	1	L7
Hg II	1623.955	5	G7
C III	1620.68	1	U5
C III	1620.59	0	U5
C III	1620.33	2	U5
C III	1620.05	3	U5
Hg II	1619.40	2	G8
Hg II	1617.75	0.5	G8
N II	1616.06	1n	L7
Hg II	1614.13	0.5	G8
Hg II	1613.355	1	G7
Hg II	1605.3	0.5	G8
C I	1602.984	5	G13
Hg II	1601.57	1	G8
Hg III	1599.42	9	M1
Hg III	1592.93	10	M1
Hg II	1591.82	0.5	G8
C III	1591.48	2	U5
N II	1590.25	2n	L7
C III	1577.89	2	U5
C III	1577.32	2+	U5
Hg II	1577.083	1	G7
C III	1576.49	3	U5
A II	1574.985	4	T4
N II	1574.28	1n	L7
N II	1573.21	1n	L7
Hg II	1568.458	1	G8
C I	1561.42	8	T2
C I	1561.292	2	U5
C I	1560.699	5	T2
C I	1560.316	4	T2
A II	1560.188	3	T4
C IV	1550.790	10	T2
C IV	1548.214	12	T2
C I	1542.202	2	G13
Hg II	1541.79	2	G8
Hg II	1540.36	0.5	G8
Hg II	1539.111	1	G7
Hg II	1533.642	3	G8
C III	1531.85	2	U5
Hg II	1530.267	3	G8
Hg III	1527.49	8	M1
Hg II	1511.565	1	G8
C I	1510.924	0.5	G13
Hg II	1495.199	0.5	G8
N I	1494.669	4	T2
N I	1492.630	5	T2
C I	1481.771	7	G13
C III	1478.30	1	U5
C III	1478.05	2	U5
Hg II	1477.770	7	G8
C III	1477.68	3	U5
N III	1472.88	C	L12
N III	1472.30	C	L12
N III	1471.69	2	L12
N III	1471.60	C	L12
N III	1471.02	1	L12
N III	1470.68	0	L12
C I	1470.20	1	L10
C I	1468.5	0	L10
A III	1468.006	2	T4
A III	1467.841	3	T4
C I	1467.450	3	G13
Hg III	1467.38	4	M1
A III	1465.712	3	T4
A III	1465.532	2	T4
C I	1463.33	3	T2
A III	1460.234	2	T4
A III	1460.077	4	T4
Hg II	1459.38	3	M2
C I	1459.054	2	G13
Hg I	1435.50	C	G15
Hg II	1429.97	1	G7
C III	1429.08	0	U5

TABLE I. (*Continued.*)

SPECTRUM	λ	INT.	REFERENCE
C III	1428.95	1	U5
C III	1428.66	0	U5
C III	1428.53	2	U5
C III	1428.17	2+	U5
C III	1427.85	3	U5
C III	1426.78	1	U5
C III	1426.45	4	U5
C III	1426.16	0	U5
Hg II	1417.002	6	G7
Hg III	1414.95	6	W1
Hg II	1414.427	9	G7
N I	1411.937	6	G12
Hg II	1404.484	5	G8
Hg I	1402.72	C	G15
Hg III	1400.53	9	M1
Hg II	1400.406	2	G7
N III	1387.31	4	L12
Hg III	1378.95	8	M1
Hg III	1377.85	8	M1
Hg II	1372.503	1	G7
O V	1371.287	10	U5
C I	1364.140	6	G13
Hg II	1361.307	9	G7
Hg III	1360.49	8	W1
C I	1359.329	2	G13
C I	1359.131	1	G13
O I	1358.507	C	TU
Hg II	1357.321	5	G7
C I	1357.058	3	G13
C I	1355.825	6	G13
O I	1355.596	C	TU
C I	1354.286	0	G12
Hg II	1354.274	0.5	G7
Hg III	1352.94	5	W1
Hg II	1350.251	2	G7
N III	1348.45	C	L12
N III	1347.56	0	L12
N III	1346.70	C	L12
N II	1346.41	0	L7
N III	1346.27	4	L12
N III	1345.69	4	L12
N II	1345.29	1	L7
O IV	1343.507	7	U5
N II	1343.37	2	L7
O IV	1342.995	4	U5
Hg II	1342.829	0.5	G8
O IV	1338.603	6	U5
C II	1335.71	40	T2
C II	1334.54	30	T2
Hg II	1331.759	15	G8
N II ?	1330.816	3	G12
C I	1329.58	6	T2
N II	1329.43	0	L7
C I	1329.101	5	T2
C I	1328.831	4	T2
N I	1327.956	6	G12
N I	1326.610	7	G12
Hg III	1326.40	8	W1
N III	1325.10	C	L12
N III	1324.40	3	L12
C II	1323.94	15	T2
N III	1323.89	C	L12
N III	1323.42	C	L12
N III	1322.90	C	L12
N III	1322.80	C	L12
N III	1322.33	C	L12
N III	1322.17	C	L12
Hg II	1321.733	10	G7
N I	1319.717	8	G12
N I	1319.039	8	G12
N I	1316.318	2	G12
C I	1315.903	4	G13
N I	1315.484	1	G12
C I	1313.471	6	G13
C I	1312.261	2	G13
C I	1311.985	2	G13
C I	1311.374	8	G13
N I	1310.973	8	G12
C I	1310.646	4	G13
N I	1310.566	8	G12
Hg II	1309.074	2	G7
C III	1308.73	2	U5
Hg II	1307.950	9	G7
Hg I	1307.76	C	G15
O I	1306.038	9	T2
Hg III	1305.61	8	W1
O I	1304.864	12	T2
O I	1302.192	12	T2
C III	1296.30	2d	U5
C I	1291.380	1	G13
C I	1289.983	3	G13
C I	1288.633	2	G13
C I	1288.445	5	G13
C I	1288.055	1	G13
C I	1280.892	4	G13
Hg III	1280.83	9	W1
C I	1280.646	2	G13
C I	1280.340	2	T2
C I	1280.154	2	G13
C I	1279.898	5	G13
C I	1279.251	6	G13
C I	1277.766	3	G13
C I	1277.550	4	T2
C I	1277.274	4	T2
C I	1277.154	2	G13
N II	1276.74	0	C13
N II	1276.18	1	C13
N II	1275.06	1	C13
C I	1275.021	5	G13
C I	1274.880	2	G13
C I	1274.131	5	G13
Hg I	1268.82	C	G15
C I	1267.633	1	G13
C I	1266.449	3	G13
C I	1261.560	1	T2
C I	1261.12	1	T2
C I	1260.955	2	T2
C I	1260.745	4	G13
C I	1260.670	2	G13
C I ?	1259.546	3	G13
Hg I	1259.24	C	G15
N II	1258.75	3	L7
C I	1257.218	2	G13
Ne III	1257.190	6	T1
C III	1256.52	1d	U5
Ne III	1255.685	5	T1
Ne III	1255.026	2	T1
C I	1253.880	1.5	G13
C I	1253.538	0.5	G13
Hg I	1250.56	C	G15
C III	1247.387	7	T2
N I	1243.297	3	T2
N I	1243.170	4	T2
N V	1242.778	7	U5
N V	1238.800	8	U5
Hg I	1235.84	C	G15
Hg I	1232.22	C	G15
N I	1231.588	1	G12
C IV	1230.511	3	U5
N I	1230.288	0b	G12
C IV	1230.046	2	U5
N I	1228.767	6	G12
N I	1228.422	4	G12
N I	1227.788	2	G12
N I	1227.226	1	G12
N I	1226.831	1	G12
N I	1225.366	4	G12
N I	1225.033	4	G12
C II	1223.99	1	U5
C II	1223.59	0	U5
Hg I	1222.38	C	G15
Hg I	1220.35	C	G15
O I	1217.645	10	T2
H^1	1215.664	C	G11
H^2	1215.31	C	TU
He II	1215.129	C	G11
Hg I	1213.90	C	G15
Hg I	1212.65	C	G15
Hg I	1208.22	C	G15
Hg I	1207.34	C	G15
A III	1205.95	1	T5
Hg II	1205.195	1	G7
Hg I	1204.24	C	G15
Hg I	1203.60	C	G15
N I	1200.706	4	T2
N I	1200.220	5	T2
N I	1199.547	6	T2
C IV	1198.58	1d	U5
A IV	1197.84	1	T4
C I	1197.812	0.5u	G13
C I	1194.656	5	G13
C I	1194.494	7	G13
C I	1194.291	2	G13
C I	1194.094	5	G13
C I	1194.027	5	G13
C I	1193.738	4	G13
C I	1193.460	3	G13
C I	1193.284	10	G13
C I	1193.005	8	G13
C I	1192.923	2	G13
C I	1192.480	2	G13
C I	1191.855	1	G13
A IV	1190.354	2	T4
C I	1189.660	6	G13
C I	1189.556	4	G13
N I	1189.213	3	G12
C I	1189.074	3	G13
N I	1188.955	4	G12
C I	1188.935	1	G13
A IV	1187.80	1	T4
N III	1184.544	8	U5
N III	1183.030	7	U5
N I	1177.673	5	G12
N I	1176.504	6b	G12
C III	1176.370	10	T2
C III	1175.986	9	T2
C III	1175.716	15	T2
C III	1175.582	5	T2
C III	1175.259	9	T2
C III	1174.934	10	T2
N I	1171.067	0	G12
N I	1170.268	1	G12
N I	1169.679	1	G12
C IV	1168.990	5+	U5
C IV	1168.873	5	U5
N I	1168.475	6u	G12
N I	1167.424	6	G12
C III	1165.87	1d	U5
C III	1165.71	0d	U5
N I	1165.566	2	G12
N I	1164.309	5	G12
N I	1163.850	6	G12
Hg II	1160.403	4	G8
N I	1159.858	1	G12
N I	1159.285	1.5	G12
C I	1159.004	5	G13
C I	1158.729	3	G13
C I	1158.398	2	G13
C I	1158.107	8	G13
C I	1158.017	7	G13
C I	1157.825	3	G13
C I	1157.391	2	G13
C I	1157.333	1	G13
C I	1156.619	5	G13
C I	1156.502	1	G13
C I	1156.059	2	G13
C I	1155.839	1	G13
O III	1153.773	3	U5
O I	1152.139	3	G12
O III	1150.882	2	U5
O III	1149.603	1	U5
C II	1141.745	1	T2
C I	1141.705	1	G13
C II	1141.623	3	T2
C I	1140.688	3	G13
C I	1140.391	1	G13
C I	1140.070	1	G13
C I	1139.894	7	G13
C I	1139.794	6	G13
C II	1139.49	0	U5
C II	1139.343	3	T2
C I	1139.142	2	G13
C I	1139.037	1	G13
C II	1138.936	2	U5
C I	1138.625	1	G13
O III	1138.545	2	U5
C I	1138.506	0.5	G13
N I	1134.980	7	T2
N I	1134.419	5+	T2
N I	1134.171	5	T2
C I	1129.927	1	G13
C I	1129.626	1	G13
Hg III	1129.18	5	W1
C I	1129.161	6	G13
C I	1128.748	1	G13
C I	1128.277	0.5	G13
Hg III	1124.08	3	W1
C I	1123.154	0.5	G13
C I	1122.776	0.5	G13
C I	1122.325	4	G13
C I	1122.179	1	G13
C I	1118.153	0.5	G13
C I	1117.706	3	G13
C I	1114.414	2	G13
C I	1112.051	0.5	G13
C IV	1107.933	4	U5
C IV	1107.600	3	U5
Hg III	1105.53	4	W1
Hg II	1104.253	2	G7
N I	1101.318	3	G12

TABLE I. (*Continued.*)

SPECTRUM	λ	INT.	REFERENCE
N I	1100.360	4	G12
Hg II	1099.337	2	G7
N I	1099.166	2u	G12
N I	1098.277	3	G12
Hg II	1098.1	1	G8
N I	1098.071	3	G12
N I	1097.221	4	G12
N I	1096.738	2	G12
N I	1096.301	2	G12
N I	1095.962	4	G12
C II	1092.740	2	U5
C II	1092.422	0	U5
C II	1092.240	0	U5
C II	1091.930	1	U5
Hg III	1090.07	3	W1
N II	1085.74	10	T2
N II	1085.546	7	T2
He II	1084.940	C	G11
N II	1084.579	9	T2
N II	1083.991	7	T2
N I	1070.935	0u	G12
N I	1069.986	2.5	G12
N I	1069.198	2	G12
N I	1068.539	3	G12
Hg III	1068.04	2	W1
N I	1067.610	1	G12
A I	1066.660	9	T4
C II	1066.138	5	T2
C II	1065.895	7−	T2
C II	1063.30	0d	U5
Hg II	1062.803	4	G8
A I	1048.218	8	T4
O I	1041.688	C	TU
O I	1040.943	C	TU
Hg II	1039.695	2	G8
O I	1039.233	C	TU
A IV	1037.931	1	T4
O VI	1037.613	9	U6
C II	1037.020	10	T2
C II	1036.332	9	T2
O VI	1031.912	10	U6
O I	1028.166	C	TU
O I	1027.441	C	TU
O I	1025.775	C	TU
H¹	1025.717	C	G11
H²	1025.42	C	TU
He II	1025.270	C	G11
C II	1010.374	7	T2
C II	1010.092	5+	T2
C II	1009.862	5	T2
N III	1006.015	6	U5
A III	1002.095	3−	T5
O I	999.494	6	T2
He II	992.361	C	G11
N III	991.579	17	U5
N III	991.514	14	U5
O I	990.797	4	T2
O I	990.213	8	T2
O I	990.121	3	T2
N III	989.804	7	T2
O I	988.775	8	T2
O I	988.64	3	T2
N III	979.919	9	U5
N III	979.842	8	U5
O I	978.618	C	TU
O I	977.961	C	TU
C III	977.020	30	T2
O I	976.451	C	TU
O I	973.684	C	TU
O I	973.244	C	TU
H¹	972.532	C	G11
H²	972.25	C	TU
He II	972.109	C	G11
O I	971.747	C	TU
Hg II	969.130	4	G8
C II	968.16	0	U5
N I	965.097	2C	TU
N I	964.632	3C	TU
N I	963.993	4C	TU
Hg II	962.740	4	G7
He II	958.696	C	G11
N IV	955.335	10	U5
N I	953.635	C	TU
N I	953.399	C	TU
O I	952.947	C	TU
N I	952.789	C	TU
O I	952.323	C	TU
N I	952.298	C	TU
O I	950.891	C	TU
O I	950.739	C	TU
O I	950.120	C	TU
H	949.739	C	G11
He II	949.326	C	G11
C IV	948.214	1	U5
O I	948.694	C	TU
C IV	948.098	2	U5
C II	946.208	2	U5
C II	945.981	1	U5
C I	945.566	3	T2
C I	945.336	2	T2
C I	945.193	1	T2
Hg II	942.630	2	G7
Hg II	940.793	6	G7
O I	939.240	C	TU
O I	938.631	C	TU
O I	938.026	C	TU
Hg II	938.0	2	G8
O I	937.848	C	TU
H	937.799	C	G11
O I	936.636	C	TU
O I	935.183	4	T2
A II	932.046	10	T4
O I	931.634	C	TU
O I	930.893	C	TU
O I	930.263	C	TU
O I	929.525	C	TU
O I	926.845	C	TU
O I	925.438	C	TU
N IV	924.274	10+	U5
N IV	923.669	10	U5
Hg II	923.393	4	G7
O IV	923.353	6	U5
N IV	923.211	12	U5
N IV	923.045	10−	U5
N IV	922.507	10	U5
O I	922.02	—	C25
N IV	921.982	10+	U5
O IV	921.364	5	U5
O IV	921.301	4	U5
A II	919.78	15	T4
N II	916.708	8	T2
N II	916.01	6	T2
N II	915.96	5	T2
Hg II	915.827	7	G7
N II	915.612	5	T2
N I	910.648	0C	TU
N I	910.281	1C	TU
N I	909.700	2C	TU
N I	907.278	C	TU
N I	906.833	C	TU
N I	906.732	C	TU
N I	906.428	3dC	TU
N I	906.212	3dC	TU
N I	905.788	3dC	TU
C II	904.482	8	T2
C II	904.144	8+	T2
C II	903.952	8−	T2
C II	903.614	8	T2
A IV	901.804	2	T4
A IV	901.168	9	T4
A IV	900.362	5	T4
O III	898.956	2	T2
A I	894.310	C	T4
Hg II	893.107	10	G7
N I	888.381	C	TU
N I	888.028	C	TU
N I	887.461	0	TU
A III	887.404	10	T4
N I	886.344	C	TU
N I	885.960	0.5C	TU
N I	885.658	1C	TU
C III	884.516	8	U5
A III	883.179	9	T4
O I	882.88	—	C25
A I	879.949	C	T4
A III	879.622	8	T4
O I	879.520	1−	U5
O I	879.077	1	U5
O I	878.957	1−	U5
A III	878.728	12	T4
O I	877.863	2	U5
O I	877.778	1	U5
A I	876.063	C	T4
N I	875.764	0C	TU
A III	875.534	9	T4
N I	875.101	0.5C	TU
N III	871.850	0	U5
A III	871.099	10	T4
A I	869.754	C	T4
A I	866.805	C	T4
O I	861.63	—	C25
C II	858.559	6	T2
N II	858.357	1	U5
C II	858.091	5	T2
O I	850.74	—	C25
A IV	850.602	25	T4
A IV	843.772	20	T4
Hg III	843.06	8	W1
A I	842.808	C	T4
A IV	840.029	15	T4
A V	836.13	2	T4
A V	835.79	1	T4
O III	835.293	7	T2
O III	835.10	5	T2
A I	835.003	C	T4
A V	834.88	4bl	T4
O II	834.467	20	T2
A I	834.397	C	T4
O III	833.749	11	T2
O II	833.332	12	T2
O III	832.93	5	T2
O II	832.762	8	T2
A V	827.350	3	T4
A V	827.052	5	T4
A I	826.371	C	T4
A I	825.348	C	T4
A V	822.161	4	T4
A I	820.129	C	T4
A I	816.466	C	T4
A I	816.233	C	T4
O I	812.09	3	C25
O I	811.69	1	C25
O I	811.43	1	C25
O I	811.02	4	C25
O I	810.62	1	C25
A I	809.933	C	T4
C II	809.770	3+	U5
C II	809.682	4	U5
A I	807.702	C	T4
A I	807.220	C	T4
C II	806.846	6	U5
A I	806.875	C	T4
C II	806.684	4	U5
C II	806.555	7	U5
C II	806.384	5	U5
O IV	802.250	5	U5
O IV	802.198	6	U5
A IV	801.913	5	T4
A I	801.359	C	TU
A IV	801.409	10	T4
A IV	801.086	10	T4
A IV	800.573	5	T4
C II	799.947	4	U5
C II	799.664	4+	U5
A I	799.137	C	TU
A I	797.744	C	TU
O II	796.661	10	U5
C II	795.134	1	U5
C II	794.964	0	U5
O I	792.92	3	C25
O I	792.50	1	C25
O I	792.20	1	C25
O I	791.93	3	C25
O I	791.48	1	C25
O IV	790.203	16	U5
Hg III	790.15	8O	W1
O IV	790.103	13	U5
O IV	787.710	15	U5
N? O?	786.474	3−3	U5−U5
C III	784.393	3	U5
O IV	779.905	10	U5
O IV	779.821	9	U5
N II	775.957	12	U5
O V	774.522	7	U5
N III	772.975	8	U5
N III	772.891	9	U5
N III	772.385	12	U5
N III	771.901	11	U5
N III	771.544	10	U5
O I	770.70	0	C25
C IV	770.379	0d	U5
O I	770.28	1	C25
O I	769.39	2	C25
A III	769.152	12	T4
N IV	765.140	17	U5
N III	764.357	15	U5
N III	763.340	14	U5
A II	762.192	2	T4
O V	762.001	10+	U5
A IV	761.470	5	T4

TABLE I. (*Continued.*)

SPECTRUM	λ	INT.	REFERENCE
O V	761.130	10	U5
O V	760.445	12	U5
A IV	760.439	3	T4
O V	760.229	10−	U5
O V	759.440	10	U5
O V	758.677	10+	U5
O I	756.7	1	C25
O I	755.8	2	C25
A IV	755.212	3	T4
A II	754.817	3	T4
A IV	754.205	4	T4
O III	752.762	4	U5
O II ?	750.226	2	U5
O II ?	749.622	1	U5
O I	749.3	1	C25
O I	748.4	1	C25
A II	748.193	4	T4
N II	746.976	8	U5
N II	745.836	6	U5
A II	745.318	5	T4
A II	744.920	5	T4
Ne I	743.70	12	T1
O II	741.293	00	U8
O II	740.838	0	U8
Hg III	740.69	6	W1
A II	740.263	12	T4
O II	739.949	1	U8
A II	737.442	1	T4
Ne I	735.89	30	T1
A II	730.929	8	T4
A II	725.542	9	T4
A II	723.353	14	T4
O II	718.562	16	U5
O II	718.484	17	U5
A II	718.083	4	T4
A V	715.65	3	T4
A V	715.60	4	T4
C III	714.879	1	U5
A V	709.197	5	T4
O III	707.315	4	U5
O III	706.298	2	U5
O III	706.224	3	U5
O III	705.762	2	U5
A V	705.352	3	T4
A II	704.516	3	T4
O III	703.850	18	U5
O III	702.899	17	U5
O III	702.822	16	U5
O III	702.332	16	U5
A IV	700.277	8	T4
A III	699.72	1−	T5
A IV	699.408	6	T4
A II	698.760	4	T4
A II	697.944	1	T4
A III	697.74	2	T4
A II	697.484	2	T4
A III	695.537	6	T4
A II	693.295	2	T4
N III	691.388	1	U5
A II	691.030	1	T4
N III	691.187	2	U5
C III	690.526	7	U5
A III	690.170	8d	T4
A IV	689.007	12bl	T4
A IV	688.392	7	T4
C II	687.355	11	U5
C II	687.059	10	U5
A II	686.50	1	T4
C II	686.480	2d	U5
N III	686.335	14	U5
N III	685.816	16	U5
N III	685.513	15	U5
N III	684.996	14	U5
A IV	683.278	10	T4
A II	679.410	8	T4
A III	676.241	6	T4
O II	673.768	7	U5
O II	672.948	8	U5
A II	672.849	3	T4
A II	671.854	10	T4
N II	671.999	6+	U5
N II	671.770	6	U5
N II	671.629	6−	U5
N II	671.391	8	U5
A II	670.947	10	T4
N II	671.014	6+	U5
N II	670.881	1	U5
N II	670.508	1+	U5
N II	670.289	2+	U5
A II	666.014	10	T4
A II	664.558	6	T4
O ?	663.139	2	U5
A II	661.868	15	T4
O ?	661.397	3	U5
N II	660.280	9	U5
O III	659.538	0	U8
O III	658.758	1	U8
(N II)	657.327	1	U5
C II	651.342	8	U5
C II	651.262	7	U5
C II	651.216	7−	U5
N II	645.167	10	U5
N II	644.825	9	U5
N II	644.621	8	U5
O II	644.148	12	U5
A III	643.256	9	T4
C II	641.875	6+	U5
A III	641.808	12	T4
C II	641.772	6	U5
C II	641.591	6	U5
A III	641.364	5	T4
A III	637.282	20bl	T4
A III	636.818	3	T4
C II	636.247	4	U5
C II	635.988	3	U5
N II	635.180	5	U5
O V	629.732	15	U5
Ne I	629.729	6	T1
N II	629.434	2	U5
N II	629.161	3	U5
Ne I	626.819	6+	T1
O IV	625.852	14+	U5
O IV	625.130	14	U5
O IV	624.617	13	U5
A III	623.767	5	T5
C III	622.144	2	U5
Ne I	619.092	4	T1
Ne I	618.668	5	T1
O II	617.051	6	U5
O IV	617.033	7	U5
O IV	616.933	8	U5
O II	616.363	4	U5
O II	616.291	7	U5
Ne I	615.623	5−	T1
O III	610.850	6−	U5
O III	610.746	8	U5
O III	610.043	7+	U5
O IV	609.829	15	U5
O III	609.705	6	U5
C III	609.275	6	U5
C III	609.025	4	U5
O IV	608.395	14	U5
A III	604.152	10	T4
A II	602.854	4	T4
Ne I	602.712	4−	T1
N III	601.878	0	U5
N III	601.468	1	U5
He I	601.418	5	G10
O II	600.585	6	U5
C II	600.532	2	U5
C II	600.369	3	U5
C II	600.265	1	U5
Ne I	600.04	2	T1
He B	600.019	−	G10
O III	599.598	18	U5
Ne I	598.86	1	T1
Ne I	598.698	2+	T1
A II	597.695	5	T4
O III	597.818	15	U5
Ne I	595.911	3	T1
C II	595.032	7d	U5
C II	594.808	6d	U5
Ne I	591.82	2	T1
He I	591.406	13	B5
Ne I	589.92	1	T1
Ne I	589.16	1	T1
Ne I	587.20	1	T1
C III	585.666	6	U5
C III	585.608	6−	U5
C III	585.496	5+	U5
C III	585.417	8b	U5
C III	585.261	6	U5
He I	584.331	10	TU
A II	583.437	8	T4
N II	582.150	5	U5
O II	580.967	7	U5
A II	580.261	8	T4
O II	580.400	6	U5
A III	579.212	3	T5
A II	578.605	4	T4
A III	578.386	4	T5
A II	578.107	4	T4
A III	577.153	3	T4
C II	577.108	2	U5
A II	576.731	5	T4
C II	576.900	1	U5
N II	574.650	6	U5
C III	574.279	12	U5
O III	574.065	00	U8
A III	573.468	4	T4
A II	573.360	6	T4
A II	572.015	5	T4
C III	566.490	4	U5
C III	565.530	7	U5
C II	564.645	5bd	U5
C II	562.577	3+	U5
C II	562.498	3	U5
C II	562.355	3	U5
C II	560.443	5d	U5
A II	560.224	7	T4
C II	560.244	4d	U5
N II	559.760	0	U5
A III	558.321	5	T4
A III	556.893	6	T4
A II	556.813	6	T4
O IV	555.262	16	U5
O II	555.121	5	U5
O II	555.056	5+	U5
C III	554.655	2	U5
O IV	554.514	18	U5
O III	554.275	0	U8
O IV	554.074	17	U5
A III	553.470	9	T4
O IV	553.328	16	U5
A II	553.122	1	T4
C II	551.894	0	U5
A II	550.899	1	T4
A II	550.475	2	T4
C II	549.568	3	U5
C II	549.507	5	U5
C II	549.375	4	U5
C II	549.317	3	U5
A II	548.779	4	T4
A II	547.983	1	T4
N II	547.813	0	U5
A II	547.460	4	T4
C II	547.288	0	U5
C II	547.169	0+	U5
A II	547.164	3	T4
A II	546.176	4	T4
A II	543.727	3	T4
Ne IV	543.884	7	T1
C II	543.475	3d	U5
A II	543.201	4	T4
C II	543.291	2d	U5
A II	542.910	3	T4
Ne IV	542.076	6	T1
A II	541.304	1	T4
Ne IV	541.124	5	T1
O II	539.853	7	U5
O II	539.547	8	U5
O II	539.086	8+	U5
A III	538.788	6	T4
O II	538.318	7	U5
C III	538.312	13	U5
C III	538.150	12	U5
O II	538.256	10	U5
C III	538.075	11−	U5
O II	537.830	9	U5
A III	537.459	6	T4
A II	537.13	3	T4
He I	537.024	3	TU
A III	536.745	8	T4
A III	535.580	7	T4
C III	535.288	10s	U5
A II	535.035	1	T4
A III	534.26	1	T4
C II	533.935	1db	U5
N II	533.809	4−	U5
N II	533.726	6	U5
N II	533.644	4−	U5
N II	533.577	5	U5
N II	533.504	4	U5
C II	532.716	3d	U5
A III	532.413	7	T4
C II	531.917	1d	U5
C II	531.775	0d	U5
A II	530.489	4	T4
C II	530.386	4d	U5
C II	530.290	3d	U5

TABLE I. (*Continued.*)

SPECTRUM	λ	INT.	REFERENCE
N III	530.268	3	U5
N III	530.037	2	U5
A III	529.900	9	T4
N II	529.860	5	U5
N II	529.713	3+	U5
N II	529.627	3+	U5
N II	529.481	3−	U5
N II	529.405	3	U5
N II	529.343	3	U5
A II	528.640	2	T4
(O III)	528.283	0	U5
A II	526.495	3	T4
O III	525.795	18	U5
A II	524.678	4	T4
A II	522.791	4	T4
He I	522.208	C	TU
Ne IV	521.810	2−	T1
Ne IV	521.730	2−	T1
O VI	519.723	2+d	U5
O VI	519.610	2d	U5
A II	519.326	6	T4
A II	518.89	2	T4
O II	518.242	5	U5
O II	517.937	4	U5
C II	517.069	1db	U5
C II	516.652	0d	U5
He I	515.612	C	TU
O II	515.640	4	U5
O II	515.498	5	U5
A II	514.301	2	T4
N II	513.845	2	U5
A III	512.769	7	T4
He I	512.094	C	TU
A III	511.565	7	T4
A III	511.497	8	T4
C III	511.527	10	U5
N II	510.757	3	U5
A II	510.550	3	T4
He I	509.993	C	TU
N III	509.897	4	U5
N III	509.586	5	U5
N II	509.018	0+	U5
N II	508.903	0	U5
He I	508.639	C	TU
N II	508.700	2	U5
A III	508.655	2	T4
A III	508.595	4	T4
N II	508.459	0+	U5
A III	508.434	9	T4
O III	508.182	18	U5
He I	507.712	C	TU
O III	507.683	17	U5
O III	507.391	16	U5
He I	507.053	C	TU
C III	506.658	0	U5
He I	506.566	C	TU
N II	506.160	3	U5
N II	506.057	2	U5
N II	505.985	1	U5
A II	505.007	1	T4
A II	504.80	1	T4
A II	503.642	2	T4
A II	502.164	2	T4
A II	502.01	1	T4
A II	501.40	1	T4
A II	501.185	2	T4
A II	500.800	1	T4
O II	500.343	1	U5
A II	499.92	1	T4
O II	499.871	2	U5
C III	499.583	7−	U5
C III	499.530	9	U5
C III	499.462	8	U5
C III	499.425	7	U5
O VI	498.431	1d	U5
O VI	498.090	0d	U5
C III	497.910	1s	U5
C III	493.587	7	U5
C III	493.519	5+	U5
C III	493.464	5+	U5
C III	493.396	5−	U5
C III	493.364	5	U5
C III	493.341	5	U5
C III	492.649	7	U5
A III	492.228	3	T4
O III	491.980	1	U5
O III	491.714	0	U5
A III	491.121	4	T4
Ne III	491.050	9	T1
(O III)	491.000	0	U5
A III	490.68	3	T4
Ne III	490.310	7	T1
Ne III	489.641	4	T1
Ne III	489.501	10	T1
A II	489.191	3	T4
A II	488.95	1	T4
Ne III	488.868	7	T1
A II	488.786	3	T4
A III	488.452	7	T4
Ne III	488.103	8−	T1
A III	487.988	7	T4
A II	487.227	2	T4
A III	487.025	7	T4
N II	485.857	0	U5
O II	485.631	4	U5
O II	485.572	1	U5
A III−O II	485.515	4−5	T4−U5
O II	485.465	0	U5
A III	485.150	6	T4
O II	485.086	6	U5
A III	484.445	5	T4
A III	484.116	5	T4
O II	484.025	2	U5
O II	483.976	5	U5
O II	483.752	4	U5
C III	483.733	5	U5
C III	483.618	4	U5
C III	483.567	3−	U5
A III	482.548	8	T4
A III	481.848	6	T4
O II	481.755	3	U5
O II	481.704	1	U5
O II	481.635	0	U5
O II, O III	481.587	4	U5
O III	481.381	2	U5
O III	481.354	3	U5
O III	480.955	4	U5
C III	477.625	3	U5
A III	476.432	7	T4
N II	475.876	1−	U5
N II	475.800	3	U5
N II	475.697	2	U5
N II	475.638	1	U5
N II	474.883	2	U5
N II	474.766	0+	U5
N II	474.686	0+	U5
N II	474.601	0−	U5
N II	474.540	0	U5
N II	474.493	0	U5
A III	473.918	6	T4
A III	473.025	6	T4
N III	472.392	5	U5
N III	472.232	4	U5
O IV	471.603	0	U5
O IV	471.273	1	U5
O II	470.408	4	U5
A III	469.968	4	T4
Ne IV	469.865	3−	T1
A III	469.831	4	T4
Ne IV	469.817	2	T1
A III	468.956	3	T4
C III	468.931	0	U5
O II	468.776	2	U5
A III	468.467	4	T4
O II	467.926	0	U5
A III	467.390	6	T4
C II	466.536	0	U5
A III	466.530	5	T4
C II	466.492	2	U5
C II	466.404	1	U5
C II	466.358	0	U5
O II	465.760	2	U5
O II	465.529	1	U5
O II	464.785	3	U5
O II	464.310	1	U5
O II	464.194	2	U5
N IV	463.743	3	U5
Ne II	462.388	14	T1
C II	461.12	1dd	U5
Ne II	460.725	15	T1
C III	460.050	8s	U5
(O III)?	459.896	1	U5
C III	459.633	15	U5
C III	459.521	14	U5
C III	459.462	13−	U5
O II	458.422	0	U5
O II	456.997	1	U5
Ne II	456.895	5−	T1
Ne II	456.344	4	T1
N III	456.078	1	U5
Ne II	455.270	7	T1
Ne II	454.648	5+	T1
N II	453.340	1	U5
N II	453.257	0+	U5
N III	452.226	11	U5
N III	451.869	10	U5
C III	450.732	9	U5
O VI	447.840	0−	U5
Ne II	447.813	8	T1
O VI	447.712	0	U5
Ne II	446.591	7	T1
Ne II	446.252	8	T1
O II	445.638	4	U5
O II	445.601	4+	U5
Ne II	445.032	7+	T1
O II	443.681	0	U5
O IV	442.873	0	U5
O IV	442.705	1	U5
O II	442.048	4	U5
O II	442.001	4+	U5
O II	440.598	2	U5
O II	440.552	3	U5
C II	438.910	1d	U5
O II	437.683	3	U5
O II	437.332	3+	U5
C II	437.102	1d	U5
O II	436.649	0	U5
O II	436.510	1	U5
O III	434.975	10	U5
O III	434.840	2	U5
O III	434.646	3	U5
N III	434.280	6	U5
O III	434.256	4	U5
N III	434.246	6−	U5
N III	434.129	5	U5
N III	434.066	7	U5
N III	434.014	6−	U5
N III	433.911	6	U5
C III	433.337	8	U5
O II	430.177	6+	U5
O II	430.041	6	U5
O II	429.918	5	U5
O II	429.716	4	U5
O II	429.647	5	U5
O II	429.557	2	U5
N III	428.244	5	U5
N III	428.180	6	U5
Ne III	427.840	3+	T1
O II	426.526	1d	U5
C II	425.326	0b	U5
O II	425.273	0	U5
O II	424.577	0	U5
Ne IV	421.584	2	T1
N IV	420.758	1	U5
C IV	419.714	14	U5
C IV	419.525	13	U5
N III	418.910	6	U5
O II ?	418.812	0	U5
N III	418.705	7	U5
C III	418.609	2d	U5
O II	418.598	1	U5
C III	416.769	5	U5
C	414.592	0d	U5
N III	413.797	0	U5
N III	413.681	0−	U5
C III	411.958	3	U5
C III	411.697	0	U5
C III	409.325	6	U5
C III	409.204	0	U5
Ne II	407.136	8	T1
Ne II	405.852	9	T1
O II	403.372	0	U5
O II	403.273	0	U5
O II	403.087	0	U5
O II	403.035	0	U5
C III	399.688	6+d	U5
C III	399.637	6d	U5
A IV	399.634	3	T4
N III	399.084	1	U5
N III	399.045	4	U5
N III	398.885	3	U5
A III	398.86	1	T4
C III	398.551	1d	U5
A IV	398.546	4	T4
C III	398.168	1d	U5
A III	397.67	1	T4
O III	397.310	0	U5
O III	397.231	1	U5
O III	397.120	2	U5
A IV	396.869	4	T4

TABLE I. (*Continued.*)

SPECTRUM	λ	INT.	REFERENCE	SPECTRUM	λ	INT.	REFERENCE	SPECTRUM	λ	INT.	REFERENCE
A III	396.38	4	T4	Ne II	355.848	1	T1	N III	314.715	8	U5
A III	395.92	1	T4	Ne II	355.647	3	T1	C III	314.395	1dd	U5
O III	395.558	12	U5	O III	355.469	5	U5	Ne III	313.92	1	T1
O II	392.322	3	U5	Ne II	355.450	2	T1	Ne III	313.677	3	T1
O II	392.002	3	U5	O III	355.333	5+	U5	Ne III	313.048	4	T1
O II	391.943	2	U5	O III	355.293	3−	U5	C IV	312.455	14	U5
O II	391.912	1	U5	O III	355.137	6	U5	C IV	312.418	15	U5
(O III)	390.832	0d	U5	Ne II	354.954	4	T1	O IV	311.726	3	U5
(O III)	390.726	0+d	U5	Ne II	353.922	2+	T1	O IV	311.679	6	U5
C III	390.055	3	U5	Ne II	353.206	3	T1	N III	311.628	3	U5
C III	389.090	7	U5	C III	353.000	3d	U5	N III	311.539	2	U5
C III	389.005	6	U5	Ne II	352.946	4	T1	O IV	311.490	5	U5
C III	388.965	5−	U5	Ne II	352.237	2+	T1	C III	311.157	0dd	U5
Ne IV	388.23	1−	T1	N IV	352.058	4	U5	C III	310.171	7	U5
O III	387.639	4	U5	N III	351.979	1	U5	Ne III	308.559	1	T1
O III	387.482	3	U5	N IV	351.931	5	U5	O III	308.306	2	U5
O III	387.398	2	U5	C III	350.330	2db	U5	O III	308.051	1	U5
N IV	387.353	4	U5	C III	350.132	0dd	U5	C IV	307.806	1s	U5
Ne IV	387.13	0+	T1	O III	349.961	1	U5	O IV	306.882	7	U5
C III	386.203	14	U5	O III	349.918	2	U5	O IV	306.621	8	U5
C IV	384.178	17	U5	O III	349.825	3	U5	N III	305.918	1	U5
C IV	384.032	16	U5	N III	348.800	0d	U5	O III	305.879	4	U5
O IV	379.919	3	U5	N III	348.690	0d	U5	O III	305.836	8−	U5
O IV	379.775	4	U5	C III	347.854	3	U5	O III	305.769	10	U5
O III	379.631	2	U5	C III	347.777	3−	U5	O III	305.703	8−	U5
O III	379.575	3	U5	O IV	346.688	3	U5	O III	305.656	9	U5
O III	379.505	4	U5	O IV	346.372	4	U5	O III	305.596	8	U5
Ne III	379.308	7	T1	O III	345.309	10	U5	N III	304.912	3	U5
C III	379.254	0d	U5	N IV	345.201	3	U5	N III	304.874	4	U5
C III	379.065	1	U5	N IV	345.107	3−	U5	N III	304.818	4d	U5
O II	377.045	0	U5	N IV	345.063	5	U5	N III	304.032	2+	U5
O II	376.745	0	U5	N IV	345.023	3	U5	N III	303.981	2	U5
O II	376.693	0	U5	N IV	344.915	3+	U5	N III	303.891	2	U5
N III	374.441	12	U5	O V	341.391	0	U5	O III	303.799	9	U5
O III	374.436	8+	U5	C III	341.242	7	U5	He II	303.779	50C	G11
O III	374.331	8	U5	C III	341.179	6	U5	O III	303.693	7+	U5
N III	374.204	11	U5	C III	341.143	5−	U5	O III	303.621	7+	U5
O III	374.165	8−	U5	C III	339.773	1s	U5	O III	303.515	7−	U5
O III	374.075	10	U5	O IV	339.436	0	U5	O III	303.460	7	U5
O III	374.005	8	U5	O IV	339.330	1	U5	C III	303.468	1	U5
O III	373.805	8+	U5	N III	338.345	2	U5	C III	303.432	4d	U5
C III	371.784	8	U5	N IV	335.050	11	U5	O III	303.411	7	U5
C III	371.747	10+	U5	N III	332.327	3	U5	N IV	303.163	4−	U5
C III	371.694	10	U5	N III	332.133	2	U5	N IV	303.123	6	U5
C III	370.951	0d	U5	Ne II	331.50	2	T1	N IV	303.079	4−	U5
C III	369.472	2	U5	Ne II	331.06	1	T1	N IV	303.048	5	U5
C III	369.415	5	U5	Ne II	330.77	3	T1	N IV	303.009	4	U5
O IV	367.192	2	U5	C III	330.687	1+	U5	C III	301.279	1	U5
C III	366.169	4d	U5	C III	330.637	1	U5	C III	301.243	3	U5
C III	365.778	1dd	U5	Ne II	330.62	2+	T1	C III	301.206	2	U5
O III	364.940	1	U5	Ne II	330.20	2	T1	Ne III	301.124	4	T1
O III	364.867	2	U5	O III	328.742	9	U5	O III	300.455	3dd	U5
O III	364.739	3	U5	O III	328.448	10	U5	N IV	300.316	3	U5
C III	363.864	6	U5	Ne II	328.08	2+	T1	O IV	299.850	4	U5
C III	363.790	5	U5	C III	327.784	1s	U5	N III	299.820	1	U5
C III	363.761	4	U5	Ne II	327.63	2	T1	O IV	299.710	2	U5
N III	362.985	6	U5	O IV	327.519	0	U5	N III	299.670	0	U5
N III	362.946	8	U5	Ne II	327.33	3	T1	O IV	299.620	2	U5
N III	362.881	8−	U5	O IV	327.320	1	U5	O IV	299.495	3	U5
N III	362.833	7	U5	Ne II	327.25	2	T1	O III	299.275	2dd	U5
Ne II	362.456	4	T1	C III	327.176	4+d	U5	N IV	297.815	5	U5
Ne II	361.427	5	T1	C III	327.112	4d	U5	N IV	297.768	3	U5
C III	360.675	5	U5	Ne II	326.77	3	T1	N IV	297.712	3	U5
C III	360.623	7	U5	Ne II	326.54	5	T1	N IV	297.644	4b	U5
C III	360.557	6	U5	C III	325.570	1d	U5	N IV	297.595	3	U5
(O III)	359.616	1	U5	Ne II	324.56	2	T1	C IV	296.951	7	U5
(O III)	359.462	0	U5	N III	323.671	4	U5	C IV	296.857	6	U5
O III	359.384	7	U5	N III	323.615	6	U5	O III	296.270	1dd	U5
O III	359.223	8−	U5	N III	323.488	5	U5	O III	296.012	4	U5
O III	359.016	8	U5	N III	323.431	4	U5	O III	295.944	3	U5
C III	358.740	4s	U5	N IV	323.175	7	U5	O IV	295.874	2	U5
Ne IV	358.70	2−	T1	N IV	322.724	9	U5	O III	295.716	6+	U5
N III	358.578	6	U5	C III	322.575	8	U5	O III	295.657	6	U5
N III	358.509	5	U5	N IV	322.570	8	U5	O III	295.619	5	U5
N III	358.469	5	U5	N IV	322.503	7	U5	O III	295.511	3	U5
N III	358.401	3	U5	O IV	321.457	1	U5	O IV	295.140	1−	U5
N III	358.356	5−	U5	C III	321.372	0dd	U5	O IV	295.051	1	U5
N III	358.327	5−	U5	N III	321.270	1d	U5	O IV	294.853	1	U5
N III	358.278	3−	U5	N III	321.161	2	U5	O IV	294.650	1+	U5
Ne II	357.534	5	T1	N III	321.071	1	U5	N III	292.595	4	U5
He I	357.507	2	G10	O III	320.979	12	U5	N III	292.447	3	U5
Ne II	356.795	5d	T1	O III	320.720	2dd	U5	C III	291.330	5	U5
O III	356.768	0	U5	He I	320.392	8	G10	O IV	291.203	1+	U5
O III	356.725	2	U5	O III	319.996	3	U5	O IV	291.054	1	U5
O III	356.625	1	U5	C III	319.266	3dd	U5	O IV	289.933	1	U5
O III	356.558	0	U5	O III	317.265	1dd	U5	O IV	289.898	2	U5
Ne II	356.534	3	T1	O III	316.967	3	U5	O IV	289.590	1	U5
Ne II	356.436	2	T1	N IV	315.053	8	U5	O IV	289.469	2	U5
Ne II	356.131	4−	T1	N III	314.877	6	U5	O IV	289.292	3	U5
Ne II	355.946	2	T1	N III	314.850	9	U5	C IV	289.230	10	U5

TABLE I. (*Continued.*)

SPECTRUM	λ	INT.	REFERENCE
C IV	289.143	9	U5
C	289.048	3?	U5
C III	288.415	0	U5
O V	286.448	6	U5
O III	286.038	0	U5
O IV	285.838	7	U5
O IV	285.714	6	U5
N IV	285.563	5	U5
N III	284.346	2	U5
N III	284.296	1+	U5
Ne III	283.894	3	G20
Ne III	283.690	5u	G20
N IV	283.579	12	U5
N IV	283.470	11	U5
N IV	283.420	10	U5
Ne III	283.206	6	G20
Ne III	283.178	3u	G20
Ne III	282.50	0+	T1
O IV–N III	282.213	1–2d	U5
N III	282.093	1d	U5
C III	281.390	2	U5
C III	280.522	2d	U5
O III	280.483	1+	U5
O III	280.412	1	U5
O III	280.328	1–	U5
O III	280.265	3	U5
O III	280.234	1	U5
O III	280.116	1+	U5
C III	280.043	3	U5
O III	280.030	2	U5
O IV	279.937	11	U5
O III	279.787	3	U5
O IV	279.633	10	U5
O IV	279.456	2	U8
O III	277.514	1	U5
O III	277.385	7	U5
O III	275.513	4	U5
O III	275.366	3	U5
O III	275.281	2	U5
C III	274.051	2d	U5
O IV	272.311	6	U5
O IV	272.270	6–	U5
O IV	272.174	5	U5
O IV	272.125	7	U5
O IV	272.076	6–	U5
O IV	271.989	6	U5
O III	271.611	0	U5
O III	271.523	1–	U5
O III	271.403	1	U5
C III	271.014	1d	U5
N IV	270.995	6	U5
O V	270.982	0	U5
C III	270.583	1d	U5
C III	270.324	0+d	U5
O IV	269.559	1d	U8
O III	268.451	1d	U5
N III	267.952	1	U5
N III	267.851	0	U5
Ne III	267.709	2	G20
Ne III	267.516	3u	G20
O III	267.121	4	U5
O III	267.050	3	U5
O III	267.030	7	U5
Ne III	267.059	3u	G20
O III	266.985	7	U5
O IV, III	266.967	6	U5
O IV	266.932	6	U5
O IV	266.729	0–	U5
O IV	266.690	0	U5
N V	266.375	7	U5
N V	266.192	6	U5
O V	265.550	4	U5
C III	265.287	0d	U5
O IV	265.062	0	U5
C III	265.029	0d	U5
N III	264.948	2	U5
N III	264.837	1	U5
O III	264.480	6	U5
O III	264.338	5d	U5
O III	264.257	4	U5
O III	263.903	0	U5
O III	263.861	3–	U5
O III	263.818	5	U5
O III	263.768	3–	U5
O III	263.728	4	U5
O III	263.692	3	U5
O III	262.882	1	U5
O III	262.729	0	U5
C IV	262.627	4	U5
C IV	262.553	3	U5
O III	262.289	0	U5
O III	262.113	2	U5
O III	261.027	4d	U5
O IV	260.556	9	U5
N IV	260.455	2	U5
O IV	260.389	10	U5
C IV	259.542	7	U5
C IV	259.471	6	U5
O IV	258.207	3	U5
O IV	258.116	2	U5
O III	256.506	3+	U5
O III	256.460	3	U5
O III	256.425	2	U5
He II	256.315	30C	G10
O IV	255.302	0	U8
O IV	255.252	5	U5
O III	255.158	1	U5
O III	255.044	0	U5
O III	253.548	0	U5
O IV	253.082	7	U5
O IV	252.948	6	U5
O IV	252.581	6d	U8
O IV	252.550		
Ne III	251.726	2	G20
Ne III	251.558	2	G20
O IV	251.148	1+	U8
Ne III	251.145	2U	G20
(O IV)	251.114	1	U8
O IV	249.365	4	U5
O IV	249.223	3	U5
C V	248.744	0	U5
C V	248.668	0	U5
O III	248.618	2	U5
O III	248.574	1+	U5
O III	248.538	1	U5
O V	248.459	6	U5
O III	248.320	1d	U5
N V	247.710	11	U5
N V	247.563	10	U5
C IV	247.415	1	U5
C IV	247.357	0	U5
N IV	247.205	10	U5
O III	247.080	1	U5
O IV	246.563	4	U5
O IV	246.503	3	U5
O IV	246.465	2	U5
O III	246.265	3	U5
C IV	245.830	5d	U5
C IV	245.775	4d	U5
O IV	245.720	1d	U5
C IV	244.907	10	U5
O III	244.049	2d	U5
He II	243.024	20C	G10
O IV	242.183	0	U5
O IV	242.140	3	U5
O IV	242.045	2	U5
O III	241.875	1	U5
O III	241.819	1–	U5
O III	241.037	2d	U5
O III	240.979	2–d	U5
O IV	240.079	1	U5
O IV	239.935	0	U5
N IV	239.693	1	U5
N IV	239.618	4	U5
O IV	239.592	3	U5
N IV	239.210	2	U5
C IV	239.196	0	U5
N IV	239.161	1+	U5
O IV	238.573	15	U5
O IV	238.361	14	U5
C IV	238.250	3d	U5
C IV	238.200	2d	U5
N IV	237.983	3	U5
N IV	237.903	2	U5
N IV	237.860	1	U5
He II	237.330	15C	G10
O III	236.710	1dd	U5
O IV	236.071	1d	U5
O IV	234.988	3	U5
He II	234.345	10C	G10
N IV	234.249	2	U5
N IV	234.195	4	U5
N IV	234.124	3	U5
O IV	233.596	6	U5
O IV	233.561	8	U5
C IV	233.53	2d	U5
O IV	233.521	6	U5
O IV	233.495	7	U5
O IV	233.457	7–	U5
He II	232.582	7C	G10
O V	231.823	7	U5
He II	231.452	4C	G10
O IV	231.302	7	U5
O IV	231.240	6	U5
O IV	231.200	6	U5
O IV	231.144	4	U5
O IV	231.101	6–	U5
O IV, V	231.070	7	U5
O IV	231.031	3	U5
O IV	230.755	2	U5
He II	230.684	2C	G10
O IV	230.682	1	U5
C IV	230.43	1d	U5
He II	230.137	1C	G10
O IV	230.040	0+	U5
O IV	229.896	0	U5
He II	229.734	0C	G10
O III	228.988	0	U5
O III	228.893	0–	U5
C IV	228.27	0dd	U5
O V	227.688	5+	U5
O V	227.636	5	U5
O V	227.549	5–	U5
O V	227.510	7	U5
O V	227.468	5	U5
O V	227.374	5+	U5
O III	226.038	1dd	U5
O IV	225.299	5	U5
N IV	225.205	5	U5
N IV	225.136	4	U5
N IV	225.098	3	U5
O IV	223.841	0–	U5
O IV	223.728	0	U5
C IV	222.791	7	U5
O IV	222.777	4	U5
O IV	222.763	5	U5
O V	222.235	3	U5
O IV	221.648	4	U5
O IV	221.515	0	U5
O V	220.352	13	U5
N IV	218.085	1d	U5
N IV	217.227	1	U5
O IV	216.960	0	U5
O V	216.018	8	U5
O V	215.245	9	U5
O V	215.104	8	U5
O V	215.034	7	U5
O IV	214.290	1–	U5
O IV	214.249	1	U5
O IV	214.209	4	U5
O IV	214.155	6	U5
O IV	214.032	5	U5
O IV	213.978	4	U5
O?	213.659	0+	U5
O?	213.533	0	U5
O IV	213.061	3–d	U5
O IV	212.974	3d	U5
O IV	212.578	2d	U5
C IV	212.421	5	U5
O IV	211.808	0d	U5
N IV	211.396	0	U5
N V	209.303	6	U5
N V	209.270	7	U5
O V	207.794	10	U5
O IV	207.348	4	U5
O IV	207.239	7	U5
O IV	207.183	6	U5
C IV	206.641	3d	U5
N IV	206.021	2+d	U5
O IV	206.002	1	U5
N IV	205.960	2d	U5
O IV	205.842	0	U5
O?	205.618	0	U5
O?	205.568	0	U5
O V	205.102	3	U5
O IV	204.996	0	U5
O IV	204.905	0–	U5
O IV	204.708	0d	U5
O V	203.935	6–	U5
O V	203.890	8	U5
O V	203.851	6–	U5
O V	203.821	7	U5
O V	203.783	6	U5
C IV	203.057	1d	U5
O IV	203.048	5	U5
O IV	202.891	4	U5
O V	202.393	7	U5
O V	202.335	5+	U5
O V	202.282	5+	U5
O V	202.226	5–	U5

TABLE I. (*Continued.*)

SPECTRUM	λ	INT.	REFERENCE	SPECTRUM	λ	INT.	REFERENCE	SPECTRUM	λ	INT.	REFERENCE
O V	202.191	5	U5	O V	182.205	2	U5	N IV	181.746	1	U5
O V	202.158	5	U5	O IV	181.995	4	U5	O IV	181.275	5	U5
O IV	201.098	1	U5	O IV	181.876	3	U5	O IV	181.150	4	U5
O IV	201.073	1−	U5	O IV	180.351	1	U5	O IV	180.481	2	U5
O IV	201.022	0	U5	O V	178.713	2	U5	O V	156.225	3	U5
O IV	200.995	2	U5	O IV	177.808	2+	U5	O V	156.158	2	U5
O IV	200.966	1−	U5	O IV	177.761	2	U5	O V	156.126	1	U5
O IV	200.915	1	U5	O IV	177.698	1	U5	O V	153.948	3	U5
O IV	200.827	1d	U8	O IV	177.659	0	U5	O IV	153.162	0d	U8
C IV	200.68	0dd	U5	O IV	177.598	0−	U5	O IV	152.355	0	U5
O V	198.031	3	U5	O V	174.558	2	U5	O IV	152.264	0−	U5
N IV	197.230	3	U5	O IV	174.220	3	U5	O V	151.548	6	U5
N IV	197.007	1d	U5	O IV	174.105	2	U5	O V	151.481	5	U5
N IV	196.954	0+d	U5	O IV	173.968	0	U5	O V	151.449	4	U5
O IV	196.435	0d	U5	O IV	173.917	2	U5	O VI	150.123	9	U5
O IV	196.348	0d	U5	O IV	173.851	1	U5	O VI	150.085	10	U5
O IV	196.009	8	U5	O IV	173.803	0	U5	O V	149.078	2	U5
O IV	195.863	7	U5	O VI	173.082	13	U5	O V	149.034	0	U5
O V	194.593	8	U5	O VI	172.935	12	U5	N V	147.424	2	U5
O V	192.906	14	U5	O V	172.168	12	U5	O V	147.261	3	U5
O V	192.800	13	U5	O IV	171.191	0	U5	O V	146.345	1	U5
O V	192.751	12	U5	O IV	171.121	2	U5	O V	144.837	1+	U5
O IV	192.244	3	U5	O IV(V)	171.071	2	U5	O V	144.802	1	U5
O IV	192.206	5	U5	O IV	170.988	0+	U5	N V	140.345	0	U5
O IV	192.169	4+	U5	O IV	170.940	0	U5	O V	140.109	0+	U5
O IV	192.139	4−	U5	O V	170.218	6	U5	O V	140.045	0	U5
O IV	191.752	3	U5	O V	169.586	0	U5	O V	139.025	5	U5
O IV	191.695	2	U5	O V	169.478	0−	U5	O V	138.108	4	U5
O IV	191.640	0	U5	O V	168.077	4	U5	O V	138.054	3	U5
O IV	191.609	2d	U5	O V	168.042	4	U5	O V	138.030	2	U5
O V	191.556	2	U5	O V	167.991	8	U5	O V	135.523	5	U5
O V	191.458	1	U5	O IV	167.145	0dd	U5	O V	133.521	3	U5
O V	191.397	0	U5	N V	166.947	2d	U5	O V	133.395	0+	U5
N V	190.242	2	U5	N V	166.865	1d	U5	O V	133.328	0	U5
N V	190.156	1	U5	O V	166.234	5	U5	O V	132.885	0	U5
O ?	188.412	0	U5	O V	166.152	4	U5	O V	132.851	2	U5
O IV	188.190	0	U5	O V	166.113	3	U5	O V	132.800	1	U5
O IV	188.152	2	U5	O V	164.986	2	U5	O VI	132.310	2	U5
O IV	186.982	0	U5	O V	164.710	4+	U5	O VI	132.218	1	U5
O IV	186.936	2	U5	O V	164.656	6	U5	O V	131.807	1+	U5
O IV	186.872	1	U5	O V	164.628	4−	U5	O V	131.750	1	U5
N V	186.153	5	U5	O V	164.578	5	U5	O VI	129.869	6	U5
N V	186.070	4	U5	O V	164.178	2	U5	O VI	129.783	5	U5
O V	185.747	9	U5	N V	162.562	4	U5	O V	128.297	0+	U5
(O IV)	185.544	1	U5	O V	162.494	4	U5	O V	128.235	0	U5
O IV	185.384	0	U5	O IV	160.141	0	U5	O V	124.598	3	U5
O VI	184.120	9	U5	O V	159.380	4+	U5	O V	122.372	0	U5
O VI	183.941	8	U5	O V	159.343	4	U5	O V	122.128	0−	U5
O IV	183.454	1+	U5	O V	158.926	2+	U5	O VI	116.419	2	U5
O IV	183.395	1	U5	O V	158.813	1d	U5	O VI	116.347	1	U5
O IV	183.353	0	U5	O IV	158.606	1	U5	O VI	115.822	4	U5
O IV	182.832	4	U5	O IV	158.553	0	U5	O VI	110.220	1	U5
O IV	182.711	3	U5	N V	158.091	0d	U5	O VI	110.148	0	U5
								O VI	104.811	2	U5

wave-lengths for the same line preference has been given to the values of Edlén in the region of wave-lengths shorter than λ800 and above that limit to the values obtained in this laboratory. The slight discrepancies between the two scales have already been discussed.[2] The available data on the first spectra of nitrogen, oxygen, and argon have been revised upon the basis of the term tables of these atoms and the few extreme ultraviolet lines for which accurate measurements are available. The letter C in the intensity column designates the wave-lengths which have been so computed. It also marks the wave-lengths of hydrogen and of ionized helium computed by Paschen[3] on theoretical grounds. The intensities given are of course comparable only among lines from the same original paper, to which reference should be made for the conditions of excitation.

No attempt has been made to include band spectra in the lists, since they can usually be distinguished by their appearance. Mention should be made, however, of three molecular spectra which sometimes are mistaken for line spectra: the many lined spectrum of hydrogen,[4] a band due to helium in the vicinity of λ600,[5] and, under certain conditions of excitation, the molecular spectrum of nitrogen.[6]

We are very grateful to Dr. B. Edlén for his kind permission to republish here so many of his own data. Grants from the Carnegie Institution

[2] J. C. Boyce and C. A. Rieke, Phys. Rev. **47**, 653 (1935).
[3] F. Paschen, Preuss. Akad. (1929), 662. See also: W. G. Penney, Phil. Mag. **9**, 661 (1930).
[4] O. W. Richardson, *Molecular Hydrogen and its Spectrum* (Yale Univ. Press, 1934).
[5] For a bibliography relating to this band see J. L. Nickerson, Phys. Rev. **47**, 707 (1935).
[6] R. T. Birge and J. J. Hopfield, Astrophys. J. **68**, 257 (1928).

TABLE II. *Extreme ultraviolet lines of boron, sodium, and silicon.*

Spectrum	λ	Int.	Reference
Si I	1991.94	2	L16
Si I	1989.01	6	L16
Si I	1986.39	4	L16
Si I	1984.50	0	L16
Si I	1983.25	4	L16
Si I	1980.64	3	L16
Si I	1979.23	3	L16
Si I	1977.62	3	L16
Si I	1963.04	00	L16
Si I	1962.13	0	L16
Si I	1961.29	00	L16
Si I	1960.16	0	L16
Si I	1958.65	0	L16
Si I	1957.92	0	L16
Si I	1956.06	0	L16
Si I ?	1955.00	1	L16
Si I	1954.71	2	L5
Si I	1953.02	0	L16
Si I	1952.53	00	L16
Si I	1951.61	0	L16
Si I	1950.23	0	L16
Si I	1947.01	1	L16
Si I	1945.03	00	L16
Si I	1942.37	00	L16
Si I	1940.69	0	L16
Si I	1934.49	00	L16
Si I	1904.643	2C	L16
Si I	1901.36	8R	L16
Si I	1893.25	5	L16
Si I	1887.74	2	L16
Si I	1883.80	0	L16
Si I	1881.883	2C	L16
Si I	1880.988	0C	L16
Si I	1875.835	2C	L16
Si I	1874.90	3	L16
Si I	1873.127	2C	L16
Si I	1865.19	0	L16
Si I	1861.76	00	L16
Si I	1855.62	00	L16
Si I	1853.17	1	L16
Si I	1852.49	3	L16
Si I	1851.82	1	L16
Si I	1850.70	5R	L16
Si I	1848.768	2C	L16
Si I	1848.17	3	L16
Si I	1847.48	4R	L16
Si I	1846.13	2	L16
Si I	1845.53	3	L16
Si I	1843.788	2C	L16
B II	1842.80	3	U6
Si I	1841.48	3	L16
Si I	1841.171	2C	L16
Si I	1838.00	1	L16
Si I	1836.54	2	L16
Si I	1829.910	2C	L16
B I	1826.52	9n	L17
Si I	1826.45	00	L16
B I	1825.97	8n	L17
Si I	1825.032	00C	L16
Si I	1822.469	2	L16
B I	1818.41	6	L17
Si I	1817.97	0	L16
B I	1817.90	5	L17
Si II	1816.98	2	L16
Si I	1814.07	6	L16
Si I	1809.05	4	L16
Si II	1808.09	1	L16
Si I	1799.16	2	L16
Si IV	1797.5	0	L5
Si I	1797.35	1	L16
Si IV	1796.1	1	L5
Si I	1790.31	2	L16
Si I	1787.78	00	L16
Si I	1784.09	0	L16
Si I	1783.24	2n	L16
Si I	1776.86	2	L16
Si I	1774.98	0	L16
Si I	1774.05	00	L16
Si I	1772.26	0	L16
Si I	1770.89	3R	L16
Si I	1769.81	3	L16
Si I	1766.09	4n	L16
Si I	1765.15	3R	L16
Si I	1759.63	2	L16
Si I	1757.34	00	L16
Si I	1753.11	3n	L16
Si I	1752.71	0	L16
Si I	1749.78	00	L16
Si I	1747.40	1	L16
Si I	1743.91	0	L16
Si I	1740.40	2n	L16
Si I	1736.58	00	L16
Si I	1734.78	1n	L16
Si IV	1727.4	4	L5
Si I	1727.37	00	L16
Si I	1724.07	00	L16
Si IV	1722.7	5	L5
Si II	1711.0	6d?	L5
Si I	1707.102	0C	L16
Si I	1704.47	3R	L16
Si I	1702.855	2C	L16
Si I	1700.623	2C	L16
Si I	1700.43	2	L16
Si I	1699.73	00	L16
Si I	1698.25	00	L16
Si I	1697.92	4R	L16
Si I	1697.60	0	L16
Si I	1696.22	3R	L16
Si I	1695.60	2	L16
Si I	1693.48	1	L16
Si I	1693.23	1	L16
Si I	1690.80	1	L16
Si I	1689.30	1	L16
Si I	1687.08	0	L16
Si I	1686.87	1	L16
Si I	1682.70	1	L16
Si I	1676.83	0	L16
Si I	1675.24	3	L16
Si I	1672.62	2	L16
Si I	1670.91	2	L16
Si I	1668.53	1	L16
Si I	1667.66	1	L16
B I	1667.42	3n	L17
B I	1666.99	2n	L17
Si I	1666.40	1	L16
Si I	1664.51	1	L16
B I	1663.07	2	L17
B I	1662.62	1	L17
Si I	1660.44	0	L16
Si I	1653.28	1	L16
Si I	1651.02	0	L16
Si I	1633.95	1n	L16
Si I	1633.04	0n	L16
Si I	1631.39	0n	L16
B I	1629.33	1	L16
Si I	1627.83	00	L16
Si I	1627.15	00	L16
Si I	1625.68	2n	L16
B II	1624.37	4	U6
B II	1624.16	4	U6
B II	1623.99	5	U6
B II	1623.77	4	U6
B II	1623.57	4	U6
Si I	1622.79	2n	L16
Si I	1620.39	1	L16
Si I	1616.55	1	L16
Si I	1615.94	1	L16
Si I	1614.63	1	L16
Si I	1609.02	0	L16
B	1607.78	0	L17
Si I	1605.86	0	L16
B I	1600.91	1n	L17
B	1600.28	0n	L17
Si I	1597.99	1	L16
Si I	1595.21	0	L16
Si I	1594.25	1	L16
Si I	1592.27	1	L16
Si I	1590.60	0	L16
B	1573.44	2n	L17
B I	1566.64	1n	L17
Si II	1563.1	3d?	L5
B	1558.93	0n	L17
Si IV(II)	1533.55	10	L5
Si	1526.9	0	C2
Si II	1526.38	8	L5
Si III	1502.00	5	L5
Si III	1501.32	5	L5
Si III	1500.39	5	L5
Si II	1485.4	3	L5
Si II	1438.9	1	L5
Si	1416.8	0	C2
Si II	1408.8	0	L5
Si IV	1402.9	8	L5
Si IV	1393.9	10	L5
Si IV	1368.72	C	L5
Si IV	1365.69	C	L5
B II	1362.460	5	U6
Si II	1309.28	2	C15
Si II	1304.41	1	C15
Si III	1303.34	–	C8
Si III	1301.13	–	C8
Si III	1298.93	–	C8
Si III	1296.73	–	C8
Si III	1294.52	–	C8
Si IV	1279.05	C	L5
Si II	1265.04	10	L5
Si II	1260.66	8	L5
Si II	1251.17	1	C15
Si	1250.3	0	C2
Si II	1248.43	1	C15
Si II	1246.75	1	C15
Si IV	1230.71	C	L5
B II	1230.160	2	U6
Si IV	1228.26	C	L5
Si IV	1211.75	C	L5
Si IV	1210.65	C	L5
Si III	1206.9	10	L5
Si II	1197.42	–	C8
Si II	1194.50	–	C8
Si II	1193.31	–	C8
Si II	1190.42	–	C8
Si	1164.0	1	C2
Si IV	1154.73	C	L5
Si III	1144.85	1	L5
Si III	1142.74	0	L5
Si IV	1127.75	C	L5
Si IV	1121.93	C	L5
Si III	1113.76	5	L5
Si III	1110.47	5	L5
Si III	1108.85	4	L5
Si	1086.9	0	C2
B II	1082.06	2	U6
B II	1081.85	2	U6
Si IV	1066.3	8	L5
B II	1048.67	0	U6
Si II	1023.75	C	L5
Si II	1020.75	C	L5
Si III	997.70	1	L5
Si III	995.23	0	L5
Si III	993.94	C	L5
Si II	993.09	1	L5
Si II	990.32	0	L5
B II	984.65	1	U6
B II	882.670	2	U6
B II	882.536	2	U6
B II	864.08	0	U6
Si IV	859.52	C	L5
Si IV	859.25	C	L5
Si IV	817.85	C	L5
Si IV	814.78	C	L5
Si IV	779.19	C	L5
Si IV	779.03	C	L5
B III	758.673	2	U6
B III	758.476	1	U6
Si IV	749.97	C	L5
B II	731.442	1	U6
B II	731.357	1	U6
B II	693.952	2	U6
B III	677.147	6	U6
B III	677.004	5	U6
Si IV	646.82	C	L5
Si IV	560.85	C	L5
Si IV	559.41	C	L5
B III	518.253	7d	U6
Na V	514.350	0	U7
Na V	511.193	1	U7
B III	510.865	3	U6
B III	510.777	2	U6
Na V	510.102	0	U7
Si	486.6	0	C2
Na V	463.263	12	U7
Na V	461.051	10	U7
Na V	459.897	7	U7
Si IV	458.09	C	L5
Si IV	457.75	C	L5
Na V	445.190	7	U7
Na V	445.046	6	U7
Na IV	412.240	8	U7
B III	411.810	3	U6
Na IV	411.333	7	U7
Na IV	410.540	6	U7
Na IV	410.371	10	U7
Na IV	409.615	8	U7
Na IV	408.682	8	U7
Na V	400.722	10	U7
Si	392.7	1	C2
Na III	380.107	8	U7
Na III	378.143	10	U7
Na II	376.375	3	U7
Na II	372.069	6	U7
Na V	369.743	3	U7
Na V	367.557	2	U7
Si IV	361.615	C	L5
Si IV	361.517	C	L5
Na IV	360.761	6	U7
Na V	360.367	8	U7
Na V	360.319	8	U7
Na V	333.910	9	U7
Na V	332.550	8	U7
Na V	330.718	0	U7
Na IV	319.638	10	U7
Na V	308.264	10	U7
Na V	307.152	8	U7
Na II	301.432	1	U7
Na II	301.311	0	U7
Na II	300.151	1	U7
Na II	282.827	0	U7
Na III	272.441	0d	U7
Na III	268.623	5	U7
Na III	267.868	6	U7
Na III	267.642	8	U7
Na III	266.893	5	U7
Na III	251.371	6	U7
Na III	250.515	8	U7
Na III	230.593	2	U7
Na III	229.868	3	U7
Na III	216.120	1	U7
Na III	215.671	4	U7
Na III	215.498	0	U7
Na III	215.340	4	U7
Na III	215.230	4	U7
Na III	215.042	2	U7
Na III	214.868	4	U7
Na III	214.596	2	U7
Na III	214.235	4	U7
Na III	207.458	0	U7
Na III	207.355	0	U7
Na III	206.871	0	U7
Na IV	206.155	3	U7
Na IV	205.956	4	U7
Na IV	205.487	6	U7
Na IV	203.959	2	U7
Na III	203.324	2	U7
Na III	203.282	2	U7
Na III	203.050	3	U7
Na III	202.760	3	U7
Na III	202.720	3	U7
Na III	202.490	2	U7
Na III	202.184	4	U7
Na IV	199.769	6	U7
Na III	194.306	1d	U7
Na III	194.166	0	U7
Na III	194.032	1	U7
Na IV	191.000	6	U7
Na IV	190.835	8	U7
Na IV	190.440	10	U7
Na IV	190.126	6	U7
Na III	189.346	1	U7
Na III	188.870	2	U7
Na III	184.218	0	U7
Na III	183.747	0	U7
Na III	183.575	0	U7
Na IV	182.282	4	U7
Na IV	182.128	6	U7
Na IV	174.008	0	U7
Na V	171.090	0d	U7
Na V	170.929	0	U7
Na V	170.631	1	U7
Na IV	168.544	5	U7
Na IV	168.409	8	U7
Na IV	168.084	10	U7
Na IV	164.841	4	U7
Na V	163.930	3	U7
Na IV	163.840	4	U7
Na V	163.616	5	U7
Na IV	163.187	6	U7
Na IV	162.445	8	U7
Na IV	157.782	3	U7
Na IV	157.599	1	U7
Na V	157.514	3	U7
Na V	157.209	5	U7
Na IV	157.090	4	U7
Na V	157.036	3	U7
Na IV	156.887	3	U7
Na IV	156.780	5	U7
Na IV	156.536	8	U7
Na IV	155.832	0	U7
Na IV	155.781	1	U7
Na IV	155.693	2d	U7
Na IV	155.622	0	U7
Na IV	155.515	4	U7
Na IV	155.445	3	U7
Na IV	155.354	0	U7
Na IV	155.248	2	U7
Na IV	155.090	1	U7
Na IV	151.303	1	U7
Na V	151.127	5	U7
Na IV	151.048	0	U7
Na IV	150.968	2	U7
Na IV	150.695	2	U7
Na IV	150.647	2	U7
Na IV	150.545	3	U7
Na IV	150.297	4	U7
Na V	149.001	4	U7
Na V	148.856	5	U7
Na IV	148.642	6	U7
Na V	147.888	1	U7
Na IV	146.397	0	U7
Na IV	146.297	1	U7
Na IV	146.060	3	U7
Na IV	145.846	0	U7
Na V	144.979	0	U7
Na V	144.661	0	U7
Na V	144.547	1	U7
Na V	144.330	2	U7
Na IV	142.688	0	U7
Na IV	142.363	1	U7
Na IV	142.232	2	U7
Na IV	139.869	0	U7
Na V	138.918	2	U7
Na V	138.809	1	U7
Na IV	137.945	0	U7
Na IV	137.714	0	U7
Na IV	137.144	0	U7
Na IV	137.062	0	U7
Na IV	136.854	1	U7
Na IV	136.748	0	U7
Na IV	136.645	0	U7
Na IV	136.550	1	U7
Na IV	136.435	0	U7
Na V	135.854	2	U7
Na V	135.791	3	U7
Na V	134.272	0	U7
Na V	134.172	0	U7
Na V	133.387	3	U7
Na V	133.164	4	U7
Na IV	132.740	0	U7
Na IV	132.465	0d	U7
Na IV	132.211	0	U7
Na V	131.633	2d	U7
Na V	131.420	2	U7
Na V	131.348	2	U7
Na V	130.725	0	U7
Na V	130.686	2	U7
Na V	129.942	1	U7
Na IV	129.464	0	U7
Na V	128.052	4	U7
Na V	128.024	4	U7
Na V	127.473	3	U7
Na V	127.447	4	U7
Na V	126.608	0	U7
Na V	126.557	0	U7
Na V	125.456	1	U7
Na V	125.432	1	U7
Na IV	125.286	6	U7
Na V	125.216	5	U7
Na V	125.183	4	U7
Na V	121.264	0	U7
Si V	118.968	6	U7
Na V	117.996	1	U7
Na V	117.876	0	U7
Si V	117.855	7	U7
Na V	117.703	0	U7
Na V	114.699	0	U7
Na V	112.003	0	U7
Na V	111.863	0	U7
Na V	111.725	0	U7
Na V	111.509	0	U7
Na V	110.901	0	U7
Na V	108.182	0	U7
Na V	107.930	0	U7
Na V	106.333	0d	U7
Si V	98.360	0	U7
Si V	97.292	2	U7
Si VI+V	96.581	3	U7
Si V	90.993	0	U7
Si V	90.594	0	U7
Si VII+V	85.706	0	U7
Si VII+V	85.328	1	U7
B IV	60.31	–	U6
B IV	52.68	–	U6
B V	48.585	C	U6
B V	40.995	C	U6
B V	38.869	C	U6

TABLE III. *Extreme ultraviolet principal lines.*

H^1	G11	C II	T2	O I	T2	Ne IV	T1	Si III	L5	Kr III	T3
1215.664	C	1335.71	40	1306.038	9	543.884	7	1113.76	5	897.801	40
1025.717	C	1334.54	30	1304.864	12	542.076	6	1110.47	5	876.674	22
972.532	C			1302.192	12	541.124	5	1108.85	4	870.825	20
		C III	T2							862.578	35
H^2		1176.370	10	O II	T2	Na II	U7	Si IV	L5	854.733	25
(Deuterium)	TU	1175.986	9	834.467	20	376.375	3	458.09	C	837.666	22
1215.31	C	1175.716	15	833.332	12	372.069	6	457.75	C		
1025.42	C	1175.582	5	832.762	8					Kr IV	T3
972.25	C	1175.259	9			Na III	U7	Si V	U7	842.035	22
		1174.934	10	O III	T2	380.107	8	118.968	6	816.822	18
He I	TU			835.293	7	378.143	10	117.855	7	805.763	7
584.331	10	C IV	T2	835.10	5						
537.024	3	1550.790	10	833.749	11	Na IV	U7	A I	T4	Xe I	TU
		1548.214	12	832.93	5	412.240	8	1066.660	9	1469.621	5
He II	G11					411.333	7	1048.218	8	1295.560	5
1640.409	C	C V	U6	O IV	U6	410.540	6				
1215.129	C	40.27		790.203	16	410.371	10	A II	T4	Xe II	TU
303.7788	C			790.103	13	409.615	8	932.046	10	1244.756	5
256.3145	C	N I	T2	787.710	15	408.682	8	919.78	15	1100.432	10
		1200.706	4								
B II	U6	1200.220	5	O V	U6	Na V	U7	A III	T4	Xe III	TU
1624.37	4	1199.547	6	629.732	15	463.263	12	887.404	10	1130.344	25
1624.16	4					461.051	10	883.179	9	1066.391	10
1623.99	5	N II	T2	Ne I	T1	459.897	7	879.622	8	1047.801	9
1623.77	4	1085.74	10	743.70	12			878.728	12	1017.680	25
1623.57	4	1085.546	7	735.89	30	Al III	U2	875.534	9	965.540	10
		1084.579	9			1862.749	10	871.099	10		
B III	U6	1083.991	7	Ne II	T1	1854.715	10			Hg I	L17
518.253	7d			462.388	14			A IV	T4	1849.68	20
		N III	U6	460.725	15	Al IV	U7	850.602	25		
B IV	U6	991.579	17			161.686	14	843.772	20	Hg II	G7
60.31		991.514	14	Ne III	T1	160.073	16	840.029	15	1942.32	50
		989.790	16	491.050	9					1649.959	30
B V	U6			490.310	7	Al V	U7	Kr I	T3		
48.585	C	N IV	U6	489.641	4	281.397	14	1235.819	13	Hg III	M1
		765.140	17	489.501	10	278.699	16	1164.868	4	1738.49	10
C I	T2			488.868	7					1677.91	10
1658.126	3	N V	U6	488.103	8—	Si II	L5	Kr II	T3	1647.49	10
1657.916	3	1242.778	7			1533.55	10	964.962	30	1592.93	10
1657.380	2	1238.800	8			1526.38	8	917.434	20		
1657.005	6										
1656.280	4										

of Washington and from the Permanent Science Fund of the American Academy of Arts and Sciences have aided our own experimental results which are included here. We are much indebted to Dr. Carol A. Rieke for her careful assistance in the preparation and checking of the tables.

BIBLIOGRAPHY

B5 Hopfield, Astrophys. J. **72**, 133 (1930).

C2 Bowen and Millikan, Phys. Rev. **23**, 1 (1924).

C8 Bowen and Millikan, Phys. Rev. **26**, 150 (1925).

C12.5 Bowen and Ingram, Phys. Rev. **28**, 444 (1926).

C13 Bowen, Phys. Rev. **29**, 231 (1927).

C15 Bowen, Phys. Rev. **31**, 34 (1928).

C25 Frerichs, Phys. Rev. **36**, 398 (1930).

G7 Paschen, Preuss. Akad. (1928), 536.

G8 Naudé, Ann. d. Physik **3**, 2 (1929).

G10 Kruger, Phys. Rev. **36**, 855 (1930).

G11 Paschen, Preuss. Akad. (1929), 662.

G12 Ekefors, Zeits. f. Physik **63**, 437 (1930).

G13 Paschen and Kruger, Ann. d. Physik **7**, 1 (1930).

G15 Beutler, Zeits. f. Physik **84**, 289 (1933).

G19 von Keussler, Zeits. f. Physik **84**, 42 (1933).

G20 von Keussler, Zeits. f. Physik **85**, 1 (1933).

L5 Fowler, Phil. Trans. Roy. Soc. **A225**, 1 (1925).

L6 Fowler, Proc. Roy. Soc. **A110**, 476 (1926).

L7 Fowler and Freeman, Proc. Roy. Soc. **A114**, 662 (1927).

L8 Fowler, Proc. Roy. Soc. **A117**, 317 (1927).

L10 Fowler and Selwyn, Proc. Roy. Soc. **A118**, 34 (1928).

L11 Fowler and Selwyn, Proc. Roy. Soc. **A120**, 312 (1928).

L12 Freeman, Proc. Roy. Soc. **A121**, 318 (1928).

L16 Fowler, Proc. Roy. Soc. **A123**, 422 (1929).

L17 Selwyn, Proc. Phys. Soc. London **41**, 392 (1929).

M1 McLennan, McLay and Crawford, Trans. Roy. Soc. Canada **22**, Sec. III, 247 (1928).

M2 McLennan, McLay and Crawford, Proc. Roy. Soc. **A134**, 41 (1931).

R1 Frisch, Zeits. f. Physik **64**, 499 (1930).

T1 Boyce, Phys. Rev. **46**, 378 (1934).

T2 Boyce and Rieke, Phys. Rev. **47**, 653 (1935).

T3 Boyce, Phys. Rev. **47**, 718 (1935).

T4 Boyce, Phys. Rev. **48**, 396 (1935).

T5 Boyce, Phys. Rev. **49**, 351 (1936).

TU Boyce, Unpublished material.

U2 Ekefors, Zeits. f. Physik **51**, 471 (1928).

U5 Edlén, Zeits. f. Physik **85**, 85 (1933).

U6 Edlén, Nova Acta Reg. Soc. Sci. Upsaliensis, Ser. IV 9, No. 6 (1934).

U7 Soderquist, Nova Acta Reg. Soc. Sci. Upsaliensis, Ser. IV 9, No. 7 (1934).

U8 Edlén, Zeits. f. Physik **93**, 726 (1935).

W1 Mack and Fromer, Phys. Rev. **48**, 357 (1935).

The Behavior of the 4930A Absorption Band of Uranine Solutions Under High Pressure

WILLIAM JAMES LYONS, *Department of Physics, St. Louis University*

(Received November 4, 1935)

The object of this investigation was to test experimentally the assumption of electromagnetic dispersion theory that the natural period of vibration of the resonators of a medium remains constant with variations in pressure. Two dilute aqueous solutions of uranine of slightly different concentrations were studied in the high pressure spectrometer. Refractive indices for the three principal lines of the mercury arc, and for the wave-length corresponding to the absorption band maximum (4390A) were determined for pressures ranging up to 915 kg per cm² in one solution, and up to 1823 kg per cm² in the other. It was found that the absorption band retained its position relative to the rest of the spectrum formed by the liquid prism under various pressures. It is concluded that the natural frequency of vibration of the resonators is affected to no measurable extent by the pressure or density of a medium.

INTRODUCTION

THE influence of pressure on the index of refraction of liquids has been studied by several investigators. The results uniformly have been an increase in the indices with increased pressures, and are quantitatively in accord with the various electromagnetic dispersion formulae. These formulae, such as Drude's:

$$\mu^2-1=\Sigma[q^2e^2N/\pi M(\nu_0^2-\nu^2)], \qquad (1)$$

where μ=refractive index, q=number of electrons per molecule, e=electronic charge, N=number of molecules per cm³, M=combined mass of the vibrating electrons in a molecule, ν_0=frequency of the absorption band of the refracting medium (natural vibration frequency of the resonators), and ν=frequency of the incident light, assume that ν_0 remains constant, with pressure changes. This implies that the absorption band of the dispersive medium does not shift to another position in the spectrum. The object of the present study was to test this conclusion, with the degree of accuracy the available equipment would allow.

The assumption that ν_0 remains constant has been indirectly verified, in the confirmation of the electromagnetic formulae (applied to liquids) by previous investigations. Eq. (1) leads directly to Newton's law:

$$(\mu^2-1)/d=K, \qquad (2)$$

where d=density of the medium, and K=a constant, the "specific refraction"; μ being the index of a particular spectral line. Using the data of Poindexter and Rosen[1] for water, the present writer found relation (2) to hold to about one percent over pressures ranging up to 1800 kg per cm². The analogous Lorenz-Lorentz law,

$$\frac{\mu^2-1}{\mu^2+2}\cdot\frac{1}{d}=K, \qquad (3)$$

which, theory indicates is valid at all pressures, has been found to hold quite accurately by Poulter and his associates,[2] and by Hayden,[3] working with glycerin. No direct study has yet been made, however, of the behavior of an absorption band with pressure changes.

It would have been of prime interest to observe the effect of changes in pressure on the absorption band to which dispersion in water is due. But, since this band lies in the ultraviolet region, this study was impossible with the available apparatus. However, it was concluded that if an increase in pressure affected the free period of the resonators, and was accompanied by an appreciable shift of the absorption band, this could be observed in a medium having an absorption maximum in the visible region. Accordingly, uranine (sodium salt of fluorescein), having an absorption maximum at 4930A, was chosen. The uranine was dissolved in water as a means of suspension. The two solutions used were made very dilute in order to obtain a narrow band, and also to permit the transmission of sufficient light for observations. No anomalous dispersion was observed. The absorption of the uranine was assumed to be independent of its presence in water. Accordingly, the center of the observed

[1] Poindexter and Rosen, Phys. Rev. **45**, 760 (1934).

[2] Poulter, Richey and Benz, Phys. Rev. **41**, 366 (1932).

[3] C. K. Hayden, Ph.D. Dissertation, St. Louis University, 1933.

absorption band in the solutions at the various pressures was taken to be the absorption maximum of uranine. The uranine molecule presumably absorbs radiation in the neighborhood of 4930A, thus giving rise to a dark line at the corresponding point of the continuous spectrum formed by the liquid prism. Known pressure and density changes are communicated to the uranine through the liquid.

Procedure and Results

The high pressure spectrometer, developed in this laboratory and described elsewhere,[4] was used in this study. At first, as the simplest method, the glass windows were made parallel to form a nondispersive cell into which one of the solutions was placed, and could be subjected to pressure. It was found, however, that the amount of transmitted light was insufficient for analysis in a glass-prism spectrometer of the usual type.

The high pressure apparatus was therefore used as a spectrometer, the glass windows being put in at oblique angles to each other, with the uranine solutions serving as the dispersive media. The angle of the liquid prism was determined by filling the cell with distilled water at a known temperature, and obtaining the angles of minimum deviation for the three or four prominent mercury arc lines at atmospheric pressure. By using the well-established refractive indices of water for these lines, values of the prism angle, in good agreement, were calculated. Glycerin was used in the cylinder around the rubber sack to transmit pressure to the solution under study.

Besides a mercury vapor arc lamp, giving the familiar 5790A, 5461A, and 4358A lines, an Ediswan Pointolite was used to furnish a continuous spectrum, against which the uranine absorption band stood out. The Pointolite was used alternately with the mercury arc through the successive stages of pressure.

Two series of observations were made; the results of both are incorporated in Fig. 1. A prism angle of 48° 8′ 11″±18″ was used with the 84 mg per liter solution, while one of 43° 32′ 45″±4″ was used with the 100 mg per liter solution. Pressures ranged up to 915 kg per cm² in the first series, and up to 1823 kg per cm² in the second.

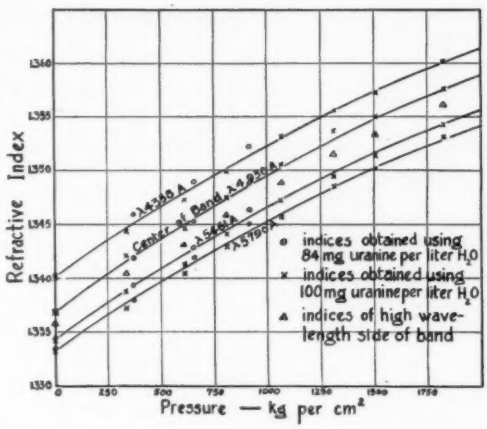

Fig. 1

Because of the dilution of the solutions the curves are sensibly the same as those for pure water, the effect of the uranine on the dispersion being negligible. The parallelism between the lines indicates that there is no measurable shift of the absorption band relative to the rest of the spectrum. While the refractive index of the medium, for the absorbed wave-length, changes under pressure, this can be charged solely to the change in the dispersion of the water, for at every pressure the index for the band center (as taken from the curve) is that appropriate to 4930A. A variation in the natural vibration frequency of the absorbing medium (the uranine, here) with pressure would be represented by a lack of parallelism between the curve for the absorption band and those for the other spectral lines. The results demonstrate, therefore, that the natural frequency of the dispersion resonators, ν_0, is affected to no appreciable extent by a change in the pressure or density of the medium. This conclusion is in accord with electromagnetic dispersion theory.

The writer is indebted to Professor Franklin E. Poindexter for his helpful advice and his generous assistance in making observations.

[4] Lyons and Poindexter, "Spectrometer for Studies at High Pressures," this issue.

A Spectrometer for Studies at High Pressures

W. JAMES LYONS AND FRANKLIN E. POINDEXTER, *Department of Physics, St. Louis University*

(Received November 4, 1935)

I. APPARATUS

VARIOUS experimenters have developed apparatus for optical studies at high pressures.[1, 2] Because of the difficulties surrounding construction sturdy enough to withstand the excessive pressures, these instruments have been of limited flexibility and spectral range. In an effort to attain these in greater degree the present high pressure spectrometer was designed.

The instrument consists uniquely of a liquid prism confined between glass walls, the whole being encased in a cylinder of thick walls, through which narrow, horizontal slits, for the entrance of light, are cut. Plate glass, approximately 6 mm thick, and elliptical in shape (*G* in Fig. 1), serve as walls or "windows" of the prism. These windows are fastened into the ends of a short rubber sack, by means of fine wire wrapped many times around near the ends of the rubber. A small rubber tube, cemented to the sack on top, and running through the cylinder, permits the introduction of the liquid under study into the sack. The use of the rubber sack is for insurance against contamination of the liquid. The windows are waxed to the steel lugs *E*, through which are cut slits, as shown by broken lines, 0.8 mm wide and 17.8 mm long at their inner ends. The lugs are, in turn, held to the cylinder by a thin layer of wax between the surfaces, the lugs having been brought up tightly by means of screws through the slits, while the wax was hot. The slits of the lugs and cylinder are, of course, adjacent to each other.

The high pressure cylinder, a vertical section of which appears in Fig. 2, is of chrome-vanadium steel, oil hardened. The inner and outer diameters are 4.45 cm and 15.24 cm, respectively; the walls, therefore, being 5.4 cm thick. The principle of "unsupported area," referred to by Bridgman,[1] is employed in packing the pistons. Rubber plugs, such as those used by Poulter,[2] serve well to stop leakage at the ends of the plungers *P* and *p*. Fitting into the bottom of the cylinder is an assembly of piston, plunger and screws (lower portion, Fig. 2). Pressures in the higher ranges are attained by screwing in *S*, and forcing the plunger *p* upward, which in turn forces liquid through the orifice *O* into the main chamber. The plunger *p* has a diameter of 1.27 cm. By means of a hollow, square-head screw, which follows it, the upper piston *R* is used for applying the initial pressures in the lower range.

Below the observation slits of the cylinder are two beveled rings, which fit onto the hollow base into which the tapered end of the cylinder sets. One ring has a scale graduated in divisions of 20′ of arc, and carries the telescope; the other, having two verniers, 180° apart, carries the collimator. A top view of the assembly with a horizontal section through the windows, appears in Fig. 3. Extending beyond the slit-end of the collimator is an arm which carries a mercury vapor arc lamp. With this apparatus the familiar yellow (5790A), green (5461A), blue (4358A), and violet (4046–4078A) lines of the mercury arc spectrum are easily observed. It is possible to tilt the arc lamp to one side to permit the use of an Ediswan Pointolite. This is done when it is desired to obtain a continuous spectrum.

II. TECHNIQUE

A direct method of measuring the pressures within the cylinder is used. It consists of a lever

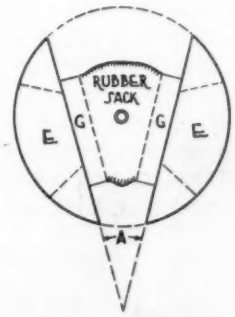

FIG. 1. Top view of prism and lugs.

[1] P. W. Bridgman, *The Physics of High Pressure* (Macmillan Co., New York, 1931).
[2] T. C. Poulter, Phys. Rev. **40**, 860 (1932).

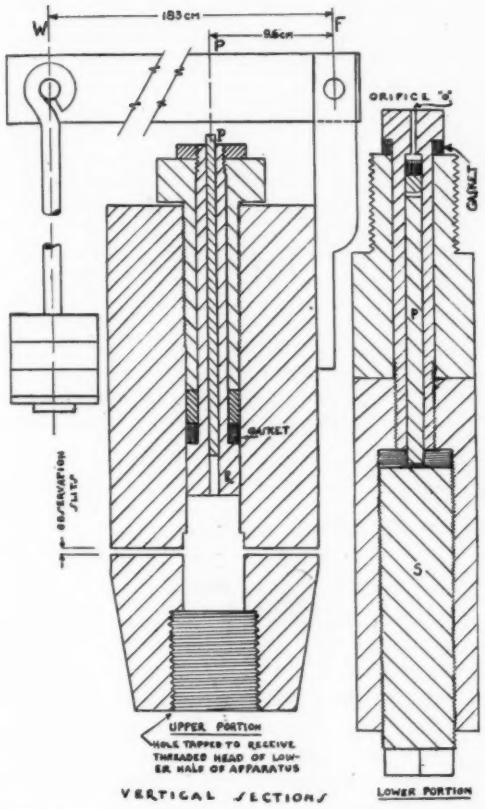

FIG. 2. Lever system and vertical sections through cylinder.

system, one force of which is the weights on a hanger at W, in Fig. 2, the other the pressure being measured, which is transmitted through the plunger P to the bar. The plunger P has a diameter of 6.35 mm. The distances along the bar from the fulcrum F are: to P, 9.6 cm, and to W, 183 cm. Thus the M. A. of the lever is 19.06. From these data it may be verified readily that a one kg weight placed at W will produce an internal pressure of 59 kg per cm². These pressures are, of course, in excess of atmospheric. The use of a spring balance at W, in addition to the weights, was resorted to, to eliminate errors due to friction. With a preassigned number of weights on the hanger, the liquid is compressed by tightening the screw S until the W-end of the bar is in approximately horizontal equilibrium. An upward pull is then exerted at W through the balance until the bar just begins to move past a certain mark on an upright; the reading of the balance is noted. Similarly, the bar is next pulled down by means of the balance, and a corresponding reading taken.

If we let P = the moment due to the internal pressure, U = the upward moment of the spring balance, D = the downward moment of the spring balance, W = the moment due to the weights at W, and F = the effective moment of frictional forces when the lever is moving up, and assume $-F$ = the moment of frictional forces when the lever is moving down, then

$$P+U=F+W, \qquad \text{for the upward movement,}$$

and

$$P-D=-F+W, \qquad \text{for the downward movement.}$$

Adding, $$2P+(U-D)=2W,$$

from which we have $$P=W-(U-D)/2.$$

Thus, the true pressure is calculated by using the weights plus one-half the difference between the downward and upward readings of the balance, as the force at W. It is estimated that the balance readings giving U and D are accurate to within 200g.

It was concluded that the most accurate method for determining the angle A of the liquid prism is to fill the sack with distilled water at a known temperature, and observe the angles of minimum deviation for the three or four prominent mercury arc lines at atmospheric pressure. We then obtain A by substituting these values, and the well-established values of the refractive indices of water for these lines in the formula,

$$\cot\frac{A}{2}=\left(\mu-\cos\frac{D}{2}\right)\Big/\sin\frac{D}{2}.$$

The values of A thus obtained for each spectral line have been, uniformly, in good agreement; their mean is used in the calculations.

Glycerin is used in the cylinder around the sack to transmit pressure to the liquid under study in the prism. Danger of corrosion of the steel parts, as would result from the use of water, is thus avoided. Furthermore, glycerin has a low coefficient of compressibility, so that high pressures can be attained with a minimum movement of the plunger and piston.

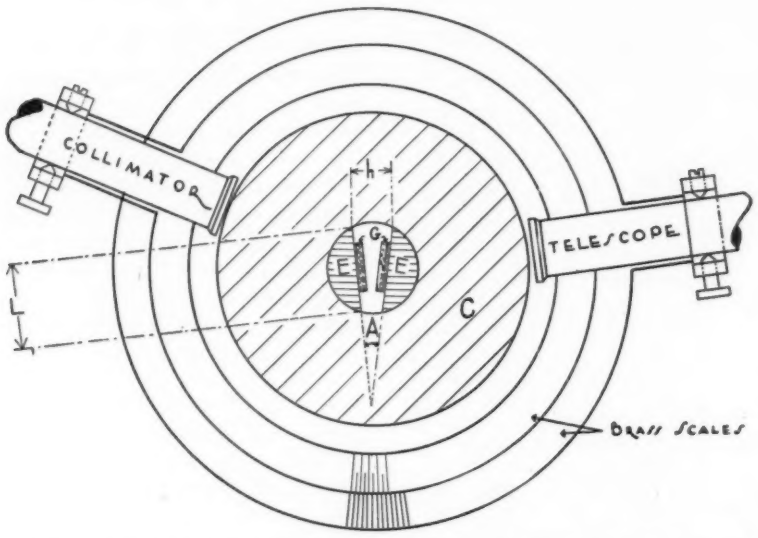

FIG. 3. Horizontal section through observation slits, with collimator and telescope.

III. ACCURACY

It is to be noted that the lens effect in the prism, due to the bulging of the glass under pressure, referred to by Poulter,[3] is negligibly small, as will be shown. The slits of the lugs upon which the windows are placed are twenty-two times as long as they are wide, and are placed perpendicular to the slit of the collimator. Therefore the cylindrical lens formed by the bulging of the glass into the slit can have no effect on the image of the collimator slit, i.e., the displacement of the image as a result of this bulging would be only perpendicular to the plane of refraction by the prism. A displacement of the image in this plane could occur only if there was an unsymmetrical bulging of the windows in their horizontal cross section. A symmetrical bulging of this type is equivalent to a very thin, liquid lens placed in the optical path before the objective of the telescope. Since such a lens does not change the direction of the rays emerging from the prism, the observed positions of the images are the same as those that would be given by flat windows. We have no reason to believe that the bulging of the windows under pressure is appreciably unsymmetrical. That there is some lens effect is indicated by the fact that it was found necessary to refocus the telescope to get clear images of the slit at higher pressures.

A calculation, by using data obtained with this apparatus,[4] was made to determine the change in the effective angle of the prism at high pressure. The eyepiece had to be moved up about 1 cm to refocus, supposedly as a result of the windows, and the lugs supporting them, bulging in a horizontal cross section. The radius of curvature of the prism windows was found to be 380 cm. By using the familiar formula, $r=y^2/x$, the displacement x of the center of the window was obtained, and from that the angle between the curved surface of each window and its plane surface under no pressure. This angle, $\Delta A/2$, was found to be on the average about 3′ 18″. The angle $(A+\Delta A)$ is the effective prism angle under pressure if only the portions near it are used to disperse the light. This, however, is the most unfavorable condition. Actually, the central portions of the windows were used, so that, effectively, ΔA is less than 6′ 36″. With this value of ΔA, and, as the prism angle, $(A+\Delta A)$, indices were calculated for spectral lines at the maximum pressure. These were compared with values of the indices obtained by neglecting ΔA. It was found that the errors in the latter were less than 0.0003. This is in the extreme, and is within the limits of experimental error.

The writers are indebted to Reverend Charles K. Hayden, S.J. for the drawings from which Figs. 2 and 3 were made.

[3] Poulter and Benz, Phys. Rev. **40**, 872 (1932).

[4] Lyons, "The Behavior of the 4930A Absorption Band of Uranine Solutions under High Pressure," this issue.

The Infrared Absorption Spectra of Mixtures of Alcohol and Water

DUDLEY WILLIAMS, R. D. WEATHERFORD AND E. K. PLYLER, *Department of Physics, University of North Carolina*

(Received December 9, 1935)

The absorption spectra of absolute ethyl alcohol and alcohol containing water were studied in the region from 1.5μ to 5μ. In the water-alcohol mixtures there appeared a band at 2.8μ not characteristic of either alcohol or water. For small concentrations of water the intensity of this band was found to increase with increasing water content. The presence of the band at 2.8μ was interpreted as indication of association between the water and alcohol molecules. This result is in agreement with the anomalous changes in volume and in specific heat which take place in mixtures of alcohol and water.

IT has been previously shown[1] that several aqueous solutions of acids and bases give rise to absorption bands in the infrared which are not characteristic of either the pure solvent or solute. These bands were interpreted as due to hydration effects in the solutions. The absorption spectra of alcoholic solutions of hydroxides were found to contain similar bands[2] and they were considered to arise from solvation effects in the solutions. The presence of these solvation bands in the spectra of these two types of solutions suggested the possible existence of associational bands in mixtures of liquids.

Fajans[3] has treated the problem of thermal effects in solutions by considering the heat of hydration of the ions. His work proved that in aqueous solutions the heat of hydration of the ions made up the greater part of the total heat of solution. For nonionizing solvents, the heat of solution is probably due to solvation effects. The results of Fajans indicate that substances which generate heat on mixing should have absorption bands on account of their associational energies. If the energy of binding is of proper size, the resulting absorption bands would be expected to occur in the near infrared.

Tests were carried out on several mixtures to ascertain if appreciable temperature changes took place. It was found that the addition of ethyl alcohol to water produced a change of temperature of several degrees. Other alcohols produced a similar change in temperature, but the study of the absorption spectra has been carried out only for various mixtures of ethyl alcohol and water. The experimental method used in this investigation has been previously described and need not be repeated here.

In order to obtain water-free alcohol for use in this study a sample of commercial absolute alcohol was dried for a week over anhydrous copper sulphate and was then distilled from metallic sodium. The water-free alcohol thus obtained was protected from air and immediately sealed in a dry bottle. Absolute ethyl alcohol and a solution containing 5 percent water was studied over the region from 1.5μ to 5μ. In the region of 2.8μ a band was observed for the cells containing water. In Fig. 1 the results for the region from 2.6μ to 3.6μ are shown. Curves *a* and *c* are for 0.03-mm cells. The absorption bands for the curves *b* and *d* were observed with a quartz spectrometer with effective slit width of 0.02μ and the band in the region of 2.8μ is well resolved. Curves *a* and *c* were observed with a fluorite prism with effective slit width of 0.08μ and the band at 2.8μ was not well separated from the alcohol band at 3.0μ. In the curves for the absolute alcohol some absorption occurs in the 2.8μ region and this is probably due to the presence of a small amount of water taken in by the alcohol when the cells were made. The bands at 3.0μ and 3.4μ are characteristic of alcohol and have been previously reported.[4] With the quartz prism the 3.0μ band occurs at 3.08μ. This change of position may in part be due to the overlapping of the 3.0μ and the 3.4μ band, but it is probably

[1] E. K. Plyler and E. S. Barr, J. Chem. Phys. **2**, 306 (1934); E. K. Plyler and W. Gordy, J. Chem. Phys. **2**, 470 (1934).

[2] E. K. Plyler and F. D. Williams, J. Chem. Phys. **2**, 565 (1934).

[3] H. S. Taylor, *Treatise on Physical Chemistry* (D. V. Nostrand Co., 1930), p. 334.

[4] E. K. Plyler and T. Burdine, Phys. Rev. **35**, 605 (1930).

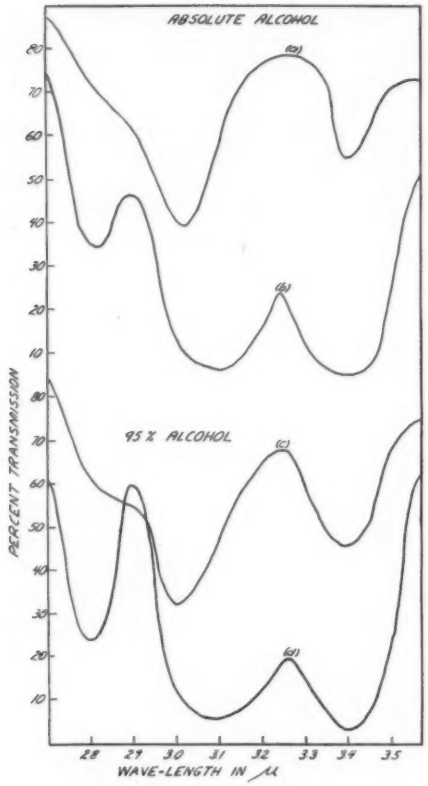

FIG. 1. The transmission of alcohol and an alcohol-water mixture in the region from 2.6μ to 3.2μ. (a) and (b), absolute alcohol; (c) and (d), 95 percent alcohol.

due to anomalous dispersion in the quartz in this region. On this account the fluorite prism was used for the other observations.

In Fig. 2 are shown the results for 100 percent alcohol and solutions in alcohol containing 5, 10 and 20 percent water. The absorption band at 2.8μ is present for the various concentrations and the intensity of it increases with increase in water. In addition to the usual chemical tests for the detection of water in alcohol, the presence of this band could be used as an indicator.

When larger quantities of water are present in the mixtures the 3μ water band overlaps the absorption of alcohol at 3μ and the band present in mixtures at 2.8μ. However, the 2.8μ band is still observed when 70 percent H_2O is in the solution. On account of the intense absorption band at 3μ in both water and alcohol, there is not much change in intensity with concentration. The observed absorption bands for the 50 percent and 70 percent water mixtures are shown in Fig. 3. The absorption band at 2.8μ is overlapped by the intense absorption at 3μ and its position cannot be determined with precision. In Fig. 2

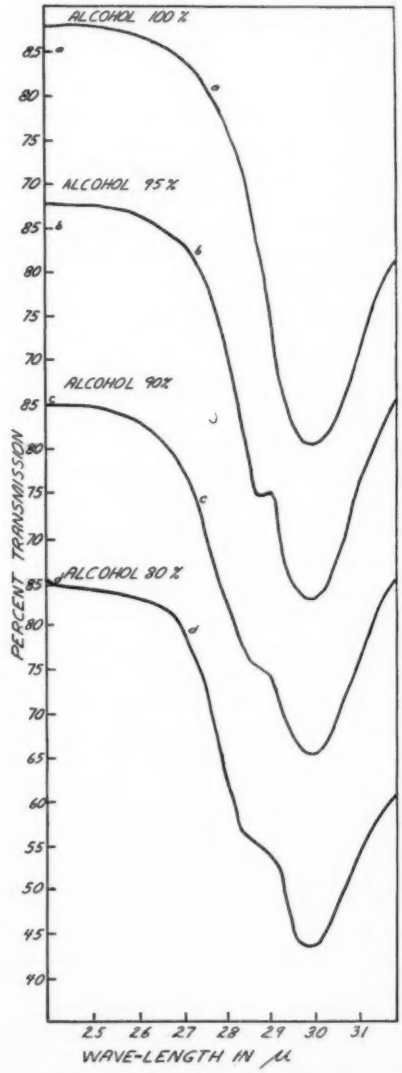

FIG. 2. The transmission of absolute alcohol and three water-alcohol mixtures in the region 2.6μ to 3.6μ. Cell thickness, 0.01 mm.

the band appears at 2.80μ to 2.85μ depending on the concentration, and in Fig. 3, where the amount of water was greater, the position is at 2.75μ to 2.80μ. It has not been determined whether this band actually changes in position with concentration or whether the change is apparent and due to overlapping with the 3μ band.

Since the 2.8μ band is not present in the absorption spectrum of liquid water or in alcohol, it must have its origin in the influence of one substance on the other. Small amounts of water added to alcohol may become diffused and act like a gas in solution. Then we should expect to have the spectrum of water vapor rather than liquid water in the mixture. The band at 2.8μ occurs in about the same region as the strong absorption bands due to water vapor at 2.66μ and 2.74μ. The main difference in the spectra of water and water vapor, besides a shift in position of the bands, is the band at 4.7μ in liquid water. The

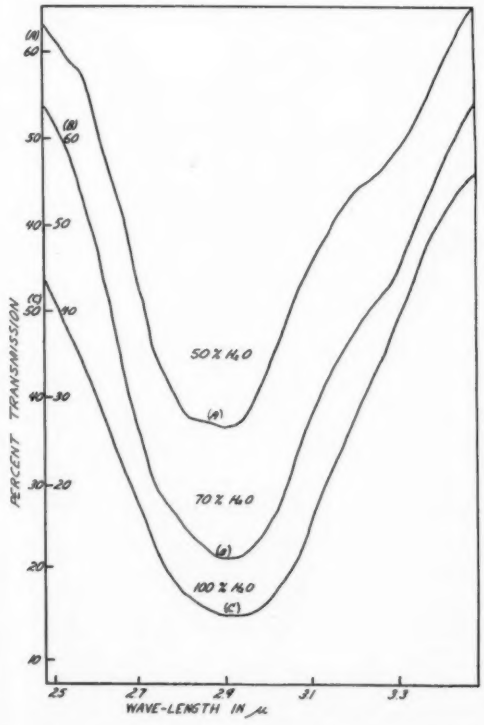

FIG. 3. Transmission of two water-alcohol mixtures and of pure water. Cell thickness, 0.03 mm.

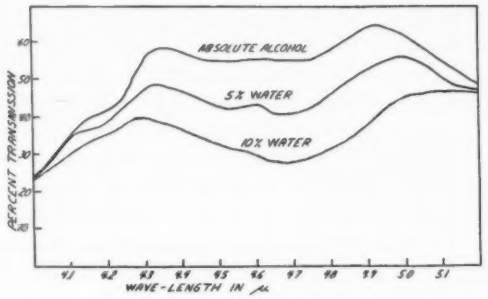

FIG. 4. Transmission of pure alcohol and two water-alcohol mixtures near the 4.7μ water band. Cell thickness, 0.05 mm.

water vapor does not have an absorption band corresponding to this and Ellis[5] has interpreted the origin of this band as due to energies of association between water molecules. If the liquid water has become dissolved into the form of vapor in solution and no association takes place with alcohol, no absorption should be present in this region. In Fig. 4 is shown the absorption spectra of ethyl alcohol and 5 and 10 percent water solutions. The curves show that the presence of water causes a decrease in the transmission in the 4.7μ region. We conclude from this result that at least some of the water molecules are associated with each other or with alcohol molecules. However, the absorption in this region does not prove that there are not some water vapor molecules present which might cause the absorption at 2.8μ.

Another interaction which might cause the presence of a band is the association of water and alcohol molecules. The energy of binding is not large and no doubt the combination would have a loose binding as compared with that existing in a water molecule. Evidently, if solvation is present, it may produce a change in all the energy levels which were present in the water and alcohol. In the associational effects which are present in liquid water the bands in the region of 3μ have been shifted in position about 0.2μ. In solvation of water and alcohol the change in position and also the intensity of bands may be different from the association observed in liquid water.

Since the alcohol and the water have an intense absorption band at 3μ, it was not possible to

[5] J. W. Ellis, Phys. Rev. **38**, 693 (1931).

study the effect on the absorption of each in this region due to the presence of the other. In Fig. 2 and Fig. 3 the bands gradually change from alcohol type, except for the 2.8μ band, to water type as the amount of water is increased. From the one band observed it is not possible to determine the origin of the band as due to modified water or alcohol or as due to vibration at an associated bond. On account of the small associational energy, the associational vibration may be present in the longer wave-length region. An attempt was made to study the changes of the water band at 6.2μ, but the absorption of alcohol in this region made it impossible to know what part of the absorption was due to water.

Since the 2.8μ band is not characteristic of either liquid water or alcohol, it must have its origin in the associational effects between alcohol and water. The anomalous changes which take place in mixtures of alcohol and water, such as in volume and in specific heat, indicate that association must occur.

The writers are grateful to Dr. R. W. Bost of the Chemistry Department, who aided in the preparation of the solutions and offered helpful suggestions.

On the Figuring and Correcting of Mirrors by Controlled Deposition of Aluminum[1]

JOHN STRONG AND E. GAVIOLA,[2] *California Institute of Technology, Pasadena, California*

(Received January 20, 1936)

It is possible to change the figure of reflecting surfaces quantitatively by controlled deposition of metals, evaporated in vacuum. The theory for calculating screens and the experimental technique are described. A spherical 12-inch mirror has been repeatedly parabolized, obtaining a surface perfect within 0.05 wave-length. A 5½-inch spherical mirror has been parabolized with the optical axis outside of its periphery. A defective parabolic mirror was corrected for turned up and down edges. A convex spherical secondary mirror was hyperbolized. The limitations and possible applications of the method are discussed.

INTRODUCTION

THE process of coating the surfaces of mirrors, prisms and diffraction gratings with a uniform film of metal by evaporation, in order to improve their optical, and chemical qualities, has been successfully and repeatedly applied.

As it is possible to obtain a uniform film by appropriate distribution of the aluminum sources[3] or by the use of a rotating screen (or both) it becomes also feasible to deposit a nonuniform coat of metal of known and controlled nonuniformity.

Experience up to date indicates that aluminum and chromium films are reasonably permanent if properly deposited. It is, therefore, possible to modify the figure of an optical surface permanently.

Mirror makers, both professional and amateur, know that all surfacing jobs require skill, patience and time but some of them much more than others. The figuring of a spherical surface is simple when compared to the difficulties encountered in the transition from a spherical to a parabolic figure. The elimination of a turned down edge is also a tedious and uncertain matter. Figures without central symmetry, like off-axis parabolic mirrors, for instance, are especially hard to obtain. By controlled deposition of aluminum, on the contrary, it is equally easy to make an axial or an off-axis parabolic mirror and to correct a turned down or a turned up edge. The procedure and technique is in all cases the same: instead of polishing off the raised zones as opticians do, one fills in the depressed zones.

The general procedure consists in distributing the aluminum sources so that, without a screen, a coating of uniform thickness would result; then a screen is designed and cut out of a sheet of metal and placed close to and in front of the surface to be modified. The function of the screen is to modify the deposit so that the desired nonuniformity in the coat is obtained. Provision must be made for rotating either the screen or the mirror during the evaporation process so that central symmetry is maintained. Once a good vacuum is obtained a calculated amount of aluminum is evaporated; the actual deposition of the metal, including the time of evacuation, takes only a few hours. A 12-inch spherical mirror was, for instance, made parabolic twice in a single day.

One of the main advantages of this method is, that if while modifying an optical surface, the result is not satisfactory, the deposited film can be dissolved away without affecting the original surface. The operation can then be repeated until the result is satisfactory. With this type of trial and error method only a few hours' work is lost. In the usual process of modifying surfaces by polishing, on the contrary, the process is not reversible; too much polishing at the wrong place may require the fine grinding of the whole surface.

PARABOLIZING OF A SPHERICAL MIRROR

The first step in the execution of the above method of figuring is to design the screen. Fig. 1 illustrates the geometry involved when it is planned to parabolize a spherical mirror. Let us assume that the spherical mirror has a diameter $2Y_0$ and radius of curvature R. The relative

[1] Part of the results contained in this paper were reported at the Meeting of the Astronomical Society of the Pacific on June 26, 1935.

[2] Fellow of the John Simon Guggenheim Memorial Foundation.

[3] The Evaporation Process and its Application to Aluminizing of Large Telescope Mirrors by John Strong, A.J.

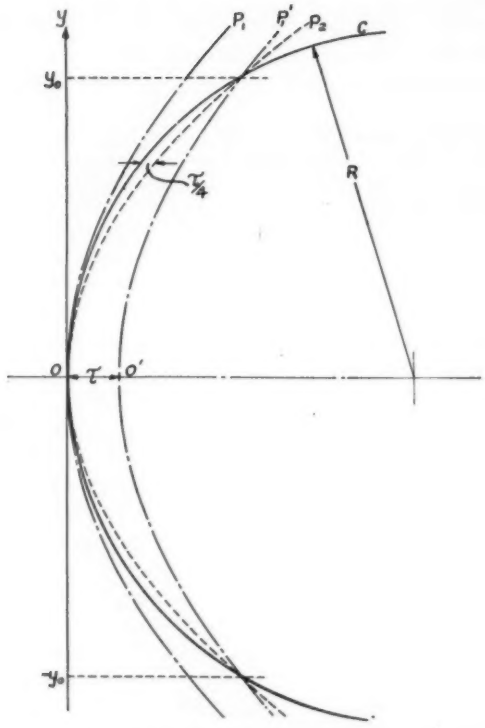

FIG. 1. Circle and parabolas important in figuring.

values of Y_0 and R have been exaggerated. Here in Fig. 1, the section of the spherical surface is represented by the circle C. Let us imagine the family of parabolas of different radii tangent to the circle at the center O. Among them there are two that demand our interest; the first, P_1', has the same radius of curvature at the apex. The other intersects the circle at the edge of the mirror and is tangent to it at the center. This one, P_2, has a slightly smaller radius of curvature than P_1. Let us displace the curve P_1 to the position P_1 by the amount τ. We see now that either of the two parabolic surfaces P_1' and P_2 will be obtained from the spherical one by filling in the space between them and the sphere with metal.

In designing a screen to do this we must calculate the thickness ΔX between the circle and parabolas as a function of the distance Y from the center O.

The equation of the circle $(X-R)^2+Y^2=R^2$ can be written in the form $X=R\pm(R^2-Y^2)^{\frac{1}{2}}$ which in second approximation and choosing the negative sign equals

$$X_C=Y^2/2R+Y^4/8R^3. \tag{1}$$

The corresponding equations for the parabolas P_1' and P_2 are

$$\text{for } P_1' \qquad X_{P_1}=Y^2/2R+\tau, \tag{2}$$

$$\text{for } P_2 \qquad X_{P_2}=Y^2/2R+Y_0^2Y^2/8R^3. \tag{3}$$

The radius in (3) is slightly smaller than in (1), as stated before, but the difference is negligible.

The differences between the first and the last two curves give us the thicknesses of the deposit in each case as a function of Y:

$$\text{for } P_1' \qquad \Delta X_1=\tau-Y^2/8R^3, \tag{4}$$

$$\text{for } P_2 \qquad \Delta X_2=Y^2(Y_0^2-Y^2)/8R^3. \tag{5}$$

τ is the amount that it was necessary to displace the parabola, P_1, with fourth-order contact in order to intersect the circumference at Y_0. $\tau=Y_0^4/8R^3$. This is also the maximum thickness of the required layer in this case. With the curve P_2 the maximum thickness is four times smaller and lies at $Y=\sqrt{2}Y_0$. Dr. R. M. Langer has kindly calculated for us that this is the most favorable case, requiring the smallest evaporation of aluminum.

The maximum thickness required to transform a sphere to P_2 can be written

$$\Delta X_{\max}=Y_0^4/32R^3=D/4096f^3 \tag{6}$$

if $D=2Y_0$ is the diameter and $f=(R/4)Y_0$ is the aperture of the mirror. We see the last thickness varies rapidly with the f value. For $D=12''$ and $f/6$ we get $\Delta X_{\max}=0.68$ wave-length; while for $D=12''$ and $f/3$ we get $\Delta X_{\max}=18.36$ wavelengths.

Screens can be designed using Eq. (4) or (5) by choosing a maximum angular opening to correspond to the maximum thickness. The ratio of the angular opening at a distance Y from the center to the maximum opening is then proportional to the ratio of the thickness at that point, as calculated from the equation, to the maximum thickness.

Fig. 2 reproduces the shape of the parabolizing screens that we have used in testing out these two methods. Screen a has a maximum angular opening of 90° at the center, b has a maximum,

again at the center, of 360°. Both decrease to an opening of 0° at the edge of the mirror. c has a maximum opening of 270° at a distance intermediate between the center and the edge. In each case $Y_0=6.19$ inches. The shape of the screen does not, of course, depend on the value of the radius of curvature of the spherical mirror, R, since a variation of R in Eq. (4) or (5) introduces only a constant factor that is taken care of when calculating the amount of aluminum to be evaporated. We call the method corresponding to the transition to P_1 the *central zone* method and the other the *intermediary zone* method of parabolizing.

The screens for both methods can also be used for mirrors of smaller diameter or for making off-axis parabolic mirrors. In the latter case a sector of constant angular opening can be covered up in the screen in order to avoid depositing aluminum beyond the edges of the zone which includes the mirror.

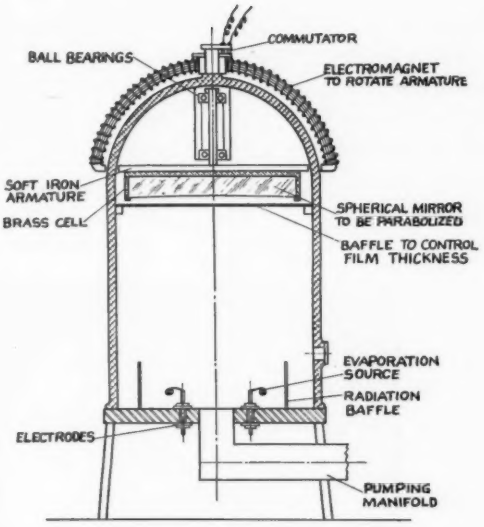

FIG. 3. Experimental arrangement.

EXPERIMENTAL ARRANGEMENT

The apparatus used consists of an evacuating system formed by two oil diffusion pumps backed by a Cenco Hypervac mechanical pump. The vacuum chamber is an aluminum bell jar (Fig. 3) resting on a platform to which it is sealed with bees-wax resin mixture (2 : 1 ratio). The platform supports six insulated binding posts to which tungsten coils loaded with aluminum are attached. The mirror to be aluminized is held face down in a brass cell which in turn is supported by a ball-bearing arrangement attached to the top of the bell-jar in such a way that the mirror can rotate freely around a vertical axis. An electromagnet is placed outside the bell jar and arranged so that it can be rotated. This acts in turn upon a soft iron armature attached to the brass mirror cell. Thus the mirror is made to rotate, and is kept turning at a rate of one or two revolutions per second during the evaporation process.

The diaphragm or parabolizing screen is placed immediately in front of the mirror and between it and the coils.

Once everything is in place and the vacuum has reached a value of 10^{-4} to 10^{-5} mm of mercury, the electromagnet is connected and set in rotation by hand; then one by one the coils are fired by applying from 10 to 20 volts potential to their ends; the rate of evaporation is controlled by observing the variations in the primary current of the transformer that feeds the tungsten coil; when the marked falling off of the primary current indicates that all aluminum in the coil has been evaporated, the circuits are disconnected and the apparatus left at rest to cool down before a second coil is fired.

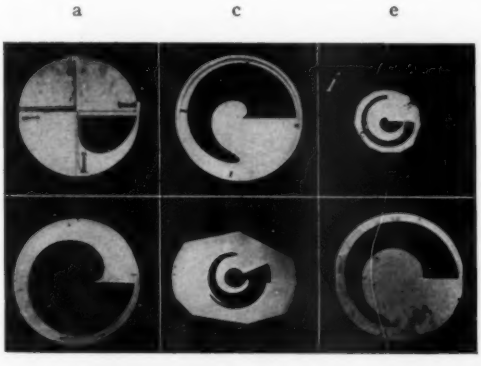

FIG. 2(a). Central zone screen with 90° maximum aperture; (b) the same with 360° maximum aperture; (c) intermediary zone screen, 2 percent maximum aperture; (d) screen used for correcting the 7-inch parabolic mirror; (e) hyperbolizing baffle employed with the convex Cassegrain mirror; (f) correcting screen for the off-axis mirror.

First Results

The first trial at parabolizing a spherical mirror was made using a $12\frac{3}{8}$-inch spherical test mirror of Pyrex glass of $152\frac{1}{4}$-inch radius of curvature. The surface of this mirror is true to a sphere within one-twentieth of a wave-length of green light ($\lambda = 5 \times 10^{-5}$ cm). Fig. 4a is a focograph at its center of curvature taken with a Foucault's knife-edge on the testing bench. Fig. 4b shows the appearance of the spherical mirror at the mean focal distance, taken with the help of a testing flat. Both represent the mirror before any correction was attempted.

The tungsten coils were arranged in a circle thus allowing the rotation of the mirror rather

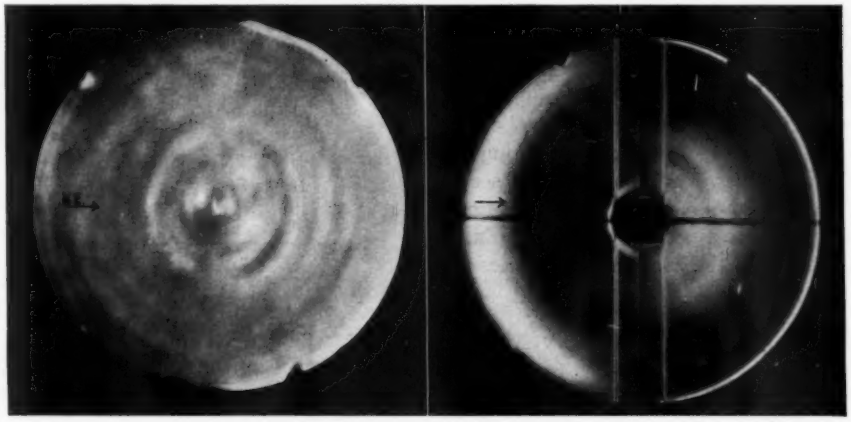

a b

FIG. 4(a) Spherical test mirror at the center of curvature. Notice the zones at 0.37 and 0.79 from the center. Their elevation is less than 1/20 of a wave-length. Contrast film and contrast paper was used to make them appear conspicuous. (b) The same mirror taken at the parabolic focus. The 0.37 zone is visible, the other one has disappeared. In this and in following focograms the direction of movement of the knife-edge is indicated by an arrow.

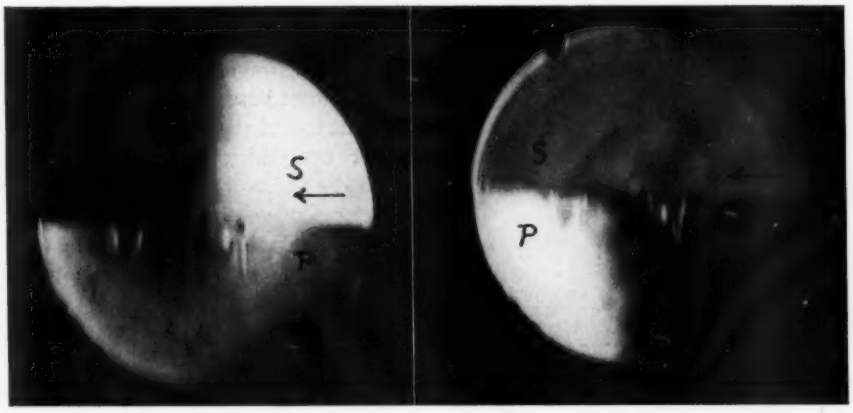

a b

FIG. 5. 12-inch spherical mirror parabolized on half its surface. (a) Focograph taken at the mean center of curvature of the parabolic half *P*. (b) At the center of curvature of the spherical part *S*. Notice the 0.37 and 0.79 zones conspicuous in Fig. 4a.

than the baffle. The central zone screen reproduced in Fig. 2a was used. The maximum thickness of deposit required for parabolizing by the central zone method was 2.6 wave-lengths (Eq. (4)). This thickness could not be obtained in a single operation. It was, therefore, necessary to reload the coils several times. The deposit thus obtained consisted of films of aluminum separated by layers of aluminum oxide which formed spontaneously when the vacuum was destroyed to reload the coils. The mirror was tested and focograms were obtained for each additional film. After the third layer, one-half of the coat was dissolved, a uniform thin film was deposited over the whole surface and the focograms reproduced in Fig. 5 were obtained at the center of curvature. This shows clearly the effect produced by the aluminum coat. Fig. 5a is taken at the mean center of curvature of the parabolized half of the mirror. This half shows the characteristic elevated intermediary zone. The spherical half appears as a concave depression. If the knife-edge is displaced toward the mirror a small distance until the spherical half is in focus, Fig. 5b is obtained. Here the parabolized part appears elevated relative to the sphere.

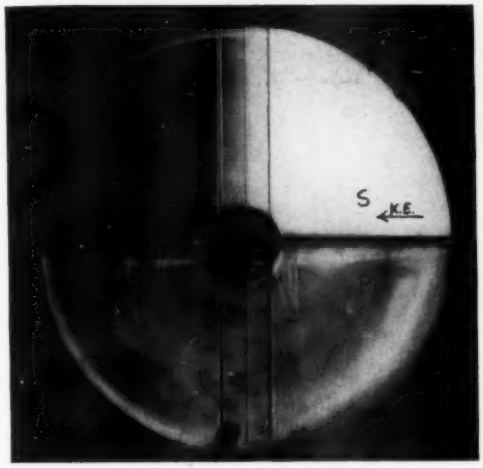

FIG. 6. The partially parabolized mirror seen from the parabolic focus after the 4th layer of aluminum was deposited. The edge of the parabolic half P appears turned up, due to "nontheoretical" distribution of sources.

As a test at the parabolic focus indicated that the mirror was still underdone, a fourth film of aluminum was vaporized while the spherical half was covered. Fig. 6 indicates the result of this operation. This focogram was taken at the parabolic focus. It can be seen that the lower half is now parabolized. Nevertheless there is a low circular zone in the outer part of this half, making the edge appear turned up. This low zone is due to the fact that the distribution of sources did not in this case fulfill the requirement that, without a screen, a uniform coat would result. This circumstance became serious in the case of the off-axis parabolic mirror that will be described later.

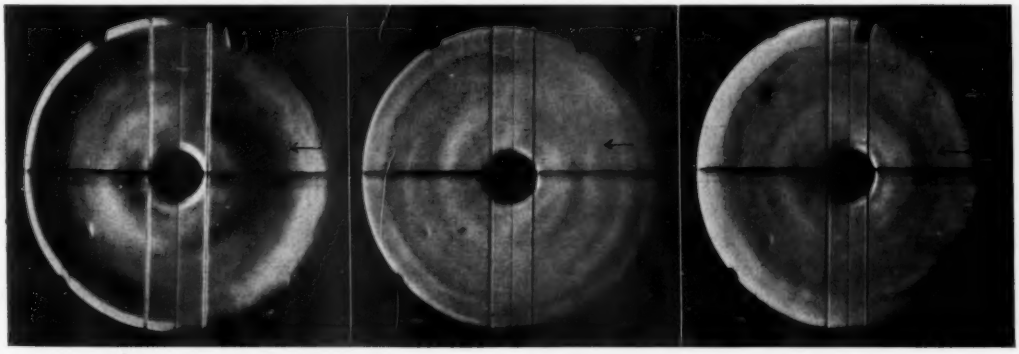

c a b

FIG. 7. 12-inch mirror parabolized with the intermediary zone screen. (a) Amount deposited just right. The 0.37 and 0.79 zones of the spherical mirror appear after the parabolizing (compare with Fig. 4a), showing that the treatment has introduced no new zones of any importance. Taken at the parabolic focus with a flat. (b) Same overcorrected: too much aluminum deposited. (c) Same undercorrected.

Parabolizing at the Intermediary Zone

The use of the intermediary zone screen (Fig. 2c) and 40-mil tungsten wire, capable of a loading of 1.29 g per coil permitted parabolizing the mirror in a single evacuation. The general procedure was the same as before. Fig. 7a, b, c, reproduces focograms of the parabolized mirror, taken with the aid of a testing flat, for three typical cases: In the first the amount of aluminum deposited is just right, in the second it is too large and the mirror is "overdone," in the third it is too small and the figuring is "underdone." It is interesting to compare 7a with 4a: it can be seen that the more prominent "zones" of the parabolized mirror were already present in the spherical glass disk; they have not been introduced by the deposition of aluminum. These zones are of heights smaller than one-twentieth of a wavelength. It is to be remembered that the zones will appear deeper in the present case since there are two reflections from the mirror as compared with one at the center of curvature.

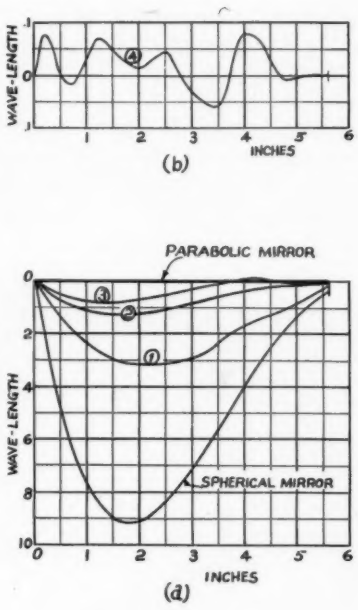

Fig. 8.

Amount of Aluminum Needed and Distribution of Sources

In order to obtain a desired figure in a single process of evaporation, it is necessary to distill just the right amount of metal. This amount can be calculated[3] in advance.

Our experiments, however, show that the actual layer thicknesses are smaller than the calculated ones, making the introduction of an empirical factor necessary. The value of this factor may be as low as 1/2. (See note added to proof.)

The first screens designed by us were calculated, assuming the distribution of sources to be such that the coat without screen would be uniform. Subsequently we found that the dimensions of the bell jar do not allow such distribution. Calculations showed that the coat without screen should be about 10 percent thicker at the center than at the edge for the present case, a prediction which was confirmed quantitatively by experiment. Although error thus introduced is negligible for thin coats it becomes important as the depth of the aluminum layer is increased.

With the intermediary zone screen for parabolizing the 12-inch mirror, where the maximum thickness of the deposit is 0.65 of a wave-length at $4\frac{1}{2}$ inches from the center, the error is barely noticeable. In the case of the central zone screen, on the other hand, where the maximum thickness reaches 2.6 wave-lengths, it becomes apparent and we have noted it already in Fig. 6, where it produced a low zone near the edge of the mirror. This error can be best eliminated by modifying the design of the screens. The simplest case would be to place the sources at the center of the jar, in which case the distribution without screen is most easily calculated.

Figuring an Off-Axis Parabolic Mirror

To make a mirror with its optical axis outside of its periphery is a difficult task with ordinary optical methods. We were able to use the intermediary zone $12\frac{3}{8}$-inch screen to parabolize a $5\frac{5}{8}$-inch spherical mirror of 63-inch radius of curvature with the axis of the parabola passing 9 mm beyond the edge of the mirror. All that is required is to have a parabolizing screen (assuming that the original glass disk has a spherical surface) more than double the size of the mirror and a bell jar of corresponding dimensions. In this case it required 15 times as much aluminum (Eq. (5)) as previously and with it the errors due

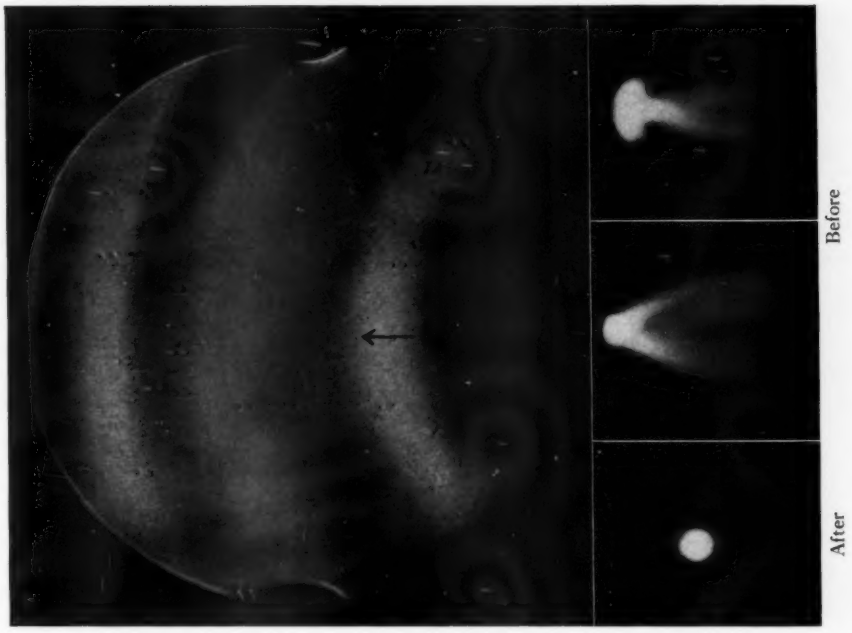

FIG. 9. Spherical mirror parabolized off-axis. (a) Focograph taken at the parabolic focus, 9 mm away from its edge, with the help of a flat. (b) Microphotographs of the image of a pinhole formed by the mirror in the off-axis set-up before (two pictures at different focal distance) and after parabolizing (the image is enlarged and blurred by vibrations of the building).

to the use of a "theoretical" screen with a "non-theoretical" arrangement of sources were magnified. The maximum thickness required was increased to nine wave-lengths. The coils had to be recharged several times before reaching that value. The final coat was thus formed by a superposition of thin aluminum layers separated by aluminum-oxide films.

The figure of the mirror was in this case followed, after the deposition of each coat, by a quantitative survey of the surface while the coils were reloaded. The method used for the survey is described in a paper to follow. Fig. 8a shows the history of this mirror. In it the X axis represents the theoretical parabolic surface; the lowest curve indicates the shape of the original spherical mirror before parabolizing; the ordinates indicate the amounts that this curve has to be raised in order to reach the parabolic figure, measured in wave-lengths. Curves 1, 2, and 3 are successive surveys of the surface during the process. When the mirror attained the figure of curve 3 it was apparent that the errors due to the use of the "theoretical" screen with the actual distribution of sources were such that it was necessary to design a new screen in order to proceed (see Fig. 2f). This was done and new layers were deposited by using the new correcting screen. The final curve of the mirror is reproduced in Fig. 8b. It can be seen that the mirror is now parabolized to less than a tenth of a wave-length. The corresponding focogram taken with the help of a testing flat at the parabolic focus, which was 9 mm outside of the edge of the glass disk, is reproduced in Fig. 9a. Fig. 9b shows direct microphotographs of the image formed, taken with a magnifying lens (14-fold magnification) before and after parabolizing. The two pictures (Fig. 9) of the image obtained with the mirror before parabolizing correspond to different focal planes. The image formed after the aluminum deposit (lower picture) appears blurred. This was

due to vibrations of the building while the photograph was taken. Its actual size, as seen by the eye, being smaller than that represented in the photograph.

Thick Layers and Bloom

Previous experience indicated that layers up to a thickness of 4 wave-lengths are generally free from bloom (a milky appearance of the surface). Beyond this bloom becomes, as a rule, increasingly conspicuous. The 9 wave-length deposit on the off-axis mirror followed the rule and exhibited some bloom. It is estimated that this bloom scattered about one percent of the light.

It is important to establish what causes the bloom and how it can be avoided. Our experiments do not allow us yet to answer these questions conclusively. All we can say provisionally is that bloom seems to be associated with low vacuum. Further experimentation will show if *ideal* conditions permit the depositing of much thicker layers without bloom. So far we have been able to obtain coats of up to 5 wave-lengths without any trace of it. Bloom can be partially, if not wholly, removed by treatment of the aluminum surface with a soft rouge pad such as is used for burnishing silver mirrors. Hard rubbing with a cotton cloth removes it completely but scratches the fresh aluminum coat.

Experiments by several authors on evaporated metallic films indicate that some of the optical properties of thin films are due to the fact that they do not show the characteristic crystalline structure of the metal until they become thicker than about 4 wave-lengths. To avoid this crystallization we have experimented with the following procedure; to form thick coats, deposit the metal layers of less than the critical thickness, the successive layers being separated by the thin oxide-films which form spontaneously if air is admitted into the bell jar. The adhesion between successive layers is as good or better than the adherence of the first one to the glass surface.

Correcting a Defective Parabolic Mirror

To correct a mirror requires first the quantitative knowledge of its actual figure. With this information it is then possible to design the appropriate screen. If the zonal errors are central symmetrical the surface can be surveyed by measuring the focal length of the different zones. Otherwise, the method described in a paper to follow is the most appropriate.

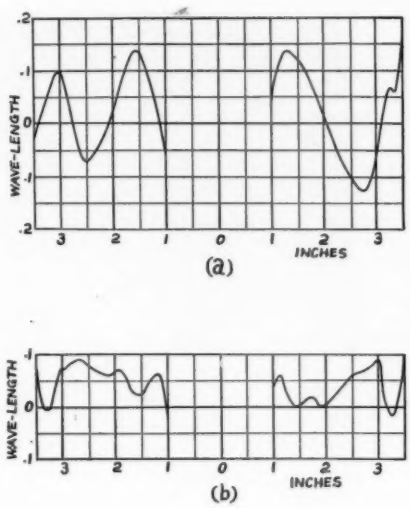

Fig. 10.

Experiments were made with a seven-inch disk having a two-inch hole in the center. Its focal length is 20.7 inches. Figs. 10a and 11a show the figure of the mirror before treatment. It is seen that the zones are asymmetric and that the outside edge appears as turned down on one side and up on the other. A central symmetric correcting screen was designed taking for each distance from the center the mean of the values corresponding to each side. The correcting deposits extended only to within one-half inch from the outside edge, as it was planned to use an aperture of only 6 inches. This outer zone received a thin uniform coat. The result produced by an aluminum coat, using this screen is indicated by Figs. 10b and 11b. As can be seen the whole central part excluding the outer $\frac{1}{2}$-inch zone has a satisfactory figure true to a parabola within a tenth of a wave-length. To our surprise the outside edge appeared now turned up on both sides, in the focograph and in the survey. This discrepancy was due to the fact that in making the latter we had introduced an improvement in the knife-edge testing arrangement so as

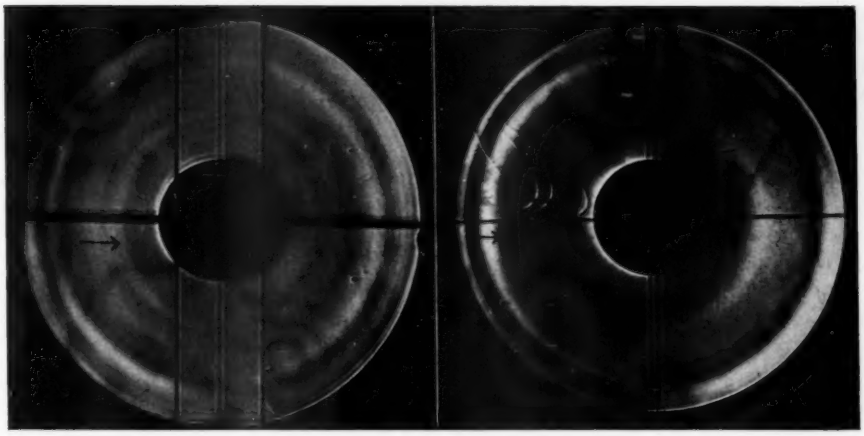

a b

FIG. 11. Defective 7-inch parabolic mirror. (a) After correcting with the screen Fig. 2d. The scratches visible are due to the testing flat and not to the 7-inch disk.

to decrease the effects of the parallax produced by the finite distance between the light source and the image (see next paper).

HYPERBOLIZING A CASSEGRAIN MIRROR

A small convex spherical mirror was transformed to an hyperbolic surface of revolution by evaporating a nonuniform film on it. This convex mirror was constructed to be used in the Cassegrain arrangement in conjunction with the above 7-inch parabolic mirror. It has foci at -7.2 inches and $+20.3$ inches giving $R=22.15$ inches and the eccentricity $e=2.094$ and a diameter $2Y_0=2\frac{3}{4}$ inches. The eccentricity is given by the expression, $e=(p+q)/(p-q)$, where p and q are the image distance and object distance, respectively.

The maximum thickness of metal required is 1.2λ at the center and at the edge. At $Y=(2)^{-\frac{1}{2}}Y_0$ the two surfaces are in contact.

For the design of the screen we have used the general expression

$$\Delta X=e^2Y^2(Y_0^2-Y^2)/8R^3, \qquad (7)$$

which gives the difference between any conic of eccentricity e which is in contact at $Y=0$ and Y_0 with a sphere with radius of curvature R. Setting $e=1$ Eq. (7) reduces to Eq. (5) for the case of a parabola.

The results of the figuring of this mirror indicate that when the maximum thickness limitation is not exceeded there is no greater difficulty encountered in going from a convex spherical mirror to a hyperbolic mirror than in going from a concave spherical mirror to a parabolic mirror. In short, if the primary surface is spherical it is possible to go directly to the hyperbola. In case the primary surface is not exactly spherical the departure of the curve will be evident with the knife-edge test in the Cassegrain set up after the mirror has been hyperbolized. Any zones which appear here may then be corrected by a second coat put on with a baffle designed especially for these zones such as the one used above with the 7-inch mirror.

CONCLUSION

The preliminary experiments reported in this paper indicate that the method of modifying the figure of a surface by controlled deposition of metals has a wide field of possible applications. It may lead to the production of cheap small Cassegrain and Herschelian reflecting telescopes for the use of schools and amateur astronomers.

The method may also have application in correcting the figure of existing telescope mirrors and also in removing zones and astigmatism where the usual methods of figuring are less expedient.

The main limitations of the method reside in the fact that it is not yet possible to deposit layers thicker than 5 wave-lengths without the disturbing appearance of bloom. This limitation may be overcome by further experiment.

Our method cannot and will not supplant the task of the optician: To apply aluminum it is first necessary to have an optically polished surface of a figure close to the desired final shape.

It is a pleasure for us to acknowledge our gratitude to Mr. Marcus H. Brown of the Optical Shop of the California Institute for his assistance in testing mirrors, to Mr. B. L. Graves, who kindly made available to us his master flat testing mirror, the 7-inch parabolic disk and the small Cassegrain reflector; to Mr. John S. Dalton of the Optical Shop of the Mount Wilson Observatory, who kindly loaned to us a testing flat and a knife-edge set and finally to Mr. W. C. Miller, who took most of the focograms reproduced in this paper.

Note added to proof, March 1, 1936: I have succeeded in getting pinhole pictures of evaporation sources. For this the arrangement consists of the source, a ½-mm hole in a thin sheet of mica at one inch distance and, beyond this one inch farther, a glass plate. Since the evaporated molecules propagate in straight lines it is possible to get a permanent reproduction of the evaporation source on the glass plate in the form of a thin metallic film. The surface density of this film varies from place to place on the plate corresponding to variations in the integrated emission from various points of the source. Fig. 12 shows a reproduction of such a picture. Here the source was a single U-shaped element of an evaporation unit formed from about 10 such U's with 40-mil tungsten wire. Each was loaded at the bottom with a drop of aluminum. This drop shows a faint outline for the element photographed in the reproduction but it will be observed, however, that far more vapor comes from the sides of the U than from the drop. This means that most of the aluminum flows out over the surface of the tungsten wire where the temperature is higher. The migration of the liquid on the wire is made evident by an accompanying decrease in the surface emissivity of the wire for visible light.

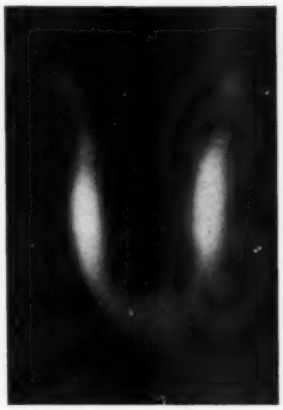

FIG. 12.

The evaporation is, then, not from point sources but it may be considered more nearly as from an ensemble of small line sources. This is especially true if all of them are vertical, or nearly so, as in the cases treated in this article. In this case more of the vapor is projected laterally. This gives rise, at least in part, to the factors referred to for computing the amount of aluminum to be evaporated to attain a given figure.

On the Quantitative Use of the Foucault Knife-Edge Test

E. GAVIOLA,[1] *California Institute of Technology, Pasadena, California*

(Received January 20, 1936)

The work described in the foregoing paper made the development of a quantitative method of surveying surfaces necessary, that could be used for local measurements and on nonsymmetric surfaces. The theory of the method and the experimental technique are described. The accuracy of the survey is better than 1/20 wave-length with visual subjective observation and could be carried up to 1/100 wave-length with objective photographic measurements. The errors of the Foucault knife-edge test, especially the one produced by parallax, are discussed. Ways of reducing or eliminating them are described.

INTRODUCTION

THE development of the technique for modifying optical surfaces, described in the previous paper, required a simple and accurate quantitative method of surveying the contour of the surface to be modified. The control of the results obtained by deposition of evaporated substances with a given screen and quantity of metal led to the same requirement. As long as the optical surface has central symmetry this requirement can be fulfilled by the well-known method of measuring the focal distances of the different circular zones with a knife-edge and integrating the results. However, if the surface does not have central symmetry, and this is often the case, this method fails. This is also the case if a purely local survey is desired or unavoidable, as in the case of a large parabolic mirror tested with a smaller flat.

The surveying method described in this paper satisfies the requirements stated above and has been of great assistance in the work of figuring by aluminizing. It may become useful as a quantitative control of figuring work in general.

DESCRIPTION OF METHOD

In Fig. 1a let OP be a spherical mirror with an elevated zone ab. We want to test it at its center of curvature C. Let L be the illuminated pinhole serving as source of light and I its image formed by the spherical part of the mirror. K represents the knife-edge. All light rays, that, like the one designated by the number 3 in the diagram, are reflected by the spherical surface, will concentrate on the real image at the point I. If the knife-edge is displaced until it touches the image and the eye is placed close behind this, looking at the mirror face, it can be observed that as the knife-edge is moved further in, the illuminated spherical part of the mirror fades out uniformly. In the case of the zone ab, the rays 4 and 5 reflected by the elements a and b are deviated counterclockwise and clockwise, respectively. When the knife-edge is at the position indicated in the figure, the element b will appear totally dark while a will appear bright when the rest of the surface fades out. Now, if one measures the positions of K at which the elements b and a darken, relatively to the position of the image I, one has data that allow the determination of the values of the angles α and β. These angles are equal to twice the inclination of the normals at the zones b and a, against the normals of the ideal spherical surface, at the corresponding points. In other words, the relative displacement of K, multiplied by the cosines of the angle between the optical axis and the observed ray, and divided by twice the radius of curvature R, is equal to the steepness of the corresponding zone, in relation to the ideal surface. If the mirror does not have a numerical aperture larger than $f/4$ the cosines can be considered to be constant and equal to unity.

When the light source is moved together with the knife-edge, as in the case of Fig. 7, the measured displacements must be multiplied by 2. These values can be plotted in a steepness diagram (Fig. 1b). The integration of this diagram reproduces the relative contour of the surface (Fig. 1c). In this last the spherical surface is represented by the axis Y; heights of the elevated zone are indicated in fractions of a

[1] Fellow of the John Simon Guggenheim Memorial Foundation.

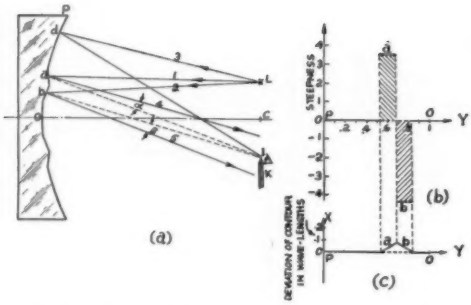

FIG. 1(a). Scheme of knife-edge arrangement. (b) Steepness diagram. (c) Contour curve.

wave-length of green light ($\lambda = 5 \times 10^{-5}$ cm). The altitude of the ridge is equal to the steepness times the width of the zone or what is the same, the surface enclosed, in the steepness diagram, by the line element a, the ordinates at the ends of a and the axis Y (shaded in the figure).

In a practical case the position of the point I is not known. The measurements have to be referred, therefore, to an arbitrary mean value. We shall consider this point more fully, later.

EXPERIMENTAL PROCEDURE

An actual measurement proceeds as follows. Once the mirror is aligned on the testing bench and the knife-edge placed in position, an easily readable scale is placed in contact with the face of the speculum, parallel to the displacement direction of the knife-edge and near the center of the former (see Fig. 7). It is advisable to draw at first a qualitative diagram of the surface as it appears for the particular focal distance chosen when the knife-edge is adjusted to cut into the real image formed by this surface. Fig. 6 shows a typical case of how the surface will appear.

Now a general plan for measurement is prepared. This involves writing down where the first dark edge or zone appears when the knife-edge is brought slowly to intersect the image. Also the points along the scale are noted at which the illumination fades out for successive positions of the knife-edge. For each position of the knife-edge there will, in general, be several such points. The "fading out" is well defined by the limits between the illuminated part of the surface and the growing dark spaces (see Fig. 6b). After the measuring plan is completed then the knife-edge for each set of limits is read on the graduated drum. Several sets of drum readings should be taken so as to avoid ambiguities in the drawing of the steepness curve. One must keep in mind that a local error in this curve produces a systematic error in the integrated contour curve.

There are several reasons for the careful preparation of a general plan or scheme of measurement. First, it simplifies the task of making readings, as each drum reading corresponds in general to several points on the mirror. Second, it avoids displacement of the knife-edge produced by thermal expansion of its support, deformations of the testing bench caused by variations in temperature and humidity because it shortens the time of measurement.

It should be remembered that one is measuring displacements of the order of less than a ten-thousandth of an inch and that readings of the drum should be reproducible with that accuracy. To control these systematic errors it is convenient to repeat, at the end of a series, the first and second measurements. The difference found, if any, can be distributed equally among the intermediary readings. If the knife-edge set up permits it, one should always make two independent measurements of the same surface, once with the edge approaching the image from the left and once from the right. The zone that appeared dark first in the one case will remain bright in the other. The average of these two measurements is free from subjective systematic errors.

The zone near the edge is generally difficult to measure on account of the light diffracted by the edge itself. This zone is, however, narrow (about $\frac{1}{8}$ inch), and the value for it can often be extrapolated if the visual observation does not discover sharp changes of slope in it. The common tendency of the beginner is to underestimate the inclination of the edges, producing a flatter contour curve than the true one. Besides this, there is the parallax error, described below, that works in the same direction.

RESULTS

To obtain an idea of the reliability and accuracy of the method, the best procedure is to measure a surface twice, with the knife-edge

entering the image from a different direction in each case, and to calculate the two contour curves independently. Fig. 2 is an example of such measurement (corresponding to the right side of the mirror illustrated by the focogram shown in Fig. 10a of the foregoing paper. The differences between the two contour lines are of the order of 2 to 3 hundredths at the left-hand edge. These figures, incidentally, give an idea of the accuracy that can be obtained by direct visual observation.

It should be stated that no special screw has been used for measuring the displacements of the knife-edge. The determinations are accurate because they are relative.

An additional and thorough test of the surveying method was performed by measuring with the help of a testing flat, a slightly undercorrected 12-inch parabolic mirror, first at the center of curvature and then at the parabolic focus. The observed difference between the two contour curves so obtained, should be equal to the theoretical difference between a perfect sphere, and a perfect parabola of corresponding radius of curvature and diameter. Fig. 3 reproduces the result of this test. The errors of the difference curve are of the order of 0.03 wave-length. This shows that a parabolic figure can be quantitatively determined at the center of curvature to 0.05 wave-length.

The difference between the measured curves can be expected to approach the theoretical values only if the focal distance chosen in the measurement with the test flat is exactly equal to half the radius of curvature chosen in the other

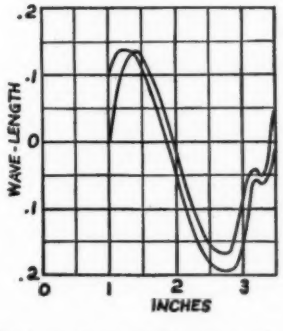

FIG. 2. Contour curves of the same mirror measured independently with the knife-edge moving in opposite directions.

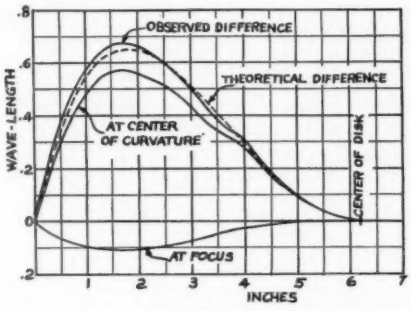

FIG. 3. Underdone parabolic mirror measured at the center of curvature and at the parabolic focus. The difference between the two curves should be equal to the theoretical contour observed at the center of curvature.

case. This can hardly be accomplished experimentally. The measurements can, however, be reduced to that case. To understand this, we must go a little deeper into the theory of the surveying.

DISCUSSION OF A PARTICULAR CASE

Let us suppose that we have a parabolic mirror, the cross section of which is represented by the expression $X = Y^2/2R + Y_0^2Y^2/8R^3$. Eq. (3) of foregoing paper and that we want to measure its contour at the center of curvature. The surface of reference is then a sphere and the deviations of the parabolic curve from it are $\Delta X = Y^2(Y_0^2 - Y^2)/8R^3$ (Eq. (5)). The thing one can measure directly is the steepness of the last function

$$d(\Delta X)/dY = Y(Y_0^2 - 2Y^2)/4R^3. \qquad (1)$$

As the measurements of any set are relative to each other, the true line of reference corresponding to the position of the ideal image is unknown. An arbitrary constant is added to the reading in order to define the zero line of the steepness diagram. This is given in Fig. 4. The scale of steepnesses is indicated on the left of the diagram, with $Y_0 = 6.19$ inches and $R = 152\frac{1}{4}$ inches. If we choose the line A–A as zero line and integrate graphically by dividing the surface between this line and the steepness curve in narrow vertical trapezes we obtain the curve D–D. The scale of elevations is at the right of the drawing. This is the contour of the parabolic surface when observed from its mean center of

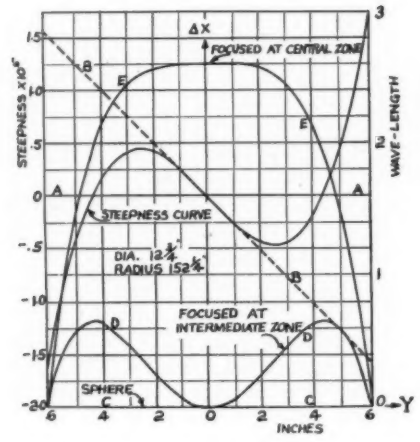

FIG. 4. Theoretical curves of a parabolic mirror measured at the center of curvature.

curvature and corresponds to Eq. (5). It represents also the amount of aluminum that must be deposited on a spherical mirror to parabolize it with an intermediary zone screen.

The zero line A–A has been chosen here so that the ends of the contour line ($-Y_0$ and $+Y_0$) be equal. If the line A–A is displaced parallel to itself, the curve D–D will rotate and change its relative form due to addition of a linear function. If it is referred, however, to an oblique Y axis, one can obtain the same ordinates as before. This means that the choice of the zero line A–A is highly arbitrary since the contour curve D–D can always be referred to any base line that fits it best, parallel to Y or not.

The apparent contour of the parabolic surface depends on the value chosen arbitrarily for its mean center of curvature. In Fig. 4 it has been chosen so that the center and the edges of the contour curve D–D are at the same level. In an actual measurement it cannot be told in advance with sufficient accuracy which radius of curvature will realize this case. But this is not necessary, for having one steepness curve, one can derive contours for any knife-edge position by simply rotating the zero line A–A.

CHANGE IN FOCAL DISTANCE

If the general equation of a parabola $X = Y^2/2R$ is differentiated, partially in regard to R one obtains

$$\delta X = -\frac{Y^2}{2R}\cdot\frac{\delta R}{R} = QY^2 \qquad (2)$$

where $-\delta R/2R^2$ is set equal to the constant Q. Adding δX (Eq. (2)) to ΔX (Eq. (5) l.c.), and differentiating in regard to Y the new steepness curve

$$d(\Delta X)/dY = Y(Y_0^2 - 2Y^2)/4R^3 + QY \qquad (3)$$

is obtained. This is identical with the previous steepness curve if referred to a Y axis inclined $2Q$ in respect to the former one A–A (Fig. 4). A variation in focal distance is then equivalent to a change of the zero line in the steepness diagram.

As an example, let us take B–B as the new zero line and repeat the graphical integration. The result is the contour line E–E which corresponds to the appearance of the parabola when the knife-edge is set at the center of curvature of the central zone. This contour line is furthermore the graphical representation of Eq. (4) of the foregoing paper and indicates the distribution of aluminum that has to be deposited when using the central zone screen.

THE ERROR OF PARALLAX AND ITS ELIMINATION

When a mirror is surveyed with the help of a testing flat and the usual knife-edge arrangement in which the pinhole or slit and the image are separated by a finite distance, an error is introduced. This does not affect the image appreciably but yet may be of considerable importance for the interpretation of the knife-edge test. This error arises only when two or more mirrors are involved. Its origin lies in the fact that in this case a ray of light is reflected twice by the mirror under test before reaching the eye and each time by a different element of its surface. Let us

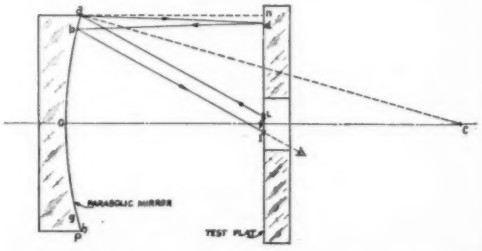

FIG. 5. Parallax when testing with a flat mirror.

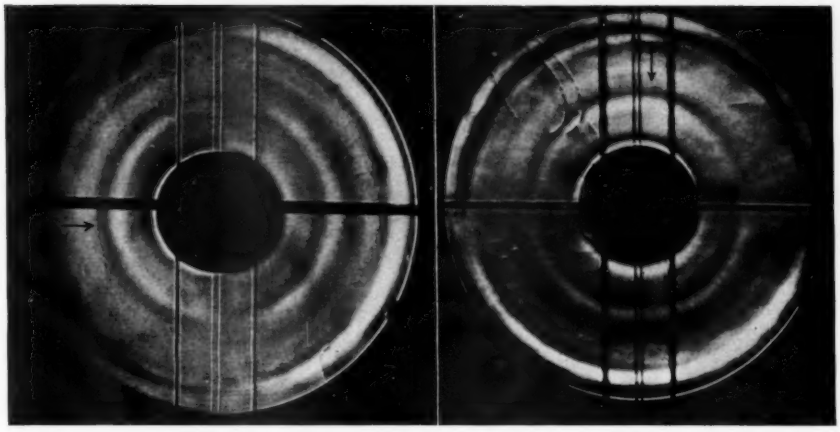

a b

FIG. 6. Two focographs of the same mirror taken with and (nearly) without parallax. (a) Knife-edge displaced parallel to the parallax vector. (b) Knife-edge displaced perpendicular to the parallax vector. Notice that in the first case the surface appears more asymmetric and smoother than in the second.

assume that light source L (Fig. 5), image I and testing flat are in the focal plane of a parabolic mirror. Let us follow the trajectory of the ray of light that starting at the source L strikes the mirror at its edge a. If the source L were at the focus f the ray reflected at a would follow the line a–n, parallel to the optical axis O–C. In the actual case it follows the direction a–d. The distance n–d and L–f are equal. After reflection at the flat the ray strikes the parabolic mirror at the point b and finally reaches the eye at I. The distance a–b is double the length n–d and equal to the separation between light source L and image I. This separation is generally of the order of several millimeters in the best cases. The displacement a–b is proportional to the distance of the flat from the parabolic mirror.

Fig. 6 of the foregoing paper gives a striking illustration of this point. The imperfections of the parabolic half appear double and displaced by about 6 mm. A first result of the parallax thus introduced is that the observed or measured inclination of the ray b–I is not determined alone by the surface element at b but also by the one in a. One is thus taking average values for elements of constant vectoral separation along the mirror. If the relative steepness of the actual surface against the theoretical surface of reference changes rapidly or periodically, considerable errors result. Let us assume, for instance, that the mirror has periodic zones of sinusoidal shape and that the difference between two successive valleys is equal to 2 cm. If the separation L–I happens to be equal to 1 cm the zones may not be seen along the diameter parallel to L–I even if the amplitude is rather large (plane of the Fig. 5). They will be more or less distorted in the areas of the surface on either side of this diameter, giving to the mirror an asymmetric aspect.

Let us consider now the case of the parabolic mirror of Fig. 5 assuming that it is under corrected so that the edge appears turned up. If one makes a horizontal cut-off (plane of the picture) the observed inclination of the edge will be the mean relative value of the elements a and b. If, now, one makes a vertical cut-off, without changing the relative positions of light source and image, the points corresponding to a and b (not in the plane of the picture but now standing 90° to this plane) will have the usual separation but they will both be at the same distance from the edge. The observed inclination will be now greater (and nearer the true one) than in the former case and the mirror will appear astigmatic.

A second result of the parallax is that the region between g and the edge appears dark for any position of the knife-edge. The apparent horizontal diameter is shortened by that amount

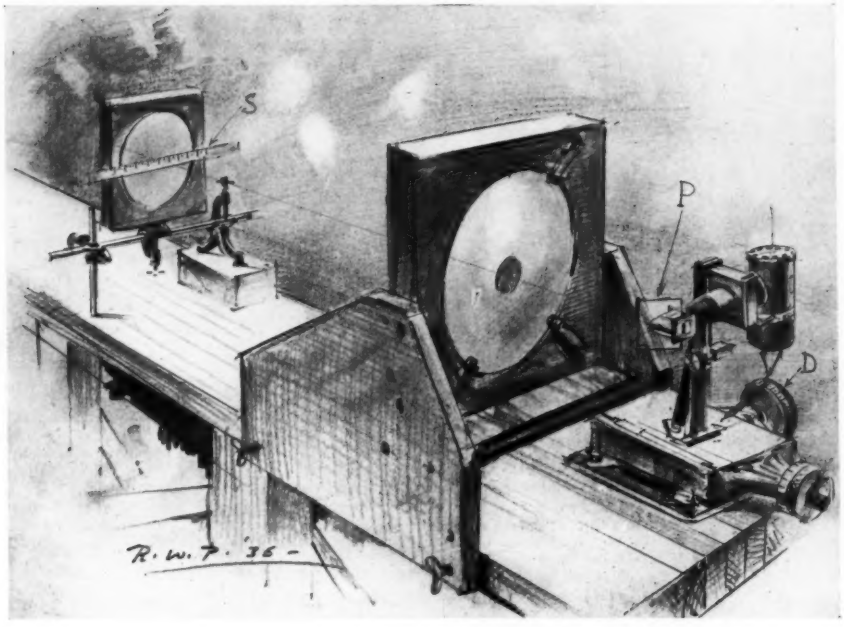

FIG. 7. Measuring a parabolic mirror at the focus with the help of a perforated flat without parallax. *P*, half-transparent thin glass plate at 45° with the optical axis. *D*, drum for measuring the transversal displacements of knife-edge and source of light. *S*, scale in contact with the surface to be surveyed. (Sketch by Russel W. Porter.)

and a focogram taken shows an elliptical image of the circular mirror.

In Fig. 6a the effect of parallax can be plainly seen. In one of the focograms the knife-edge was displaced along the parallax vector and the zone near the edge appears turned down on one side and up on the other and the zones in the central part appear flat and smooth. In Fig. 6b, taken with the knife-edge moving in a direction perpendicular to the parallax vector, the edge of the mirror appears turned up symmetrically and the central zones appear steeper and better defined. In both cases the surface observed was a 7-inch parabolic mirror tested with the help of a flat. The parallax was 8 mm.

The parallax error can be considerably reduced by displacing the knife-edge always in a direction perpendicular to the line connecting the light source with the image. This is done in some optical shops. It can be completely eliminated by using a half transparent plate arrangement, as the one pictured in Fig. 7. The only disadvantage of this set-up is that the light dispersed by the half-transparent surface during the first reflection produces a uniformly faintly lit background, for the observations, instead of a black one. A very thin plate must be used. Otherwise, the astigmatism due to the plane parallel becomes apparent; light coming from opposite ends of the diameter of the mirror contained in the plane of incidence traverses the half-transparent plate under different inclinations, meeting different glass thicknesses in their path.

PRECISION MEASUREMENTS

If it is desired to increase the accuracy of the surveying method here described one can take two main measures: (a) To increase the precision of the readings of the positions of the dark and bright zones on the surface of the mirror using an observing telescope, and (a) to improve the determination of the displacement of the knife-edge by using a good micrometer screw and a divided drum of a size that permits direct reading to 10^{-4} inch. Better still is to take a suc-

cession of focographs of equal exposure time on a roll film, corresponding to equal displacements of the knife-edge. If the film is then developed uniformly, a very accurate steepness curve can be obtained. The scale in front of the mirror is unnecessary in this case as the position can be measured on the photograph.

Conclusion

The method described here for surveying optical surfaces may not be completely new. It may have been used in one form or another in optical shops or by amateur mirror makers.

The elimination of parallax, while using two or more optical surfaces in combination, by employing a half-transparent thin glass plate, has been previously accomplished by Mr. Harold A. Lower of San Diego, California, and probably by several other opticians and amateur astronomers. To my knowledge, no description of these methods has, however, appeared in the literature. This fact made it appear desirable to publish this paper.

I wish to express here my thanks to Dr. John Strong for his constant cooperation and valuable assistance; to Messers B. L. Graves, Harold Lower and Roger Hayward for placing at my disposal diverse mirrors; to Mr. John S. Dalton for loaning me the knife-edge set (to which the half-transparent plate was added) reproduced in Fig. 7; to Mr. Russel W. Porter for making this drawing, and to Dr. R. M. Langer, who made many helpful suggestions during this work.

Objective Measurements of Graininess of Photographic Materials

A. VAN KREVELD, *Laboratory of the Netherlands Foundation for Photographic and Cinematographic Research*

(Received October 22, 1935)

INTRODUCTION

IN a former paper[1] the author has described a general theoretical basis for expressing and measuring the graininess and resolving power of photographic emulsions with respect to their different applications. Two properties of this system are:

1. All quantities, which are used, can be measured *objectively*.

2. To speak of "the" graininess and "the" resolving power of photographic emulsions has no meaning since for each application a special "quality" must be defined. This quality indicates the suitability of the emulsion for the application in question.

This paper will deal with the practical realization of the measurements as far as graininess is concerned.

First we shall make some general remarks. If we wish to have an objective measure for the practical graininess we cannot use the real grain size; this statement is made by nearly all authors.[2] Thus neither the method of measuring the size of the grains with the microscope nor the method of Eggert and Archenhold[3] based on the Callier effect (also giving the real grain size) may be applied to practical purposes.

The reason for this is simply that the resolving power of the optical systems used in practice (enlarger, microphotometer, sound-film system, projecting lens) is much too low to separate the individual grains. All these systems integrate the density over an area of at least $100\mu^2$. So we are not interested in the size of the individual grains but only in their grouping, in their distribution over the plate.

It is clear, that the grain size distribution *has* a certain influence on the grouping of the grains, but it is not the only factor. Other possible factors are: The inhomogeneity of the undeveloped emulsion and the clustering of the grains caused by the developer. For the present we are not interested in these individual factors but only in the final result of them, that is the practical graininess.

If we formulate the problem in this way, a quite natural measure for the graininess suggests itself. We simply use some registrating microphotometer, measure with it an area of constant density and compute the graininess from the fluctuations in the registrogram.

This method was proposed by Dunham.[4] The author of the present article gave an exact definition of it as part of the general system mentioned above and described an apparatus to measure it in a direct way.[5]

THE PRACTICAL GRAININESS

Fig. 1 shows the registrogram of a homogeneous black area, bordered by unexposed parts. XAY is the reference line, which indicates the zero of the galvanometer. The logarithmic density D is obtained from: $D=\log AB/AC$.

Now we draw the horizontal average density line EF and measure the total area of the density "waves" lying on both sides of it. This can be done with a planimeter after enlarging the registrogram. If we divide this area by the length EF of the black area in question we find an average deviation δ, which implies a certain

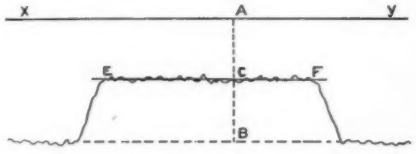

FIG. 1. Registrogram of a homogeneous black area, bordered by clear parts.

[1] A. van Kreveld, Phot. J. **74**, 590–596 (1934).

[2] A. C. Hardy in F. Ross, *The Physics of the Developed Image* (Rochester, 1924), pp. 21–34; A. Küster, Agfa-Veröffentlichungen **3**, 93 (1933); S. D. Threadgold, Kinotechnik **14**, 297 (1932); Ornstein, Moll and Burger, *Objective Spectralphotometrie* (Braunschweig 1932), p. 75.

[3] J. Eggert and G. Archenhold, Zeits. f. physik. Chemie **110**, 497 (1924).

[4] Th. Dunham, Bericht VIII. Int. Phot. Congress p. 294 (1932).

[5] A. van Kreveld, Communication IX Int. Phot. Congress, Paris, 1935 (not yet printed).

average deviation from the density ΔD, obtained from: $\Delta D = \log (AC+\delta)/AC = (\delta \times 0.434)/AC$.

Now one might think, that two emulsions, for which ΔD is the same function of the density, have also equal graininess-qualities. For most applications however this conception is too simple.

We shall give two examples:

1. The negative-positive process; if we have two emulsions with the same $\Delta D(D)$ function but of different contrast, by using a softer printing material for the emulsion with the steeper gradation, we obtain prints of similar appearance except that the print made from the emulsion with the steeper gradation has a lower graininess.

2. In photographic photometry light intensities are computed from measured densities. A certain inaccuracy of the density will lead to an inaccuracy in the intensity which will be smaller the steeper the density curve of the emulsion.

So in both examples the steeper emulsion is the better and we see that it is not sufficient to measure ΔD, but that the density curve must also be considered. And the practical measure for the two above examples is not ΔD but the relative deviation from the intensity $\Delta J/J$, computed by means of the density curve from the formula: $\Delta J/J = \Delta D/(dD/d \log J)$, $dD/d \log J$ being the slope of the density curve.

For the formulae for other applications see the former paper of the author.[1]

Experiments on ΔD

In order to obtain a verification (perhaps superfluous) of the contention that the fluctuations of the density are caused by the silver grains only, we made the following experiments:

1. A microphotogram was made of a plate of homogeneous density, such as shown in Fig. 1. Subsequently we bathed the plate in water for an hour, pressed a microscope coverglass on it in order to make the surface of the gelatin quite flat and registered the plate under these conditions. The fluctuations of the density line were practically unchanged.

Fig. 2. Registrogram of a plate freed from silver grains.

2. The same plate was bathed in Farmer's reducer, which dissolved the silver grains. The plate was washed, dried and registered again. The fluctuations had disappeared. Only some isolated deviations at one side of the line indicated the scratches and dust on the surface of the emulsion (see Fig. 2).

A second question which interested us was: what are the mathematical properties of the registrogram? Is it a simple error curve or does it show any periodicity or other remarkable properties?

To answer these questions we have analyzed eight registrograms systematically. The data are given in Table I.

Table I. *The plates for the statistical analysis.*

No. of Plate	Emulsion	Development	Density
1	Ilford special rapid	Rodinal 1 : 20 6 minutes 18°C	0.04 (=fog)
2			0.10
3			0.39
4	Ilford Empress		0.02 (=fog)
5			0.07
6		paraphenylenediamine according to Eder[6] 30 minutes, 18°C	0.43
7	Ilford special rapid		0.09 (=fog)
8			0.14

Each density was measured over a length of 2 mm. As the magnification of the Moll microphotometer,[7] which we used, was $\times 50$, the length of each registrogram was 100 mm. The image of the slit of the microphotometer, projected on to the photographic plate, had a size of $250 \times 14\mu$.

The deviations on the registrograms are too small to be measured exactly. For that reason we reproduced them with a magnification of $\times 4$ on "Mimosa"-Aktographenpapier, which is a very sensitive contrast paper. During the exposure this paper was covered with a piece of cellophane, printed with a quadratic millimeter scale parallel to the reference line of the registrogram (see Fig. 3). This facilitated the measurements.

Each curve was measured as follows: From the millimeter scale an arbitrary horizontal line was chosen and the distances r of the points of the curve to this reference line were read from millimeter to millimeter. From the 400 readings r obtained in this way the mean was taken and thus we determined the horizontal average density line. Then the deviations from this line were calculated and their frequency law was

[6] J. Eder, *Rezepte, Tabellen, Arbeitsvorschriften*, 14–15 edition (Wien, 1933), p. 76.

[7] Ornstein, Moll and Burger, reference 2, p. 60.

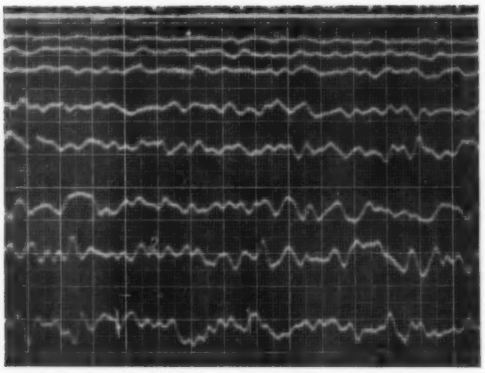

FIG. 3. Enlarged registrograms printed with millimeter scale.

determined. The frequency laws of the eight plates are given in Fig. 4.

The crosses indicate the observed frequencies. The full-drawn line in each figure is the Gaussian frequency law, $y=(h/\pi^{\frac{1}{2}})\exp(-h^2x^2)$, with the same mean value and the same mean deviation as the observed values.

We see that the observations satisfy the Gaussian law fairly well, especially when we consider that each frequency law is based on not more than 400 measurements. A slight systematical dissymmetry towards the positive side cannot be denied; it is due to dust and scratches on the surface of the plate, which cause naturally only positive deviations. For that reason the plates for our following experiments were finished very carefully and dried in a special box free from dust.

The fact that the Gaussian law holds does not imply that the registrograms are real error curves, for the succession of the deviations might still fit some special law. We studied this question by applying the following statistical method:

Let i be a fixed interval of the successive numbers of the readings r. Then we subtract reading No. 1 from reading No. $1+i$, No. 2 from No. $2+i$, No. 3 from No. $3+i$ and so on. In this way we obtain $400-i$ differences, of which we take the mean, say m. Now we chose another value for i and again calculate m. Thus we find m as a function of i. The results are given in Table II.

The first column gives the mean deviation (in millimeters of the enlarged registrogram), which is proportional to ΔD.

The second column gives the first column multiplied by $\sqrt{2}$; the further columns give m for different values of i. Under each value of i the original distance on the plate corresponding to this interval is given in parenthesis.

If the registrograms are real error curves, m will be independent of i and will satisfy the equation: $m=\Delta D\times\sqrt{2}$.

The table shows, that this equation holds for the Nos. 2, 3, 4, 5, 7 and 8, with the precision to be expected, but only when the interval i is not too small.

For the smaller intervals we find: $m<\Delta D\sqrt{2}$.

This effect is due to the width of the microphotometer slit, which causes a certain correlation between neighboring readings. At all events we may *conclude that the undulating density lines are Gaussian error curves.*

The plates Nos. 1 and 6 however seem to be exceptions. For these plates m is smaller than $\Delta D\times\sqrt{2}$ even for the larger intervals. It appeared

TABLE II. *The values of m as a function of i.*

Values of i			36	24	18	12	8	6	4	3	2	1
Corresponding Distances on the Plate			(180μ)	(120μ)	(90μ)	(60μ)	(40μ)	(30μ)	(20μ)	(15μ)	(10μ)	(5μ)
Plate No.	$\Delta D\times$const.	$\Delta D\times\sqrt{2}\times$const.	values of $m\times$constant									
1	2.15	**3.03**	2.86	2.77	2.89	2.76	2.70	2.70	2.65	2.22	1.95	—*
2	2.18	**3.09**	3.03	3.11	3.37	2.99	3.01	3.20	2.87	2.68	2.21	1.27
3	1.83	**2.58**	2.60	2.42	2.37	2.49	2.23	2.15	2.34	2.26	**1.96**	1.19
4	1.20	**1.69**	1.82	1.79	1.74	1.65	1.59	1.60	1.56	1.40	1.12	0.63
5	1.74	**2.44**	2.40	2.36	2.46	2.31	2.32	2.23	2.13	1.86	1.44	0.80
6	1.22	**1.72**	1.41	1.47	1.42	1.35	1.49	1.46	1.31	1.25	0.99	0.57
7	2.51	**3.55**	3.54	3.80	3.41	3.32	2.92	2.59	2.23	1.58	1.32	0.72
8	1.45	**2.03**	2.19	1.94	2.00	1.97	2.10	1.94	1.68	—*	1.01	0.54

*Not measured.

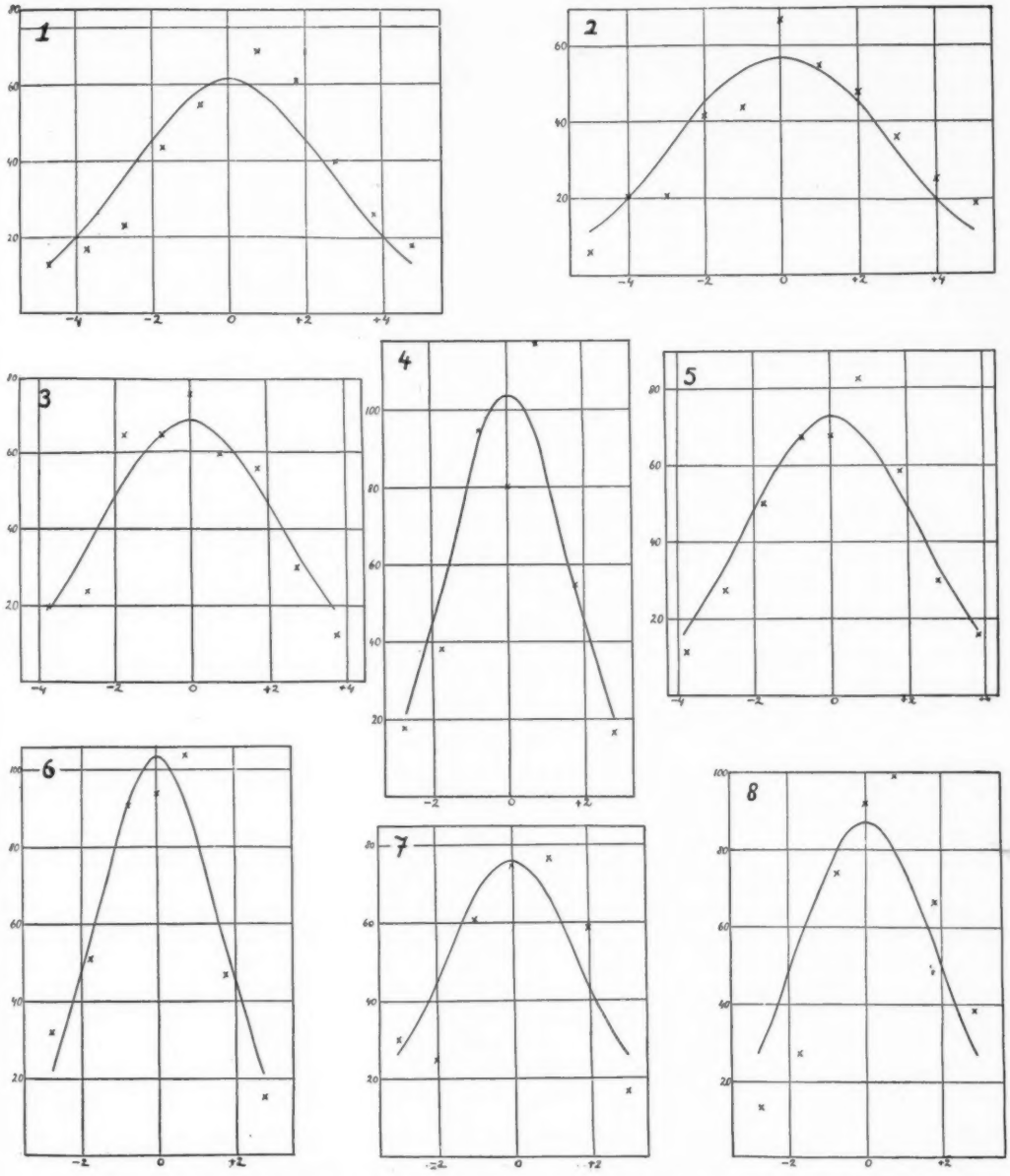

FIG. 4. Observed frequency laws of the eight registrograms, compared with Gaussian frequencies.

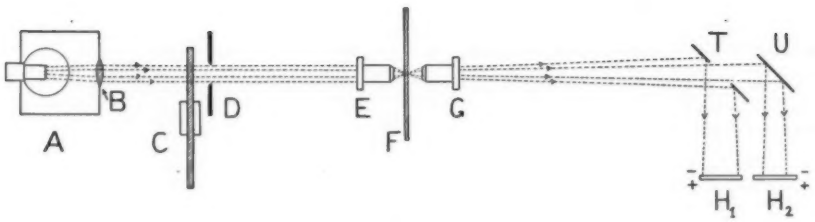

FIG. 5. Optical part of the graininess meter.

that this effect was caused by a slight systematical decrease of the density along the registrogram. This effect causes too high a value of ΔD, while it influences m only slightly.

This example shows clearly what kind of difficulty must be expected in the direct measurement of ΔD: we cannot separate the graininess from possible systematical variations.

The Gaussian properties of the error curves however give us a means to avoid this difficulty. We simply calculate the mean difference m for an interval i, which is sufficiently larger than the width of the slit, and then compute ΔD from:

$$\Delta D = m/\sqrt{2}.$$

The drawback is that this method requires so much time. For this reason we have constructed an instrument, which performs the measuring and integrating of the fluctuations automatically, thus yielding m without lengthy calculations. The principle of this instrument is as follows: The image of the plate formed by the microphotometer is projected on two barrier layer cells, placed next to each other, in such a way, that half of the image falls on the one cell, the other half on the second cell. The cells are connected in opposite direction, so that when the plate is quite homogeneous, the resulting current is zero. When the plate shows graininess however, the halves of the image contain different and varying amounts of light. Therefore by moving the plate in the microphotometer, an alternating current is set up, which is directed in a special way and provides a measure for m.

THE GRAININESS METER

The optical part of the instrument is shown in Fig. 5. Certain improvements have been made on the original form.[5]

The main parts are reproduced from the microphotometer of Moll.[7] A is the lamphouse, which contains a 6-volt motorcar lamp. The spiral of the lamp is focused by the lens B (a simple magnifying glass) on the diaphragm D. This replaces the first slit of the microphotometer. It is clear that a slit would not offer any advantage in our case; we have taken a circular hole (of diameter 1.5 mm) since this is the shape with the simplest optical properties: C is a circular gray wedge, which controls the total amount of light. The hole is focused on the negative F by means of the lens E, a microscope apochromate of Zeiss (numerical aperture 0.30; mag. $\times 10$). The image formed on the negative is focused (with a magnification of $\times 30$) by a second apochromate G of the same type on the mirror T. This mirror serves to divide the image into two parts. It has an elliptical hole in its silver layer with an area of half the image. Now the image is projected in such a way, that it is concentric with the hole. Consequently the light of the inner half of the image passes through the mirror, while the outer half is reflected on the barrier layer cell H_1. The inner half of the image is reflected by a second mirror U on a second barrier layer cell H_2. The cells are connected as shown in Fig. 6. From this figure we see that the Moll galvanometer J measures the difference of the currents which flow through the cells.

To perform a measurement, the negative is rotated in its plane by means of a synchronic motor. The center of the rotation is about 1 mm out of the optical axis, so that different parts of the plate pass the light beam successively. Consequently the amount of light, falling on the barrier layer cells varies continually and in the galvanometer J a fluctuating current is set up, the mean of which is a measure for the quantity

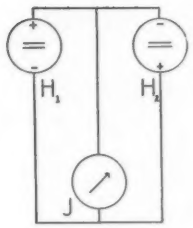

FIG. 6. Connection of the barrier layer cells.

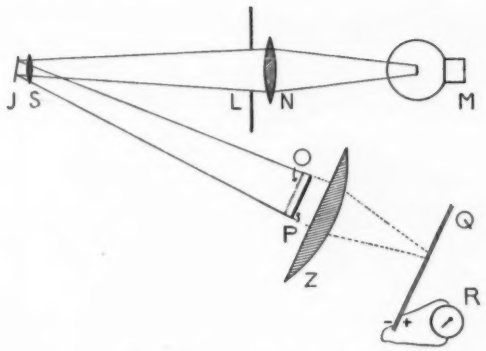

FIG. 7. The optical rectifier.

m, mentioned above. Now this current is alternating, so its algebraic mean is zero. What we want, is the mean of the absolute value of the current and this is measured by the second part of the apparatus, the rectifier (see Fig. 7) in the following way: A diaphragm L of rectangular form is illuminated by an incandescent lamp M and a condenser N. The light is concentrated on the mirror of the Moll galvanometer J and by the lens S an image of the diaphragm is formed in O.

When the alternating current flows through J, the image O moves to and fro and follows the fluctuations of the current. When there is no current, the image O is projected exactly on a strip of black metal P of the same breadth as O, but when O moves, its light passes along the right and the left of P and falls on a lens Z which focuses the mirror J on the barrier layer cell Q. In this way Q also produces a fluctuating current, but this current is rectified. It flows through a Siemens galvanometer R, which has an internal resistance of 275 ohms and is aperiodic with 10,000 ohms. Its oscillation time is 24 seconds. We have shunted this galvanometer with 300 ohm. Therefore it has become very slow and does not follow the fast fluctuations, but indicates the mean current. From its reading m and ΔD can easily be calculated.

One systematic error might be expected, namely a nonlinear distortion caused by the barrier layer cells. We could not find, however, such an effect. The only nonlinear correction to be made is the correction for the edges of the image O, which are not perfectly sharp.[7a]

It is obvious that ΔD, being a statistical magnitude, cannot be measured with great precision. The mean deviation between two measurements of the same spot of the plate appears to be 10–15 percent. By repeating each measurement four times we reach a precision of about 5–8 percent. For practical purposes this is quite sufficient.

Another difficulty is caused by the large densities. These reduce the light intensity to such an extent that the current produced by the cells H becomes too small for exact measurement. Because of this densities up to only 1.3 could be measured.

If the barrier layer cells H would be replaced by vacuum cells connected to an amplifier, the sensibility of the system would greatly increase, so that large densities could also be measured.

RESULTS

The first series of measurements with the graininess meter was performed in order to obtain general data about ΔD. We used the following emulsions:

I. Ilford special rapid
II. Ilford ordinary
III. Ilford double express
IV. Mimosa finograin

and the following developers:

A. Metol, 8.6 g; Borax, 19 g; Na_2CO_3, 5.3 g; $Na_2SO_3 \cdot 7H_2O$, 75 g; KBr, 0.5 g; water up to 1000 cm³ [Reinders and Beukers[8]].

B. Hydroquinone, 3 g; $K_2S_2O_8$, 3 g; KBr, 3 g; KOH, 12 g; water up to 1000 cm³.

[7a] This correction will be described in a following paper. It has not been applied to the data given in this paper. It causes a somewhat higher ΔD at the larger densities so that the maxima of the $\Delta D(D)$ curves become flatter than those of Fig. 9.

[8] W. Reinders and M. Beukers, Bericht VIII. Int. Phot. Congress, p. 177.

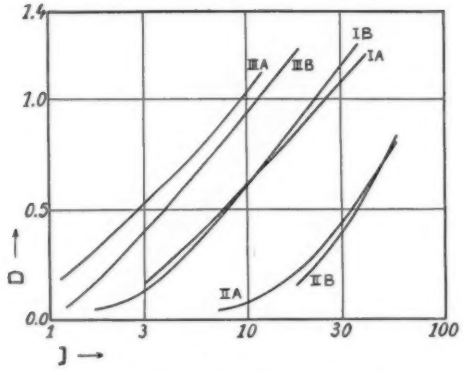

FIG. 8. Density curves of the measured plates. A. Metol developer. B. Hydroquinone developer.

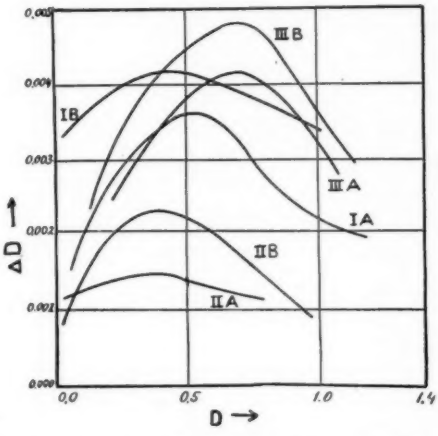

FIG. 9. ΔD as a function of the density. A. Metol. B. Hydroquinone.

Temperature of both developers 18°C; time of development 6 minutes.

Since the "Mimosa" plates appeared to be very inhomogeneous and fogged, they could not be used. Six combinations of emulsion and developer remained.

The plates were exposed to the light of an electric lamp which had passed through a monochromatic filter (maximum at 4600A). At about 1 cm in front of the plate an opal glass was placed in order to avoid dust and scatches on the filter being projected on to the plate. The variation of the intensity was obtained by varying the current of the lamp. The latter was calibrated by means of the well-known method of Ornstein.[9] With each value of the current an area of about 15×15 mm was exposed. Fig. 8 shows the density curves measured with the graininess meter (fog subtracted). Fig. 9 shows ΔD as a function of the density (fog included). Table III gives $\Delta J/J$ (computed from ΔD), as a function of the density (fog subtracted). We conclude from these data:

1. The metol developer causes a higher sensitivity and a somewhat lower $\Delta J/J$ (which means a lower graininess for many applications) than the hydroquinone developer.

2. ΔD as a function of the density has a maximum at a density of about 0.3–0.6.

3. The quantity $\Delta J/J$ decreases with increasing density (is not constant, as would appear from our provisional, inaccurate measurements).

[9] Ornstein, van der Held and Vermeulen, J. O. S. A. **20**, 573 (1930).

TABLE III. *$\Delta J/J$ in percent, as a function of the density A. Metol. B. Hydroquinone.*

PLATE NUMBER										
IA	D	0.05	0.08	0.14	0.25	0.34	0.46	0.67	0.90	1.11
	$\Delta J/J$	*3.1*	*1.5*	*1.1*	*0.74*	*0.74*	*0.85*	*0.64*	*0.46*	*0.42*
IB	D	0.17	0.28	0.38	0.47	0.67	0.87			
	$\Delta J/J$	*1.3*	*1.1*	*1.1*	*1.5*	*0.85*	*0.81*			
IIA	D	0.05	0.22	0.38	0.57	0.78				
	$\Delta J/J$	*1.3*	*0.40*	*0.33*	*0.23*	*0.21*				
IIB	D	0.17	0.34	0.55	0.91					
	$\Delta J/J$	*0.48*	*0.46*	*0.33*	*0.13*					
IIIA	D	0.18	0.33	0.40	0.63	0.77	0.84			
	$\Delta J/J$	*0.99*	*1.06*	*1.2*	*0.98*	*0.85*	*0.71*			
IIIB	D	0.06	0.17	0.30	0.37	0.53	0.66	0.78	1.00	
	$\Delta J/J$	*0.85*	*1.1*	*1.01*	*1.01*	*1.1*	*1.06*	*0.85*	*0.63*	

The curves of Fig. 9 show a remarkable accordance with the curves of *subjective graininess*, obtained by Hardy and Jones.[10] The measurements are being continued.

The author is greatly indebted to Professor L. S. Ornstein for his interest in this paper.

[10] A. C. Hardy, reference 2.

On the Characteristic Function of Hamilton, the Eiconal of Bruns, and Their Use in Optics*

M. HERZBERGER, *Kodak Research Laboratories, Eastman Kodak Company*

(Received January 28, 1936)

IN a previous paper,[1] the author derived from the law of Snellius a certain differential invariant, and promised to give the laws which can be obtained by integrating this differential law. This promise will be fulfilled in this paper. By using our tetrality principle, we find four types of characteristic functions, which, according to Hamilton, determine all the qualities of the optical system.

H. Bruns[2] was the first to give the eiconal in explicit form for some special kinds of image formation. T. Smith in England, and H. Boegehold and the author in Germany have published several papers on this subject, but these papers seem not to be very well known in America. For this reason, the author has given a systematic introductory report, which is as complete as possible. This is greatly facilitated by the introduction of the new tetrality principle.

Let a ray be defined by an arbitrary point $\mathbf{a}$ and the unit vector $\mathbf{s}$ in its direction; let n be the refractive index of the object space, and n', $\mathbf{a}'$, $\mathbf{s}'$ the corresponding quantities in the image space. Then, for three neighboring rays ($\mathbf{a}$, $\mathbf{s}$; $\mathbf{a}+d\mathbf{a}$, $\mathbf{s}+d\mathbf{s}$; $\mathbf{a}+\delta\mathbf{a}$, $\mathbf{s}+\delta\mathbf{s}$) the following is true, according to formula (10) of my previous paper:

$$n(d\mathbf{s}\delta\mathbf{a}-\delta\mathbf{s}d\mathbf{a})=n'(d\mathbf{s}'\delta\mathbf{a}'-\delta\mathbf{s}'d\mathbf{a}'). \qquad (1)$$

The magnitude on the left side is an invariant which does not change if we shift the three points $\mathbf{a}$, $\mathbf{a}+d\mathbf{a}$, $\mathbf{a}+\delta\mathbf{a}$, in an arbitrary but continuous way. Eq. (1) is then nothing more than the integrability condition, i.e., that the four forms:

$$\begin{aligned} dS&=n'\mathbf{s}'d\mathbf{a}'-n\mathbf{s}d\mathbf{a}, \quad dV=-\mathbf{a}'dn'\mathbf{s}'-n\mathbf{s}d\mathbf{a}, \\ dV'&=n'\mathbf{s}'d\mathbf{a}'+\mathbf{a}dn\mathbf{s}, \quad dW=-\mathbf{a}'dn'\mathbf{s}'+\mathbf{a}dn\mathbf{s} \end{aligned} \qquad (2)$$

are total differentials. This theorem was developed by W. R. Hamilton.

You can assume either point coordinates x, y, z, x', y', z', or angle coordinates ξ, η, ζ, ξ', η', ζ', or mixed coordinates for an arbitrary Cartesian coordinate system in object and image space, and find from (2) the following equations:

$$\begin{aligned} \partial S/\partial x'&=n'\xi', \quad \partial S/\partial x=-n\xi, \\ \partial S/\partial y'&=n'\eta', \quad \partial S/\partial y=-n\eta, \\ \partial S/\partial z'&=n'\zeta', \quad \partial S/\partial z=-n\zeta, \end{aligned} \qquad (3)$$

if S is given as a function of x, y, z, x', y', z'. Of course, the manifold of rays is only four dimensional, so we have too many variables, which, however, can be eliminated with the help of (3), if we consider that

$$\begin{aligned} n^2&=n^2(\xi^2+\eta^2+\zeta^2)=n^2\mathbf{s}^2 \\ &=\left(\frac{\partial S}{\partial x}\right)^2+\left(\frac{\partial S}{\partial y}\right)^2+\left(\frac{\partial S}{\partial z}\right)^2, \\ n'^2&=n'^2(\xi'^2+\eta'^2+\zeta'^2)=n'^2\mathbf{s}'^2 \\ &=\left(\frac{\partial S}{\partial x'}\right)^2+\left(\frac{\partial S}{\partial y'}\right)^2+\left(\frac{\partial S}{\partial z'}\right)^2. \end{aligned} \qquad (4)$$

The function, S, therefore, cannot be any arbitrary function of its six variables, but can only be one which satisfies the two differential Eqs. (4). We can deal with the other three functions in the same way. That is the method Hamilton tried to follow in dealing with optical problems, and which led him to the important results which are stated in his papers. But this is extremely difficult, and no one has succeeded until now, except for the case of the plane mirror, in finding this Hamiltonian function for a given optical system or for an optical system with given qualities. That is the reason why Hamilton's work, in spite of its importance, has had no effect on the development of optics in the past century, and only a few scientists, for instance, Maxwell, Rayleigh, Clausius, and Larmor, have developed optical problems by Hamilton's method.

Independent of Hamilton, whose papers until recently appeared only in the "Transactions of

* Communication No. 583.

[1] M. Herzberger, J. Opt. Soc. Am. 25, 295 (1935).

[2] H. Bruns, Abh. der Phys. Klasse der Kgl. sächs. Ges. der Wiss. 21, 325 (1895).

the Irish Society," which is difficult to get on the Continent, Bruns in 1895 developed formulae (2), as a kind of application of the theory of contact transformations given by S. Lie. However, in developing formulae (2), he differed from Hamilton, and his method opened a fertile field for further investigation.

Since the straight lines of three-dimensional space form a four-dimensional manifold, we should choose our functions, which Bruns called "eiconals" (Greek "eicon": image), so that they depend on only four variables.

If we consider a Cartesian coordinate system, and assume that **a** determines a point x, y in the plane $z=0$, and **a'** a point x', y' in the plane $z'=0$, we can regard a ray as being defined by these four coordinates. If S is an arbitrary function of these four variables, we get a coordination of rays in object and image space where all optical laws hold true if we consider Eq. (2); that is, if we coordinate the rays given by

$$\begin{aligned} n\xi &= -\partial S/\partial x, \quad n'\xi' = \partial S/\partial x' \\ n\eta &= -\partial S/\partial y, \quad n'\eta' = \partial S/\partial y'. \end{aligned} \tag{5}$$

We have said that S may be an arbitrary function of x, y, x', y', but, of course, only those functions may be used which give a relation between actual object and image rays. That means that Eqs. (3) must be soluble according to x, y, $\eta\xi$, $n\eta$ and $n'\xi'$, $n'\eta'$, x', y', respectively. This gives the condition

$$\frac{\partial^2 S}{\partial x \partial x'} \cdot \frac{\partial^2 S}{\partial y \partial y'} - \frac{\partial^2 S}{\partial x \partial y'} \cdot \frac{\partial^2 S}{\partial x' \partial y} \neq 0. \tag{6}$$

Every function of x, y, x', y', which fulfills condition (6) gives an optical image formation.

In the same way, the optical image formation can be given by the angle eiconal W. The function W may be regarded as an arbitrary function of $n\xi$, $n\eta$, $n'\xi'$, $n'\eta'$, such that

$$W_{n\xi,\, n'\xi'} W_{n\eta,\, n'\eta'} - W_{n\xi,\, n'\eta'} W_{n'\xi',\, n\eta} \neq 0, \tag{6a}$$

if we use the usual abbreviation for derivatives. The coordinates of the points where the ray intersects object and image plane are then given by

$$\begin{aligned} x &= \partial W/\partial n\xi, \quad x' = -\partial W/\partial n'\xi', \\ y &= \partial W/\partial n\eta, \quad y' = -\partial W/\partial n'\eta', \end{aligned} \tag{7}$$

and the same holds true for the two mixed eiconals.

In the following discussion, we shall deal especially with rotation-symmetrical systems. Then, if we rotate the object ray about the axis of symmetry, the image ray must rotate in the same way. Thus, S must be a function of the three variables

$$a_s = x^2 + y^2, \quad b_s = 2(xx' + yy'), \quad c_s = x'^2 + y'^2 \tag{8}$$

and, similarly, W must be a function of

$$\begin{aligned} a_w = (n\xi)^2 + (n\eta)^2, \quad b_w = 2(n\xi n'\xi' + n\eta n'\eta'), \\ c_w = (n'\xi')^2 + (n'\eta')^2. \end{aligned} \tag{9}$$

Hereafter, we shall drop the suffix from a, b, c, as the choice of the eiconal will indicate clearly enough which is meant.

If we introduce (5) into Eqs. (3), they can be written

$$\begin{aligned} n\xi &= -2S_a x - 2S_b x', \quad n\eta = -2S_a y - 2S_b y', \\ n'\xi' &= 2S_b x + 2S_c x', \quad n'\eta' = 2S_b y + 2S_c y'. \end{aligned} \tag{10}$$

Similarly, we get from (7)

$$\begin{aligned} x &= 2W_a n\xi + 2W_b n'\xi', \\ y &= 2W_a n\eta + 2W_b n'\eta', \\ x' &= -2W_b n\xi - 2W_c n'\xi', \\ y' &= -2W_b n\eta - 2W_c n'\eta', \end{aligned} \tag{10a}$$

and the mixed eiconal V gives

$$\begin{aligned} n\xi &= -2V_a x - 2V_b n'\xi', \\ n\eta &= -2V_a y - 2V_b n'\eta', \\ x' &= -2V_b x - 2V_c n'\xi', \\ y' &= -2V_b y - 2V_c n'\eta', \end{aligned} \tag{10b}$$

where V is a function of

$$\begin{aligned} a = x^2 + y^2, \quad b = 2(xn'\xi' + yn'\eta'), \\ c = (n'\xi')^2 + (n'\eta')^2. \end{aligned} \tag{11}$$

The functions S, W, and V may be given as arbitrary functions of a, b, c, if only condition (6) is fulfilled, which is equivalent to

$$S_b \neq 0, \quad V_b \neq 0, \quad W_b \neq 0. \tag{12}$$

These are the fundamental equations from which our further investigations will begin.

It is sometimes confusing to read papers on this subject because different authors have used different letters to denote the eiconals. We shall

list here the most important of the different notations:

Hamilton	V	T	—	W
Bruns	E	E	E	E
T. Smith	V	E	—	—
Boegehold and Herzberger	S, E	W	V	V'

We shall now investigate the way in which the eiconals change if we shift the object or image plane. The points x^*, y^*; $x^{*\prime}$, $y^{*\prime}$, at which the ray intersects the new object and image coordinate plane, are given by

$$\begin{aligned} x^* &= x + \frac{z}{[n^2-(n^2\xi^2+n^2\eta^2)]^{\frac{1}{2}}} n\xi, \\ y^* &= y + \frac{z}{[n^2-(n^2\xi^2+n^2\eta^2)]^{\frac{1}{2}}} n\eta, \\ x^{*\prime} &= x' + \frac{z'}{[n'^2-(n'^2\xi'^2+n'^2\eta'^2)]^{\frac{1}{2}}} n'\xi', \\ y^{*\prime} &= y' + \frac{z'}{[n'^2-(n'^2\xi'^2+n'^2\eta'^2)]^{\frac{1}{2}}} n'\eta'. \end{aligned} \tag{13}$$

We recognize that a shifting of the object can be described in a simple way only if we use the eiconal V' or W, and a shifting of the image plane only by the use of W or V, and to describe both simply, we must use W. The change of the functions, by shifting the origin the amount z or z', is given by

$$\begin{aligned} &V_c^* = V_c - \tfrac{1}{2}z'/[n'^2-c]^{\frac{1}{2}} \\ \text{or}\quad &V_a^{*\prime} = V_a' + \tfrac{1}{2}z/[n^2-a]^{\frac{1}{2}} \\ \text{or}\quad &W_a^* = W_a + \tfrac{1}{2}z/[n^2-a]^{\frac{1}{2}}, \\ &W_c^* = W_c - \tfrac{1}{2}z'/[n'^2-c]^{\frac{1}{2}} \end{aligned} \tag{14}$$

or, integrated,

$$\begin{aligned} V^* &= V + z'[n'^2-c]^{\frac{1}{2}}, \\ V^{*\prime} &= V' - z[n^2-a]^{\frac{1}{2}}, \\ W^* &= W - z[n^2-a]^{\frac{1}{2}} + z'[n'^2-c]^{\frac{1}{2}}. \end{aligned} \tag{15}$$

This last equation suggested to the author the introduction of

$$\begin{aligned} [n^2-a]^{\frac{1}{2}} &= \alpha = n\cos\sigma, \\ [n'^2-c]^{\frac{1}{2}} &= \gamma = n'\cos\sigma', \end{aligned} \tag{16}$$

as a set of new variables into the angle eiconal. (σ, σ' are the angles between the ray and the optical axis.) We get in this case

$$W^* = W(\alpha, b, \gamma) - z\alpha + z'\gamma,$$

as a simple formula for shifting the coordinate origin. This means that all theorems containing only W_b and the second or higher derivatives of W are independent of the chosen origin, a very convenient fact for general investigation.

Eq. (16) gives us

$$\begin{aligned} W_a &= W_a d\alpha/da = -(1/2\alpha)W_a, \\ W_c &= W_\gamma d\gamma/dc = -(1/2\gamma)W_\gamma. \end{aligned} \tag{17}$$

And if we introduce (16) into our Eqs. (10a) we get

$$\begin{aligned} x &= -(W_a/\alpha)n\xi + 2W_b n'\xi', \\ x' &= -2W_b n\xi + (W_\gamma/\gamma)n'\xi'. \end{aligned} \tag{18}$$

These equations will be investigated in our next paper.

Now let us consider the use of the eiconal. The formulae (2) are valid without restriction. For instance, if object and image plane are conjugated to each other, so that to each point of the object plane corresponds an image point in the image plane, S has the same value for all rays coming from any one object point ($d\mathfrak{a} = d\mathfrak{a}' = 0$, therefore $dS = 0$, S is constant). We see that, in this case, S is a function of only two variables, namely, the coordinates x, y, in the object plane. It is very useful to know this, but if we want to investigate the image formation for the four-dimensional manifold of all the rays, or of all the rays in the neighborhood of a particular ray, the eiconal S cannot be used.

In general, we can say that the eiconal S cannot be used for general investigation if two points in the object and image plane are conjugated, the eiconal W cannot be used if parallel entering rays leave the system parallel to each other, especially in telescopic systems, and the mixed eiconals cannot be used if object or image plane is at the corresponding focal point. In either case, the reason for this is that the coordinates do not determine the light rays in a one-to-one correspondence.

For all general investigations of systems with finite focal length, the angle eiconal proves to be best adapted. For investigation of the image formation of a single plane, the mixed eiconal V seems most efficient. For investigations in the neighborhood of the axis, the so-called image error theory, W and S seem to be equally useful. The latter should be applied in such a manner

that the origin for the object space is at the axial point of the object, but the origin for the image space is at the so-called exit pupil. In this way, we can best investigate separately the influence of aperture and field.

In his next paper, the author will give a practical application of this theory, and show how, given the eiconal W, all points in space which have a sharp or rotationally symmetrical image may be found. This paper will also give a simple generalization of the laws of Gaussian optics which is valid for each skew ray.

Applied Electron Optics

V. K. ZWORYKIN AND G. A. MORTON, *Electronic Research Laboratory, RCA Manufacturing Co., Inc., Camden, N. J.*

(Received February 12, 1936)

THE beginnings of electron optics can almost be said to predate the discovery of the electron itself. It was well known to the earliest investigators that an object in the path of a cathode-ray beam would cast a sharp shadow on a fluorescent screen which was bombarded by these rays. In this respect, at least, it was known that cathode rays resembled light rays.

It was not long after the discovery of the electron itself that such workers as Classen,[1] Busch,[2] and later Knoll and Ruska[3] began the calculation of electron paths and thus laid the ground work for the true science of electron optics. Since that time these trajectories have been studied in increasing detail as the importance of electron optics has become more and more widely recognized.

The calculation of the paths through fields having radial symmetry is of particular interest. This type of field, either electrostatic or magnetic, can be shown to cause the electron paths to bend in a manner similar to the way in which light is bent when going through a lens. It is therefore possible to replace a radially symmetric electronic system with an analogous optical lens system. This use of an optical analog often simplifies both qualitative and quantitative study of an electron lens system. It is this possibility of replacing an electronic system by an analogous optical lens system that gives our subject its name, and this replacement by an optical analog often (but not always) simplifies both qualitative and quantitative study of an electron "lens" system.

The behavior of electrons passing through an aperture at potential V from a region of field strength E_1 into a region of field strength E_2 illustrates the similarity between electron rays and light rays. In this case the aperture will cause the electrons to converge just as would a spherical lens of focal length[4] $f=4V/(E_2-E_1)$. Just as the glass lens will image a light source, so will the aperture be capable of producing an electron image. Furthermore, it has been shown that any cylindrically symmetrical configuration of an electrostatic field will produce either a positive or negative lens action if the electron path is not too far from the axis of symmetry.[5]

It is not our purpose to present a theoretical study of the "optics" of electrons, as there are many excellent articles dealing with the subject,[6] but rather to discuss certain practical details concerning the formation of electron images. Furthermore, we shall limit our discussion to the formation of images by means of electrostatic fields rather than systems involving magnetic lenses or combined magnetic and electrostatic lenses.

Two very important practical applications of electron optics illustrate the use of the electron lens as a means of forming an image of an emitter. The first is the electron gun which is used to concentrate the electrons from a cathode into a very small image or spot. In this case, both image and object are close to the axis of the lens and factors such as curvature of the image field, distortion within the image, etc., are not of great importance. A typical example of an electron gun is shown in Fig. 1. This system consists of two lenses (shown in the optical analog under the diagram of the gun) which image, not the cathode itself, but a point close to the cathode (known as the cross-over) onto the screen. This type of electron optics plays an important role in cathode-ray oscillographs in general and in cathode-ray television in particular. A more detailed description will be found in numerous papers covering this phase of electron optics.[7]

The second field of application, the electron microscope, is one in which electron optics are

[1] J. Classen, Physik. Zeits. **9**, 762 (1908).
[2] Busch, Physik. Zeits. **23**, 438 (1922).
[3] M. Knoll and E. Ruska, Zeits. f. tech. Physik **12**, 396 (1931); Ann. d. Physik **12**, 607 (1932).
[4] C. J. Davisson, Phys. Rev. **42**, 580 (1932); L. H. Bedford, Proc. Phys. Soc. **46**, 882 (1934).
[5] H. Busch, Ann. d. Physik **81**, 974 (1926); Archiv f. Elektrotechnik **18**, 583 (1927).
[6] E. Brüche and O. Scherzer, *Geometrische Elektronenoptik* (Julius Springer, 1934).
[7] V. K. Zworykin, J. Frank. Inst. **215**, 535 (1933); V. K. Zworykin, J. Inst. Elec. Eng. **73**, October (1933); I. G. Maloff and D. W. Epstein, Proc. I. R. E. **22**, 1386 (1934).

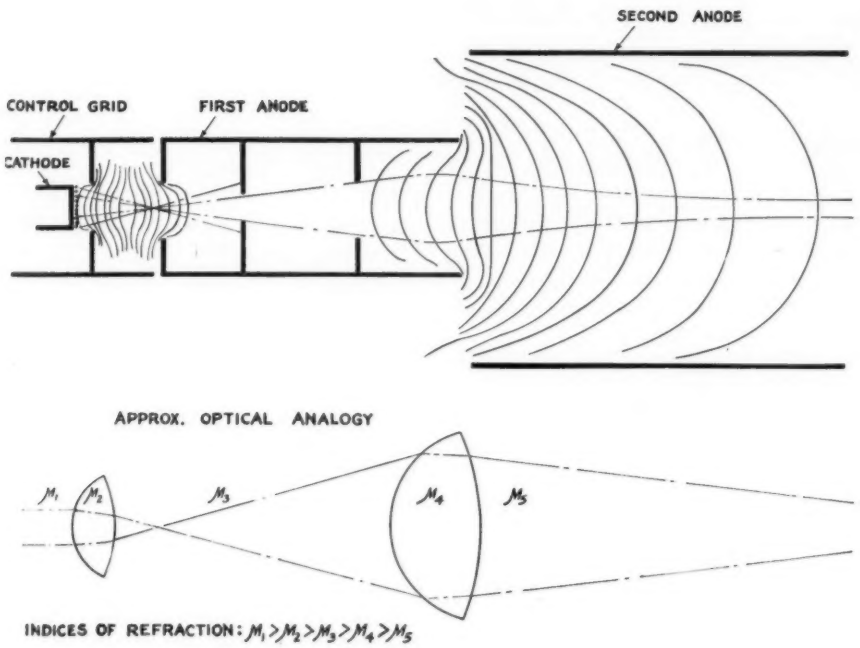

FIG. 1. Electron gun.

used to image a small object into a very much enlarged reproduction. This use differs from the example given above in that the internal details of the object are important rather than the outline alone, hence such problems as image distortion and aberration must be considered. However, in the case of the electron microscope the angle between the axis and any electron "ray" is, in general, small, so that corrections for defects of the lenses are comparatively simple. Fig. 2 illustrates a typical electron microscope given in Brüche and Scherzer's excellent monograph on electron optics.[6] There are a great many types of these microscopes, most of which make use of combined electrostatic and magnetic fields, and a complete discussion of them is beyond the scope of this paper.

In the course of our study of electron optics there arose the problem of producing an electron image of an extended object; furthermore, it was necessary to do this solely by electrostatic means. The optical analog of this system is the lens system of a copying camera. A satisfactory solution of this problem requires that: (1) the image be free from distortion, (2) the circle of confusion be small, (3) the effective aperture of the lens large, and (4) the area of the object and image large. The magnification of this system should be close to unity, that is, from one-half to three.

As a basis for this system, let us consider the field between two coaxial cylinders of equal diameters. Fig. 3 illustrates diagrammatically this type of image tube. The cathode is a semitransparent photoelectric surface which will be described in detail later. The viewing screen is similar to those used in the cathode-ray oscillograph, formed by spreading a thin layer of special willemite on the glass end plate of the tube. A potential is applied between the two cylinders, the cathode and adjoining cylinder being negative, while the screen and long cylinder are made positive. When a light image is projected on the photo-cathode, electrons are released in proportion to the intensity of the light falling on any given area. These electrons are focused by the electrostatic lens between the two cylinders into an inverted image on the fluorescent screen.

Since this system is to form the basis of the

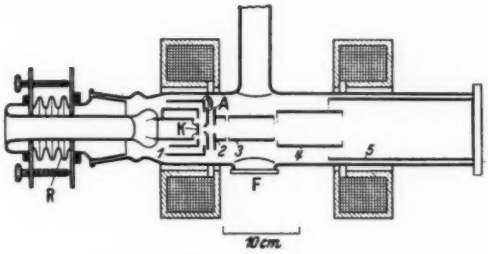

FIG. 2. Electron microscope.

image tube, it is worth while to examine it in detail, both from a theoretical and an experimental aspect. The potential distribution for this configuration can be obtained by solving the Laplace differential equation with appropriate boundary conditions as determined by the cathode and cylinder walls. This solution leads to the following integrals for the potential, together with its first and second derivatives along the axis:

$$\phi(z)=\frac{2}{\pi}\int_0^\infty \frac{A\cos 2ku\cdot\sin 2kzdk}{kJ_0(ik)},$$

$$\phi'(z)=\frac{4}{\pi}\int_0^\infty \frac{A\cos 2ku\cdot\cos 2kzdk}{J_0(ik)},$$

$$\phi''(z)=-\frac{8}{\pi}\int^\infty \frac{Ak\cos 2ku\cdot\sin 2kzdk}{J_0(ik)},$$

where z = the distance along the axis of the cylinder measured in lens diameters.
A = the difference in potential between the cylinders.
u = the cathode to lens distance in lens diameters.
and $\phi(z)$, $\phi'(z)$, and $\phi''(z)$ = the potential and its first and second derivatives along the tube axis.

A plot of the potential and its second derivative are shown in Fig. 4. With this potential distribution, together with a suitable form of the ray equation

$$\frac{d^2r}{dz^2}+\frac{\phi'}{2\phi}\frac{dr}{dz}+\frac{\phi''}{4\phi}r=0,$$

paths of electrons may be calculated.

With these calculated paths the image position and the magnification may be determined. The former is found by locating the intersection of the paths of an electron leaving the center of the cathode with zero initial velocity (i.e., the axis of the tube) and an electron leaving the cathode with a radial initial velocity. The magnification is determined by finding the radial distance from the axis of the tube, at which an electron leaving the cathode with zero velocity from a point off the axis intersects the image plane. The electron path for $u=0.9$ diameter is shown in the lower diagram of Fig. 4.

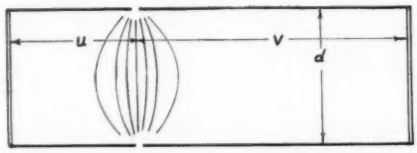

FIG. 3. Simple fixed focus image tube.

The position of the image is determined by the distance u between cathode and juncture of the two cylinders, which, for convenience, we shall call the "lens." Determinations of lens-image distance v in terms of u have been made experimentally as well as theoretically, by using a tube having a movable cathode and screen. Fig. 5 shows the result of both types of determination on the curve giving "u" *vs.* "v" (both in terms of gun diameters). This figure also shows the magnification plotted against $v/2u$. This plot illustrates that over a wide range the magnification is quite accurately given by $m=v/2u$. It should be noted that the image position and magnification is independent of the potential between the two cylinders.

The practical difficulty with this system lies in the fact that it is almost impossible to construct and mount the cylinders in such a way that the image will be perfectly in focus, and to construct the tube in such a manner that its mechanical dimensions can be changed after the tube has been exhausted and sealed is rather impractical, though not impossible.

In order to focus the system electrically, it is necessary to change the curvature of the equipotential surfaces near the "lens" without so changing the field close to the cathode that the distortion of the image is increased. This could best be done by making the cylinder from cathode to the lens out of resistive material so that a potential gradient could be established along it. Experimentally, it is found that if the cathode

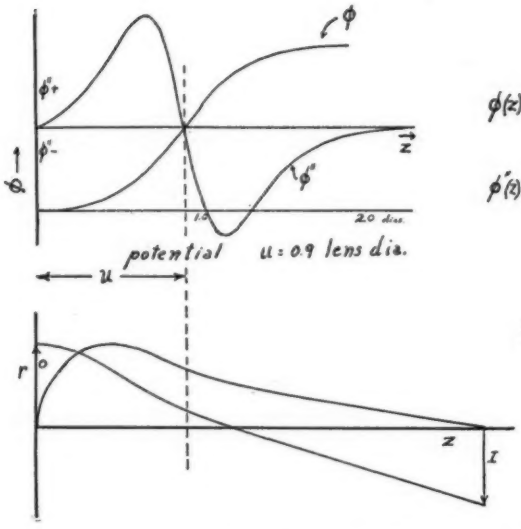

$$\phi(z) = (E_2 - E_1)\frac{2}{\pi}\int_0^\infty \frac{\cos(2ku)\sin(2kz)\,dk}{k\,J_1(ik)}$$

$$\phi'(z) = (E_2 - E_1)\frac{2}{\pi}\int_0^\infty \frac{k\cos(2ku)\sin(2kz)\,dz}{J_1(ik)}$$

$$\frac{d^2r}{dz^2} + \frac{\phi'}{2\phi}\frac{dr}{dz} + \frac{\phi''}{4\phi}r = 0$$

FIG. 4. Potential distribution and electron paths in simple image tube.

cylinder is subdivided into four or more rings, each at a progressively higher potential, the distortion of the image is no greater than for the mechanically focused tube. The magnification of this type of tube is given by the same relation as in the former case, that is $m = v/2u$.

These two types of tube will give a fairly satisfactory image if the percentage of the cathode area used is small. However, the image suffers from two defects: First, from pin cushion distortion, and second, a truly sharp focus can only be had at one value of radius on the screen. A study of the pattern shows that the image field is curved in such a way as to be concave from the lens side. Fig. 6 is a photograph of the image on the fluorescent screen when the entire cathode is illuminated with a rectangular grid. Without changing the actual lens system, we have two means for correcting the above-mentioned distortion: first, by producing a radial gradient over the cathode, and second, by properly shaping the cathode surface.

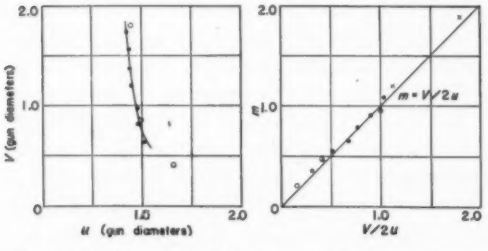

FIG. 5. (left) Lens object distance *vs.* lens image distance. (right) Magnification *vs.* $v/2u$. Experimental: black dot, fixed focus; cross, variable focus. Calculated: circle, fixed focus.

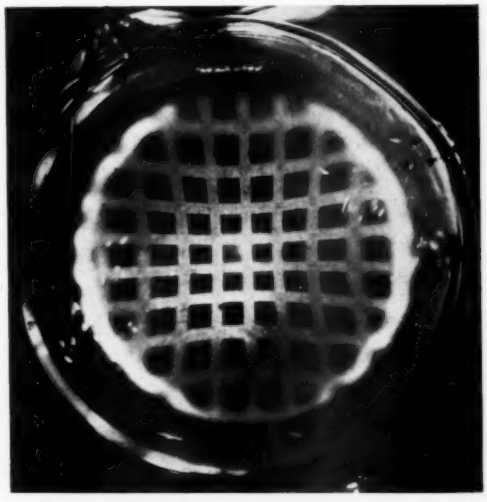

FIG. 6. Photograph showing the image distortion in uncorrected image tube.

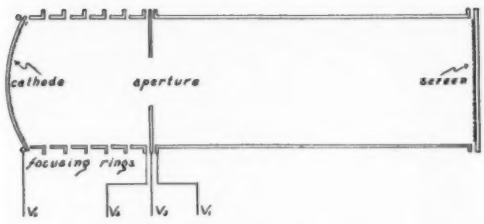

FIG. 7. Variable focus image tube with corrected cathode.

The first method is not at present of much practical importance, but it is of interest theoretically. It can be accomplished by making the semitransparent cathode film resistive and passing a current radially outward from the center. For perfect correction, the resistance of the film should not, however, be uniform, but should be lowest at the center, increasing approximately proportional to the square of the radius towards the rim. By making the center positive and correctly proportioning the resistance, both pin cushion and defocus effects can be corrected. However, since electrical contact must be made to the center of the film, it is impossible to avoid a blemish at the center of the image.

It is interesting to note that these cathodes can be made self-correcting for a given value of light by making the film of uniform high resistance. When thus made the photoelectric current produces a gradient over the cathode just as did the radial current in the previous case. The disadvantage of this solution to the problem is that the correction is complete for one value of light only and, furthermore, the illumination over the optical image must be fairly uniform.

The second method, that of shaping the cathode, is much more practicable and can be made to yield an excellent image over the entire cathode area. This method of correcting the image is possible because the primary causes of the defects are the distortion of the equipotential surfaces due to the cathode surface and the nature of the lens itself, which has the properties of a simple spherical lens. The correction is effected by using a cathode surface which is concave towards the lens. It is found experimentally that if the cathode is spherical and of radius equal to the lens distance "u," very satisfactory results are obtained.

Fig. 7 shows diagrammatically the construction of an image tube with curved cathode and focusing rings. It should be mentioned here that it is unnecessary to bring out separate leads for each of the rings making up the focusing cylinders. Instead, the potential divider supplying the voltage to these rings can be mounted within the tube itself. A photograph of the image produced by this type of tube with the same grid pattern used in Fig. 6 is shown in Fig. 8. It will be seen that the image is uniformly sharp and

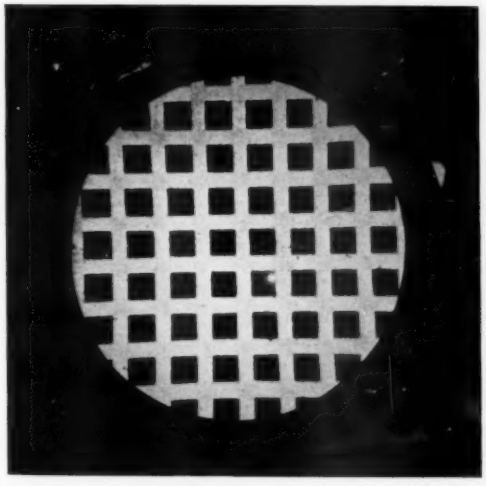

FIG. 8. Undistorted image from corrected image tube.

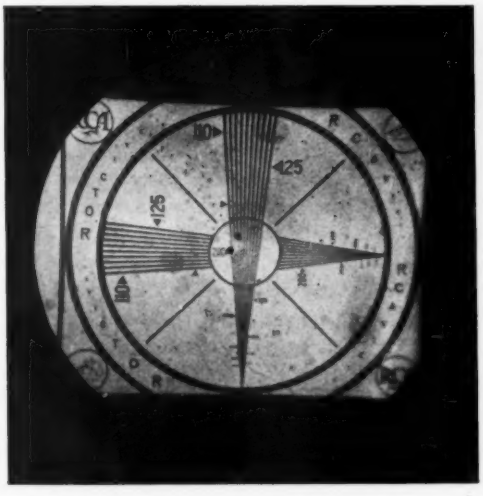

FIG. 8A. Resolution pattern.

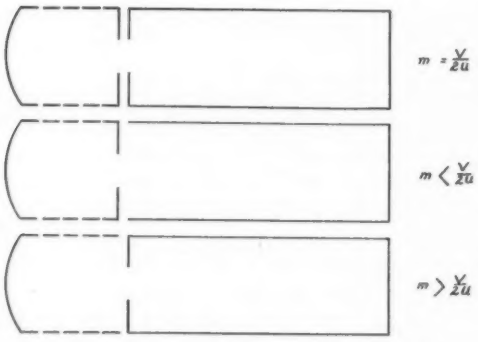

FIG. 9. Arrangement of apertures in image tube.

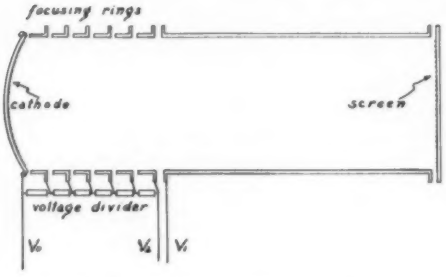

FIG. 10. Image tube, variable magnification.

that the pin cushion distortion is negligible. Fig. 8A shows a resolution pattern obtained using the corrected cathode.

In the foregoing, we have considered only lens systems with no apertures. While the presence of apertures somewhat complicates our picture of the electrostatic field making up the electron lens, certain general features remain the same. The field is cylindrically symmetrical as before, the lens system as a whole is positive and capable of producing a real image, and finally, the same type of image distortion occurs as in the tubes described above unless a corrected cathode is used.

Three arrangements of apertures applied to the type of tube just described are shown in Fig. 9. The first case is that of two symmetrical apertures. With this system the magnification will be found to be $m=v/2u$, as before. However, the focal length for a given ratio of V_1/V_2 is shorter. This means, in a practical case, that the voltage difference between the anode cylinder and the final focusing ring can be made less, with a consequent simplification of the insulation problem and decrease in the danger of cold cathode discharge.

In cases where the apertures are not symmetrical, the magnification is no longer given by the

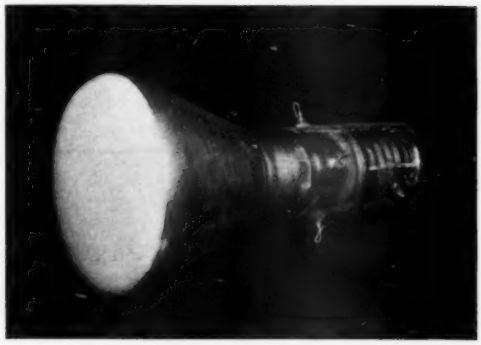

FIG. 11. 9-inch image tube.

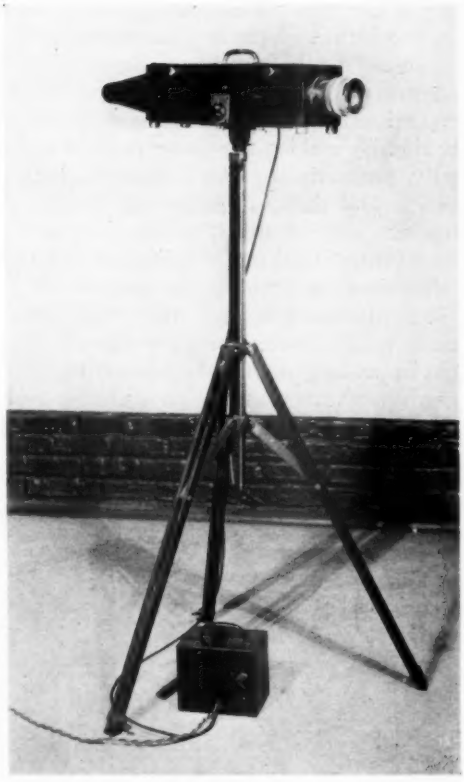

FIG. 12. Electron telescope.

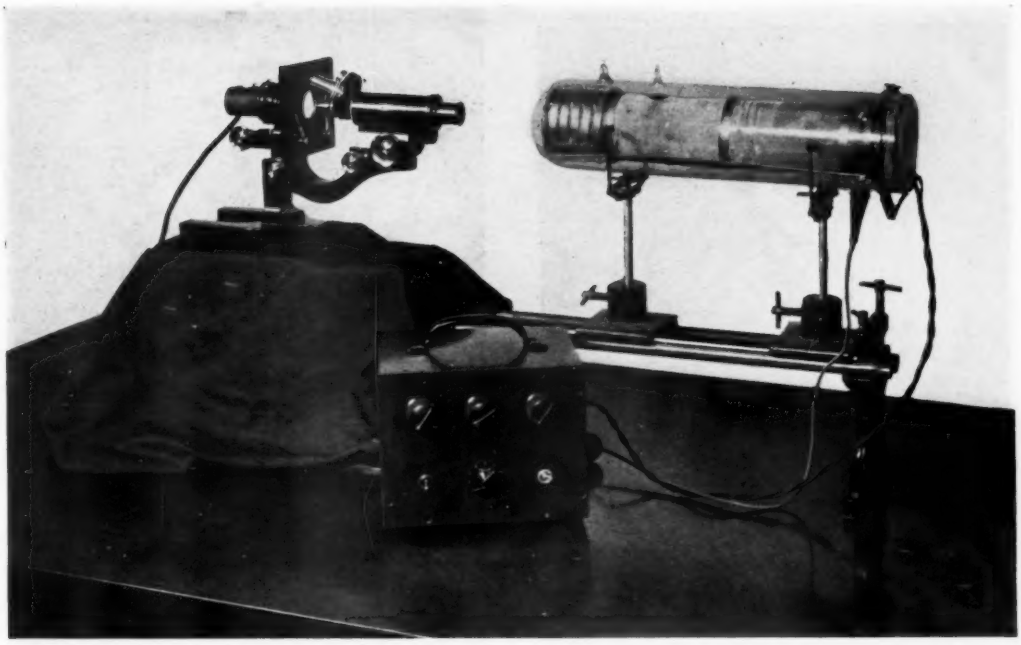

FIG. 13. Infrared microscope.

relation $m=v/2u$. If the aperture on the anode cylinder is smaller than the aperture on the final focusing ring, the magnification is greater than that given by the above relation, while if the anode aperture is the larger, the magnification is less. The use of unsymmetrical apertures allows a wide variation in magnification in tubes which otherwise have identical construction.

The final case to be considered is that shown in Fig. 10. This type of lens system has an aperture, whose potential V_3 can be varied, placed midway between the anode cylinder and the final focusing ring. It should be noted that when the aperture potential V_3 equals the anode voltage, the conditions are similar to the case just described where the aperture on the anode cylinder is smaller than that on the focusing ring and the magnification will be greater than $v/2u$. Likewise, when V_3 is made equal to the ring potential, the magnification is a minimum. For intermediate values of V_3 the magnification lies in between these extremes.

The pin cushion distortion is a maximum when V_3 is at ring potential or less, but decreases rapidly to a constant value as V_3 is increased. Over nearly the entire range of magnification, a curved cathode will correct this distortion fairly satisfactorily. With this arrangement it is possible to construct a tube which gives a very satisfactory image and whose magnification can be controlled electrically.

The construction of the photosensitive cathode to be used in any given image tube will, of course, depend upon the spectral region in which maximum sensitivity is desired. A cathode which has excellent sensitivity in the visible and infrared can be formed as follows: A metal layer is sputtered onto the curved glass disk to be used as the cathode. This layer serves to form an inert conducting backing for the photosensitive layer. Next, a layer of silver is evaporated onto the backing metal. The cathode is mounted and the tube baked and exhausted in the ordinary way. The activation of the cathode is quite similar to that used for the ordinary cesium photo-cell. The silver is oxidized by an electric discharge in oxygen at 1 or 2 mm pressure. Cesium is admitted from a side tube and the cathode is baked to

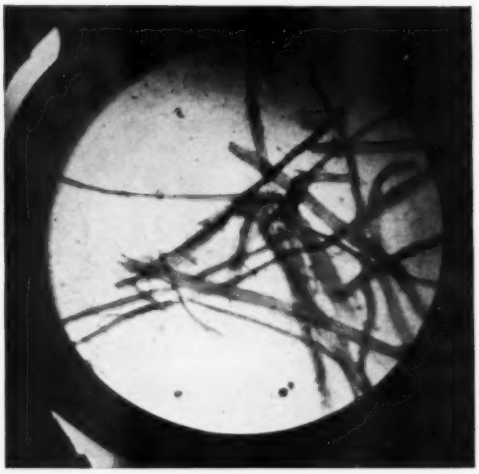

FIG. 14. Infrared micrographs, black gum fiber.

FIG. 16. Cartoon picture projected in infrared on image tube.

FIG. 15. Infrared micrographs, daphnia.

FIG. 17. Scene from the fluorescent screen of image tube.

promote a reaction between the silver oxide and the cesium. Cathodes formed in this manner can be made to have a photosensitivity of 5 microamperes per lumen or better, and a spectral response extending well into the infrared. A typical variable magnification image tube of the type described having a 9-inch viewing screen is shown in Fig. 11.

An interesting use to which the image tube may be put is exemplified in the electron telescope. A large aperture lens is mounted so as to image the scene towards which the telescope is pointed onto an infrared sensitive cathode of an image tube. Fig. 12 shows an example of a portable electron telescope. The electron picture falling on the fluorescent screen renders visible the

infrared image. Such a device can be used to test haze and smoke penetration by infrared, for signalling, etc.

Another application is in connection with infrared microscopy. Fig. 13 shows an image tube and microscope arranged for infrared work. The visible images of micro-specimens on the fluorescent screen are shown in Figs. 14 and 15.

The next two pictures (Figs. 16 and 17) were made by photographing the fluorescent screen while an infrared picture was projected on the cathode. They illustrate fairly well the resolution and fidelity of the image obtainable.

In conclusion, the authors wish to express their thanks to Dr. E. G. Ramberg for his aid in the theoretical work involved, and to the members of the laboratory staff whose cooperation made this work possible.

Gloss Investigations Using Reflected Images of a Target Pattern*

RICHARD S. HUNTER, *National Bureau of Standards*

(Received March 18, 1936)

A target pattern of concentric rings varying from fine lines to broad bands has been placed in the open face of a desk lamp. This luminous target is useful in the study of the gloss characteristics of the more glossy surfaces. The lines and bands of various sizes in the target provide means for studying surfaces of a wide range of "distinctness-of-reflected-image" gloss. Records may be made of which lines and bands are visible by reflection from different surfaces. Such records serve as permanent gloss values for the different surfaces studied. The dark areas of the target immediately adjacent to the luminous areas provide ideal conditions for the identification of surface "bloom." The best gloss differentiations are made when the lamp is used in a darkened room so that the luminous pattern is the only source of light illuminating the surfaces inspected. Photographic records of gloss and unusual gloss effects are discussed.

I. INTRODUCTION

IN a recent circular[1] of the Scientific Section of the National Paint, Varnish and Lacquer Association, the author described an instrument to measure "distinctness-of-reflected-image" gloss and to study other gloss effects. In this gloss comparator two identical, illuminated targets consisting of concentric rings varying from fine lines to wide bands were used. The narrowest lines which could be seen after reflection from any given surface were used as the criterion of the distinctness-of-image gloss of that surface. A measuring device which gave variable amounts of diffusion to one of the targets was used to arrange these distinctness-of-image comparisons on a continuous scale.

Shortly after this gloss comparator was introduced, it was realized that perhaps the luminous target itself, without the accompanying instrument, might be useful in gloss-control work and studies of gloss differences. Accordingly, an enlargement of the gloss-comparator target was printed on a photographic plate and mounted in the face of a desk lamp, as illustrated in Fig. 1. This lamp has proved so useful in studies of gloss that it is thought worth while to describe its use in detail.

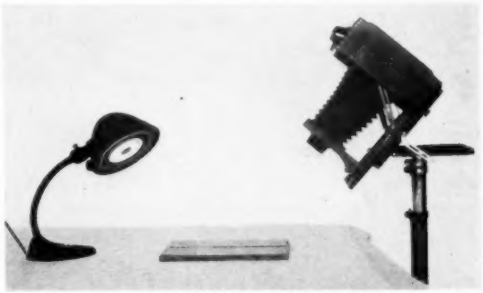

FIG. 1. Target pattern mounted in desk lamp, two panels in position for comparison, and camera to photograph images of target pattern reflected in panel surfaces.

II. APPARATUS AND METHOD

In Fig. 2 a 90° quadrant of the target is reproduced to full scale. Each of the lines and bands in the target is designated with a letter by which it may be identified. The advantages which the device offers when used for studies of gloss and gloss differences are: (1) It affords reproducible conditions for the study of glossy materials; (2) the lines and bands of varying size in the target provide means for studying surfaces over a wide range of distinctness-of-image gloss; (3) permanent records of this type of gloss may be obtained by identification of the rings and bands which are visible after reflection from any given surface, and (4) the dark areas in the target may be used for determining the differences in "bloom" between glossy surfaces.

The design of the circular target was reached through a trial-and-error development during the building of the earlier instrument.[1] Rectangular and straight-line targets were tried

* Paper presented before the Optical Society of America, New York City, February 21, 1936. Publication Approved by the Director of the National Bureau of Standards of the U. S. Department of Commerce.

[1] Scientific Section Circular No. 493 of the National Paint, Varnish and Lacquer Association, Washington, D. C. (October 1935). In this circular are described the gloss comparator and also the different appearance effects identified with glossiness. A bibliography on gloss-measuring methods is included.

FIG. 2. One quarter circle of the target pattern reproduced full scale, with letters to identify the different rings and lines.

first, but it was discovered that the images reflected by many surfaces varied as the surfaces were rotated in their own plane. The circular target, of course, gives the imaging powers from source lines in all directions. The widths of the lines and bands have been graded to give fairly even steps in distinctness-of-image reflection. To illustrate the differentiations thus made possible, three pairs of typical target images have been photographed with the combination of camera and lamp shown in Fig. 1. These photographs are reproduced in Fig. 3.

The lamp makes possible the finest distinctions in gloss when it is used in an otherwise darkened room. However, since the ordinary glossy appearance of any surface varies with the surrounding field of view and with other illuminations, it is, in many cases, advisable to make gloss comparisons with outside light present in order to realize more closely the actual conditions of gloss observation. It is best to obtain flat panels of the materials to be studied as curved surfaces reflect distorted images, which are more difficult to evaluate. A mild example of this distortion is seen in Fig. 3, where the panel $a-l$ possesses a slight curvature.

For detecting gloss differences, the two panels to be compared are placed side by side and viewed so that part of the image of the face of the lamp is seen reflected from each surface. The distance of the surfaces from the lamp and the angle of view are always important and should be noted where permanent records are to be kept. If the test panels are moved toward the lamp, finer lines in the target may be distinguished. Also, a shift of the surfaces toward the lamp will make their lightness and color characteristics more pronounced. When the surfaces are moved away from the lamp, the finer lines in the pattern disappear, and color and lightness becomes more difficult to recognize. As the angle of view approaches grazing incidence, images reflected in the surfaces become more distinct. Thus many of the very flat, matt surfaces will reflect distinguishable images at near grazing incidence.

When the lamp is used as a source for obtaining the distinctness-of-image gloss ratings of individual surfaces, instead of simply for com-

paring two surfaces, these surfaces must, in turn, all be placed in the same position relative to the lamp and should be viewed from the same position. The exterior lighting conditions must also be constant and the following factors specified in presenting the results:

1. Distance from lamp to test surface
2. Distance from observer to test surface
3. Direction of view (unless otherwise specified, approximately 45°)
4. Amount of light present from sources outside the lamp.

When these factors are recorded, reproducible conditions for the identification of the lines of the target are established, and observations made at separate times may be used as records of the gloss of the surfaces tested.

The observer, who wishes to describe the appearance of the target image reflected in some particular glossy surface, names and describes the appearance of the least distinct ring. That is, he records the letter which identifies this ring and perhaps a modifying letter to indicate whether this ring is sharp, fairly plain, or indistinct; also whether it appears as a continuous ring, or shows only irregularly from certain parts of the surface. In order of descending "distinctness-of-image," the letters identifying the rings in the target are: A_1, A_2, A, B, C, D, and E. In addition, there are two auxiliary rings (D_1 and X) which are occasionally used in describing the appearance of surfaces. The following modifying letters are suggested for the above designations: *g*—good definition, *f*—fair definition, *p*—poor definition. This system gives a distinctness-of-image gloss scale of seven letter ratings and twenty-one steps, three steps for each rating. Three letters, which serve to indicate the appearance of a surface aside from its distinctness-of-image gloss, are suggested: *n*—nonuniform, *w*—wavy, *s*—specks and scratches. Other characteristics of surfaces, such as bloom, particular types of texture, and unusual appearance may also be designated.

In the innermost band of rings, the letter A_1 represents resolution by the eye of the two rings close together just outside the center of the target. A_2 represents resolution of the third ring as separate from the other two, but A_2 would mean. when reported, that the observer could not, under the given conditions, resolve the A_1 pair as separate and distinct rings. The letter A

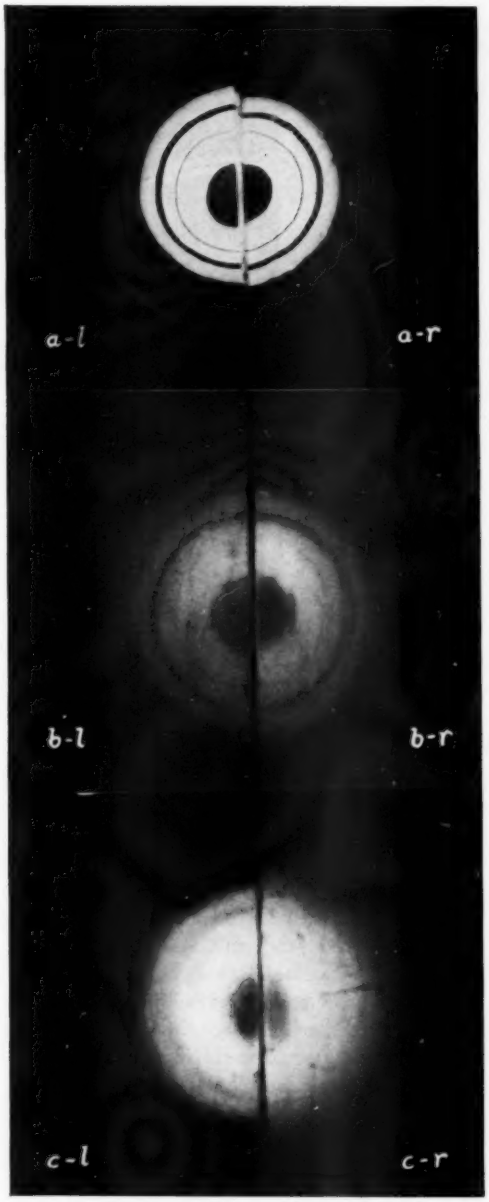

FIG. 3. Comparison of three pairs of panels using the gloss-inspection lamp. *a*, olive-green enamels; *b*, white, resinous paints; and *c*, rubbed furniture finishes. Distances of camera to surface and lamp to surface both about 30 cm; room dark.

indicates identification of the three rings as a single band without their separate resolution.

III. Representative Results

This gloss-rating scale was used by a number of observers to grade the three pairs of panels illustrated in Fig. 3. The results of their observations are given in Table I.

Each pair of panels was observed at two distances from the lamp (30 and 90 cm); in each instance the observer's eyes were slightly farther from the test surfaces than the test surfaces were from the lamp. The direction of view was 45°; the room was dark.

The observer's rating, *g*, *f*, or *p*, is placed opposite the designation (A_1, A_2, ···) of the ring which was least discernible. A mean rating is assigned at the bottom of each set of observations. To obtain these means, it is assumed that the distinctness-of-image gloss scale is a uniform continuous scale of 21 steps from "*pE*," at the bottom, to "gA_1" at the top. Tenths of a step were computed from the averages of the six observers. Below the sharpness-of-image ratings in the table are crosses to indicate the observers' identifications of nonuniformities, surface waviness, and specks or scratches.

From the photographic record in Fig. 3, and the gloss data recorded in Table I, the degree of consistency between visual and photographic records of gloss may be seen. Note, for instance, that panels $a-l$ and $b-r$ were designated "wavy" by all observers in the visual test; also these panels in the photograph show the typical distortion due to waviness. The distinctness of the images reproduced in the figure do not

TABLE I. *Tabulation of distinctness-of-image gloss ratings by six observers of the three pairs of surfaces compared in Fig. 3. Surfaces were observed at two distances and surface characteristics noted.*

Distance from Lamp to Sample		30 cm						90 cm					
Observers		RSH	DBJ	KSG	GWH	HJK	WNH	RSH	DBJ	KSG	GWH	HJK	WNH
Panel *a–l*	A_1	*f*	*g*	*f*	*g*	*f*	*g*	–	–	–	–	–	–
	A_2	–	–	–	–	–	–	–	–	–	–	–	–
	A	–	–	–	–	–	–	*f*	*f*	*p*	*p*	*p*	*f*
	B	–	–	–	–	–	–	–	–	–	–	–	–
	C	–	–	–	–	–	–	–	–	–	–	–	–
	D	–	–	–	–	–	–	–	–	–	–	–	–
	E	–	–	–	–	–	–	–	–	–	–	–	–
Mean Rating		$(f+0.5)A_1$						$(p+0.5)A$					
nonuniformities		–	–	–	–	–	–	–	x	–	x	–	–
waviness		–	x	x	x	x	x	x	x	x	x	x	x
specks scratches		x	–	x	x	x	x	–	–	x	–	–	–
Panel *b–l*	A_1	*f*	*p*	*p*	*p*	*f*	*p*	–	–	–	–	–	–
	A_2	–	–	–	–	–	–	–	–	–	–	–	–
	A	–	–	–	–	–	–	–	–	–	–	–	*f*
	B	–	–	–	–	–	–	*f*	*g*	*p*	*f*	*f*	–
	C	–	–	–	–	–	–	–	–	–	–	–	–
	D	–	–	–	–	–	–	–	–	–	–	–	–
	E	–	–	–	–	–	–	–	–	–	–	–	–
Mean Rating		$(p+0.3)A_1$						$(f+0.5)B$					
nonuniformities		x	–	x	x	–	–	–	–	–	–	–	–
waviness		–	–	–	–	–	–	x	x	x	x	–	–
specks scratches		x	–	x	x	x	–	x	–	–	x	x	–
Panel *c–l*	A_1	–	–	–	–	–	–	–	–	–	–	–	–
	A_2	–	–	–	–	–	–	–	–	–	–	–	–
	A	–	–	–	–	–	–	–	–	–	–	–	–
	B	–	–	–	–	–	–	–	–	–	–	–	–
	C	*f*	*p*	*f*	*f*	*f*	*f*	–	–	–	–	–	–
	D	–	–	–	–	–	–	*p*	*f*	*p*	*p*	*p*	*g*
	E	–	–	–	–	–	–	–	–	–	–	–	–
Mean Rating		$(f-0.2)C$						$(p+0.5)D$					
nonuniformities		–	–	–	x	–	–	–	–	–	–	–	–
waviness		–	–	–	–	–	–	–	–	–	–	–	–
specks scratches		x	x	x	x	x	–	x	–	x	x	–	x

Distance from Lamp to Sample		30 cm						90 cm					
Observers		RSH	DBJ	KSG	GWH	HJK	WNH	RSH	DBJ	KSG	GWH	HJK	WNH
Panel *a–r*	A_1	*g*	*g*	*g*	*g*	*g*	*g*	–	–	–	–	–	–
	A_2	–	–	–	–	–	–	–	*g*	*f*	–	–	*p*
	A	–	–	–	–	–	–	*g*	–	–	*f*	*g*	–
	B	–	–	–	–	–	–	–	–	–	–	–	–
	C	–	–	–	–	–	–	–	–	–	–	–	–
	D	–	–	–	–	–	–	–	–	–	–	–	–
	E	–	–	–	–	–	–	–	–	–	–	–	–
Mean Rating		gA_1						$(p-0.2)A_2$					
nonuniformities		–	–	–	–	–	–	–	–	–	–	–	–
waviness		–	–	–	–	–	–	x	–	–	–	–	–
specks scratches		x	–	x	x	x	x	x	x	x	x	–	–
Panel *b–r*	A_1	*p*	*p*	*p*	*p*	*p*	*p*	–	–	–	–	–	–
	A_2	–	–	–	–	–	–	–	–	–	–	–	–
	A	–	–	–	–	–	–	–	–	–	–	–	*p*
	B	–	–	–	–	–	–	*p*	*p*	*p*	*p*	*p*	–
	C	–	–	–	–	–	–	–	–	–	–	–	–
	D	–	–	–	–	–	–	–	–	–	–	–	–
	E	–	–	–	–	–	–	–	–	–	–	–	–
Mean Rating		pA_1						$(p+0.5)B$					
nonuniformities		x	x	–	x	x	x	–	x	–	–	x	–
waviness		x	x	x	x	x	x	x	x	x	x	x	x
specks scratches		–	–	x	x	x	–	–	x	x	x	–	–
Panel *c–r*	A_1	–	–	–	–	–	–	–	–	–	–	–	–
	A_2	–	–	–	–	–	–	–	–	–	–	–	–
	A	–	–	–	–	–	–	–	–	–	–	–	–
	B	–	–	–	–	–	–	–	–	–	–	–	–
	C	–	–	–	–	–	–	–	–	–	–	–	–
	D	*p*	*p*	–	–	–	–	–	–	–	–	–	–
	E	–	–	*f*	*g*	*f*	*g*	*f*	*g*	*p*	*p*	*p*	*p*
Mean Rating		*gE*						$(p+0.5)E$					
nonuniformities		–	–	–	–	–	–	–	–	–	–	–	–
waviness		–	–	–	–	–	–	–	–	–	–	–	–
specks scratches		x	x	x	x	x	x	x	–	x	x	–	–

exactly correspond to the 30-cm ratings given in the table because of slight changes in reproduction introduced in the various printing processes.

When it is considered that the gloss inspection lamp and the method of rating gloss were both new to these observers, the agreement among them seems quite satisfactory. The lamp is shown to be capable of establishing twenty-one steps on a distinctness-of-image scale. The range of this scale may be adjusted to give the best gloss differentiations of any particular type of glossy material. This adjustment is usually accomplished by varying the distances of lamp to test surface and test surface to observer. Glossy surfaces which reflect sharp images should be compared at greater distances from the lamp, while better differentiations are made on the less glossy surfaces by approaching them closer to the lamp. The average observed, distinctness-of-image gloss differences, expressed in gloss steps between the *l* and *r* panels of each pair at the two distances recorded in Table I, are as follows:

	Distances	
Sample	30 cm	90 cm
a pair	0.5	2.3
b pair	0.3	1.0
c pair	4.8	3.0

Thus it can be seen that the glossy *a* pair of panels showed an average difference of only one-half a step at 30 cm, while at 90 cm this difference was more than two steps. The converse is true for the *c* pair of low gloss panels; thus, viewed at 30 cm, the average difference was 4.8 steps, but at 90 cm the difference recognized was only 3.0 steps.

The preparation recently of a specification for the gloss of automobile enamels furnishes an example of the practical use of this flexible gloss scale. Representative test samples of such glossy enamels, some weathered and some fresh, were used for trial observations to determine under what conditions the best gloss differentiations could be made. It was found that at a lamp-to-surface distance of one meter, a lamp-to-observer distance of 1½ meters and an angle of view equal to 30°, practically the complete gloss scale could be used. The test room was dark, the lamp was placed on a bench, the test panels were placed on the floor, and the observers viewed the images of the lamp target reflected in the various surfaces while standing. Tentatively, the distinctness-of-image gloss requirements were chosen as follows: fresh surfaces: *B* fair, or higher, after 168 hours of accelerated weathering: *C* good, or higher.

In comparing the superior and inferior enamels, it was found that the better grade materials retained their gloss more effectively through accelerated weathering.

IV. Identification of Differences in "Bloom," Objective Gloss and Texture

"Bloom," objective gloss, and surface texture were three of the types of gloss identified in the earlier publication.[1] It is not possible to arrange, by means of the lamp, these factors along a scale such as used in the case of distinctness-of-image gloss. However, the lamp and target have proved useful in identifying differences in these three types of surface appearance and in furnishing qualitative, rather than quantitative, data on them.

When using the gloss-inspection lamp for the identification of "bloom," one inspects the image of the black spot in the center of the target and the other dark areas in the target. "Bloom" is indicated as a haze in these dark areas of the image. The two glossy olive-green enamel panels compared in Fig. 3 for distinctness-of-image gloss showed also a pronounced difference in "bloom." This effect is quite appreciable in the left panel of Fig. 4 which is another print from the *a* pair negative of Fig. 3, but less dense. In the *b* pair of white surfaces, Fig. 3, $b-l$ reflects the sharper images, and also shows more "bloom" than $b-r$. "Bloom" is shown only by surfaces which reflect images.

Objective gloss is more popularly thought of as "shininess." With the gloss lamp and target, it is recognized by the brilliance of reflected images but is not readily measurable. There are a number of other gloss meters, however, which give records of specular reflectance, such as, for instance, the instrument[2] designed by the author

[2] Hunter, "The Glossmeter," Scientific Section Circular No. 456 of the National Paint, Varnish and Lacquer Association, Washington, D. C. (April 1934).

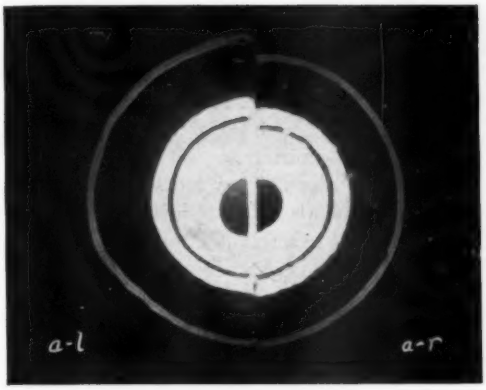

FIG. 4. Comparison of *a* pair of panels shown in Fig. 3 printed from same negative as in Fig. 3, but with low density to show effect of bloom on panel *a*—*l*.

in the spring of 1934. References to methods for measuring objective gloss as well as other gloss factors are given in the previous circular.[1]

With regard to comparisons of surface texture and the evaluation of irregularities, this lamp is useful as a source of nearly unidirectional light. Nonuniformities, waviness, and specks or scratches were evaluated qualitatively by the observers who compared the six surfaces and obtained the results shown in Table I. Surface irregularities, blemishes, and texture show up distinctly in illumination from a single direction but are less visible in illumination which is well diffused. Texture is most distinct at the angle of specular reflection, and photographs at this angle with the camera focused on the surface tested, give, in our experience, the best records of texture. All the surfaces photographed in Fig. 3 show irregularities, but they are out of focus because the camera was focused on the image of the target.

V. Value of Gloss Photographs

It can be appreciated that photographs such as are shown in Figs. 3 and 4 are better and more complete records of glossiness and serve better for comparing gloss than values obtained on any gloss scale. This is because the glossiness of a surface arises from a combination of several factors and these combined factors are seldom expressible as a variation in one dimension. Because of the advantages of the photographic method, the earlier gloss comparator[1] was designed to take a camera directly into the instrument. The camera is always placed in the same position in the instrument; no careful adjusting and focusing are necessary, and the exposures are timed by a prepared table. With the gloss-inspection lamp, on the other hand, it is necessary to set the camera up carefully in the desired position to photograph the effect sought. In spite of the greater care which is necessary, this ability to use the camera in any position is sometimes an advantage because it gives greater latitude for the study of gloss effects.

A 5 by 7 plate camera was used to obtain the photographs shown in Figs. 3 and 4. This was set up as shown in Fig. 1 where the camera lens and the lamp target are both about 30 cm from the gloss surfaces. The lens of the camera was stopped down to about 3 mm so that as much detail as possible would be obtained from the out-of-focus test surfaces.

VI. General Technique

As already implied, the observer who wishes to analyze gloss effects must recognize that two distinctly different modes of appearance, as well as several appearance effects, are always possible. One mode results when the observer fixates upon the glossy surface itself; the other when he fixates the image of some object reflected in that surface. Surface texture, formation, and structure are appreciated when the eye is focused upon the surfaces being studied. On the other hand, form of reflected images, gloss contrasts, and the distribution of light reflected by surfaces are usually appreciated when the observer fixates the images of objects reflected in the glossy surfaces. For this reason, one who wishes to photograph surface features and texture focuses the camera upon the glossy surface, while one who wishes to photograph image reflections, "bloom," or contrasts, as in Fig. 3, focuses the camera upon the image of the target reflected in the test specimens. In this latter case, pimples, irregularities, and grain in the surfaces can be seen, but they are out of focus.

In conclusion, it may be repeated that the gloss inspection lamp is a convenient source of light for the general study of gloss-appearance effects. The wide variety of ways in which it can

be used makes it possible to identify many effects that are not appreciated when using other apparatus. Thus, as described in section II, the distances of the test surface from the lamp and observer and the surrounding lighting can be varied to obtain the conditions which give best discriminations of distinctness-of-image gloss for the particular type of surfaces being studied. Furthermore, unusual gloss effects can often be seen which do not fall directly into one of the classes identified in the previous publication.[1] By using the gloss-inspection lamp to study these effects, and trying different methods of illuminating and viewing the samples, satisfactory conditions for the identification of many effects may be found.

For example, an unusual effect which appeared in comparing the *c* pair of furniture finishes photographed in Fig. 3 may be described. When these two surfaces were compared from a direction considerably to one side of the direction of image reflection shown, panel *c–r*, which shows distinctly the lower distinctness-of-image gloss, appeared to have a cleaner and glossier finish than panel *c–l*. The effect on *c–l*, which appeared to be similar to "bloom" or reflection haze, detracted considerably from its appearance and yet it was only identified under rather exceptional conditions of illumination.

Directional distribution measurements of reflection as recommended by McNicholas[3] may eventually lead to a more definite understanding of the conditions under which some of these appearance effects are likely to occur, and such measurements are now in progress; but for the present, empirical methods which are discovered by trial, using devices such as this lamp, offer the best means of identifying and recording the presence of unusual gloss types. Because there is so much latitude in establishing external conditions for the use of this lamp, it is believed that it will prove valuable in examining many types of gloss effects.

[3] McNicholas, "Absolute Methods in Reflectometry," Bur. Standards J. Research **1**, 29 (1928), Research Paper No. 3.

APRIL, 1936 J. O. S. A. VOLUME 26

Erratum: Theory of Microscope Vision

M. HERZBERGER, *Eastman Kodak Company*

(J. O. S. A. **26**, 52 (1936))

ON page 61 of this article, left column, second line from the bottom, leave out the words "Russian authors, in particular."